



Fermilab

UPC 086

UPC No. 86

THE AMATEUR MAGNET BUILDER'S HANDBOOK

A.V. Tollestrup

February 22, 1979

This incorporates the work of many people over the last two years in the Doubler Division. References to specific names will be made at the proper points.

Additional sections will be issued as they are ready.

1. Introduction

This report will cover magnet construction up through number 150 which took place at the end of December, 1978. We have in this group almost 100 magnets that have had measurements made on them either in the vertical dewar or in the Magnet Test Facility. This set of magnets will be used as a data base to estimate what the systematic and random errors are made during construction and also to try and set realistic limits on what errors may be expected in the future.

We attempted to make #160 a magnet that would satisfy all of the criteria necessary for an operating doubler magnet, however, in incorporating the necessary changes to make such a magnet a number of troubles were encountered. All of these troubles have been met in some form before and are generally reappearing for a second time. At this point we are faced with the task of identifying these troubles, their symptoms, and instituting a suitable quality control program to eliminate them. Troubles exist with controlling shorts, wire size, mechanical tolerances, short sample tests on the wire, and the quality of the test program itself. In addition, we must set up a system that will allow us to speedily react to any indication of trouble.

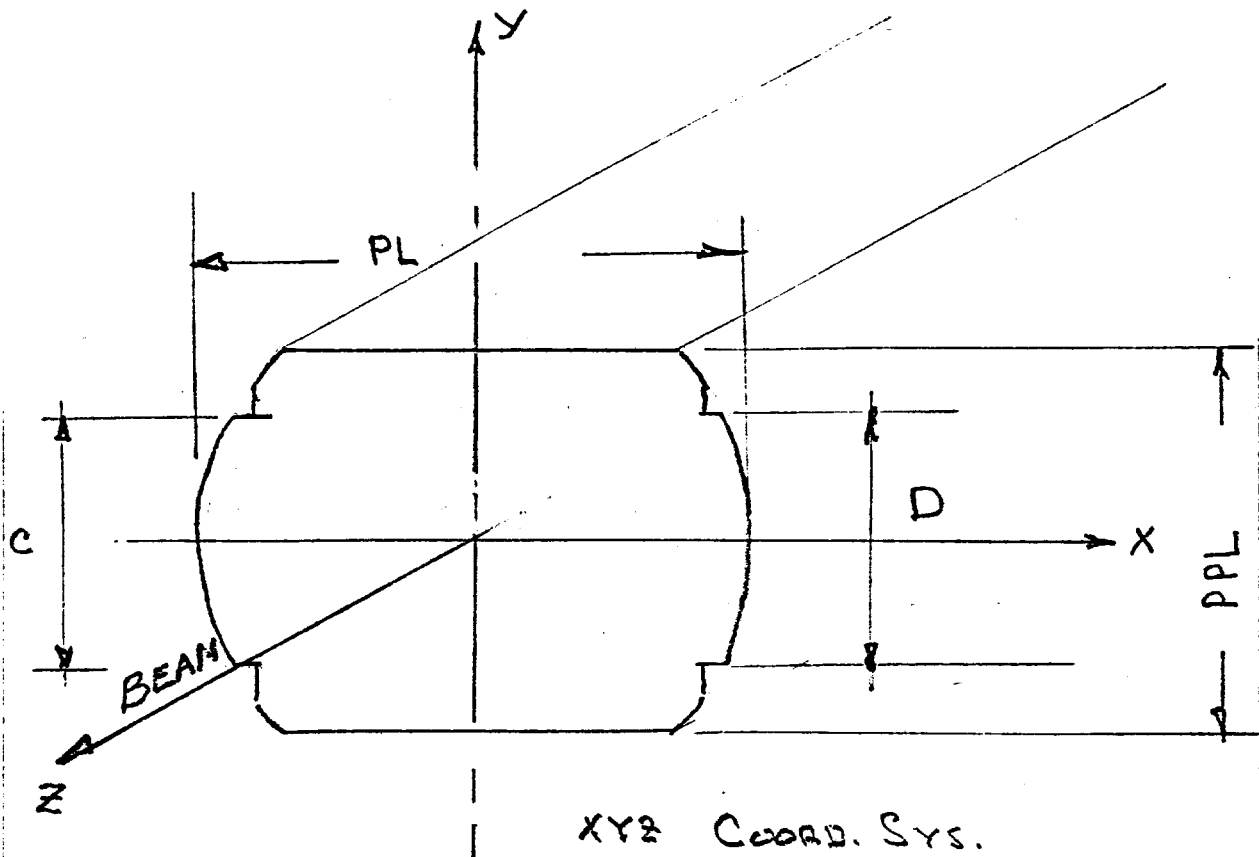
The quality control system should be as diffuse as possible with simple tests employing "go-no go" limits and using unskilled people as much as possible. It is realized that such a program will occasionally produce bad test results. At this point there should be a skilled group of people that can access as rapidly as possible whether there is trouble with a magnet or whether the test has simply not been

carried out well. In any case, the work on that particular magnet must be stopped until the problem is properly understood. As we go through the magnet description in this report an attempt will be made to define as many "go-no-go" tests and limits as are possible at this stage.

1.1 Properties of Multipoles and Description of Coordinate System

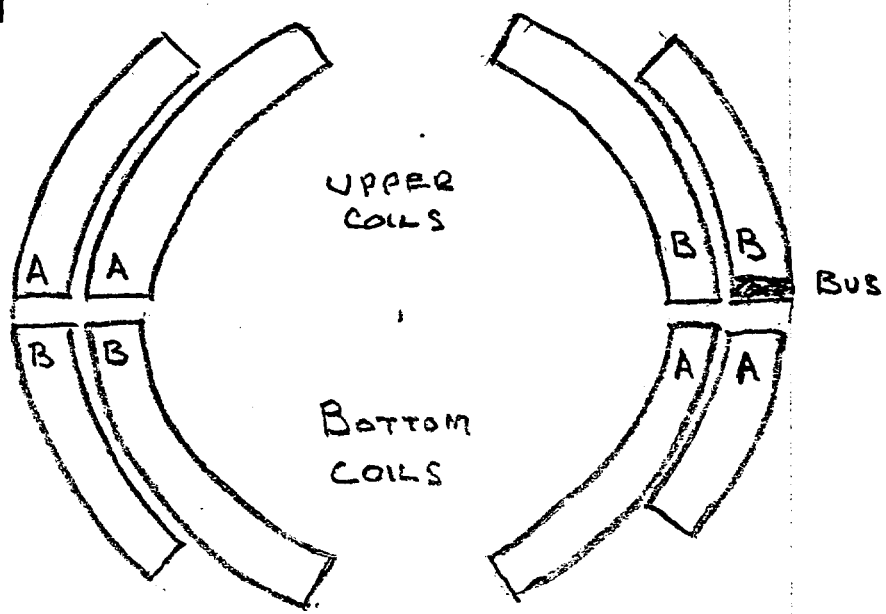
The bore of the magnet is 1.5" in radius. Inside of this volume a coordinate system is set up such that the beam travels along the z axis in a positive direction. Looking upstream the y axis is vertical and the x axis is to the right, thus, defining a right-handed coordinate system. The inside of the ring is then in the minus x direction. Figure 1.1 shows a cross section of the coil with letters on it that are used in the magnet assembly building to designate various portions of the coil. The buss is located in the plus x upper, outer coil median plane and crosses over at the ends where the connections from magnet-to-magnet are made on the minus x side of center. In addition to the coil labels, collar dimensions are shown in the top part of the picture. C and D refer to little shoulders on the sides of the collars; PL and PPL refer to the parting line and perpendicular to the parting line directions respectively. This same coordinate system is used for the room temperature measurements.

In this coordinate system we can express the fields by the following equations.



UPPER LEFT

LOWER LEFT



Nomenclature for COIL SIZE MEASUREMENTS.

LOOKING UPSTREAM

Figure 1.1.1

The vector potential is given by:

$$A_z (r, \phi) = \sum_n (C_n \sin n\phi + D_n \cos n\phi) (r/r_0)^n$$

where ϕ is measured from the + x axis and r_0 sets the scale.

$$B_\phi = + \frac{\delta A_z}{\delta r} = + \sum_n \frac{r^{(n-1)}}{r_0^n} (C_n \sin n\phi + D_n \cos n\phi)$$

$$B_r = - \frac{1}{r} \frac{\partial A_z}{\partial \phi} = - \sum_n \frac{r^{(n-1)}}{r_0^n} (C_n \cos n\phi - D_n \sin n\phi)$$

$$B_x = B_r \cos\phi - B_\phi \sin\phi$$

$$B_y = B_r \sin\phi + B_\phi \cos\phi$$

$$B_x = - \sum_n n \frac{r^{n-1}}{r_0^n} \{C_n \cos (n-1)\phi - D_n \sin (n-1)\phi\}$$

$$B_y = \sum_n n \frac{r^{n-1}}{r_0^n} \{C_n \sin (n-1)\phi + D_n \cos (n-1)\phi\}$$

at $y = 0$, we have $\phi = 0$ and $x = r$, so:

$$B_x (X) = - \sum_n n C_n \frac{x^{n-1}}{r_0^n} = B_0 \sum_1^\infty a_n X^n$$

$$B_y (X) = \sum_n n D_n \frac{x^{n-1}}{r_0^n} = B_0 \sum_1^\infty b_n X^n$$

where a_n, b_n are the usual multipole coefficients.

In these equations, the units will be chosen such that x is measured in inches. This is not a capricious adherence to the inch system but rather comes about because 1 inch represents

two thirds the magnet aperture. At this radius the multipoles up through the 30-pole are all of the order of 10^{-4} , and hence, this multiplier may be suppressed. In everything that follows in this report the units will be expressed in terms of 10^{-4} at 1 inch for all of the multipoles.

The useful aperture of these magnets is about 1". In this connection, it is worth remembering some simple properties of multipoles. The first is that on a circle of a constant radius, any given multipole has a magnetic field vector whose magnitude is constant in value. Second, as one travels around a circle of constant radius, the vector of the multipole rotates $\frac{n}{2} - 1$ times, where n is the multipole order. One can easily verify this by thinking about a quadrupole field. Finally, recall that the amplitude of the multipole is proportional to $r^{\frac{n}{2} - 1}$.

Our present magnet is very rich in multipoles. These largely arise from the sharp corners on the coil blocks; the inner one of which is located at about 72° and the outer one of which is located at about 36° . Symmetry requires that all of the a_n 's are zero, and all of the odd b_n 's are zero. Thus, when we come to the analysis of the field as measured by the Magnet Test Facility (MTF). We will have some handle on the size of the magnet errors by looking at the coefficients that should not be there for a perfectly symmetric magnet.

The calculated value of the multipole coefficients in the body of the magnet as well as the integral values are listed in the Table 1.1.1 below. It should be mentioned at this point that all of the theoretical calculations on the magnetic field resulting from a given current distribution have been done by S. Snowdon.

Table 1.1.1

N	# Pole	Body b_n	Integral b_n
0	Dipole	1	1
2	Sextupole	7.28	.41
4	Decapole	3.19	1.11
6	14-Pole	4.67	4.42
8	18-Pole	-12.22	-12.08
10	22-Pole	3.73	3.64
12	26-Pole	-.83	-.82
14	30-Pole	.07	.07

An examination of the table in combination with the little theorems about multipoles given in the previous will indicate that if we know the multipoles up through the 30th that then we will know the magnetic field everywhere inside of a 1" circle to an accuracy of better than $\frac{1}{2}$ gauss out of 45,000. Figure 1.1.2 shows the magnetic field calculated from this set of multipoles along the x axis. It is noted that there is a sextapole component

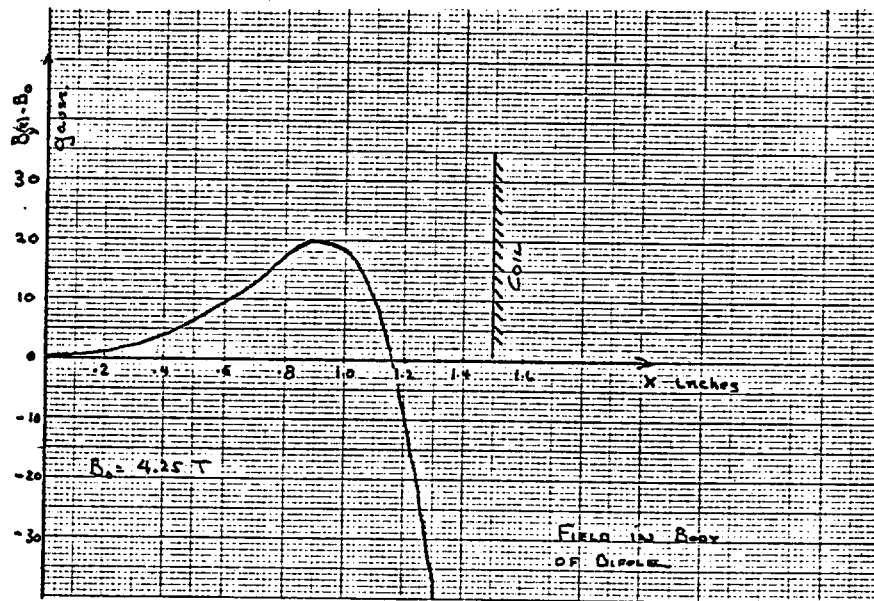


Figure 1.1.2

to this field. This component is necessary in order that the integral of B_y through the magnet be independent of x. This occurs because the ends of the magnet are curved in a circular fashion

and hence as one moves out in x , the magnet becomes slightly shorter. This parabolic shortening of the magnet is compensated for by making the field slightly stronger at larger x . This will be discussed in more detail later.

Figure 1.1.3 shows a plot of the $\int B dl$ through the magnet as a function of x . It is noted that the useful aperture is

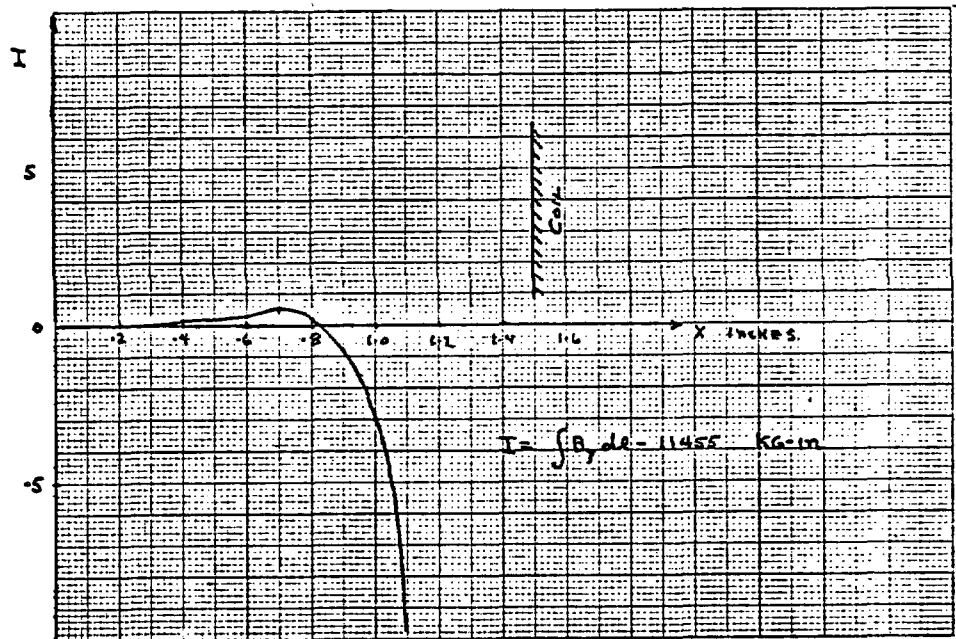


Figure 1.1.3

limited to a ± 0.8 " and that past this point the field very rapidly deteriorates. The second important point to note is that the aperture in the x direction is larger than it is in the y direction. The sum of all the multipoles very nearly cancels at about $x = 1$. However, when one moves off the $y = 0$ plane, all of the multipole vectors are rotated by different amounts and this fortuitous cancellation no longer takes place.

A magnet with such a rich harmonic structure has not been used up to the present for an accelerator. Iron pole tips have been a very convenient filter to smooth the field. However, if one is to take advantage of superconductivity, it will be necessary to solve the problem of controlling this harmonic structure carefully. In fact, this represents the major challenge to the designer of the accelerator for the future.

1.3 Philosophy of Magnet Construction and Control of Errors

A simple calculation of the accuracy that it is necessary to use when constructing a magnet, will indicate that the conductors must have their position controlled to the order of .001". It is not clear that modern technology is capable of this feat while at the same time maintaining the cost of the magnet at a manageable level. However, our experience has led to a new philosophy of magnet construction. An examination of the magnet cross section shows that the uniform field is based upon approximating a current sheet with a cosinusoidal distribution of current density. However, due to the finite thickness of the wires, the current sheet becomes two rather massive current blocks, whose thickness is far from negligible. In fact, the corners of these current blocks are the sources of the higher harmonics that are displayed in Table 1.1.1. For instance, it is apparent that there are two angles in the coil that can be adjusted such that the sextapole and decapole components of the field are made to vanish (remember that for a simple current sheet cut at 60° , the sextapole vanishes). Thus, the first harmonic of the field over which the gross geometry of the coil does not have a strong influence is the 14-pole. The group of three very strong harmonics 14, 18, and 22, is mainly the result of the corners, and we have very little control over the amplitude of these harmonics. All of the lower harmonics are available for our control by changing the angles that the current blocks occupy.

Once this is realized, a new philosophy for the control of the magnets becomes possible. Suppose we have a machine that will

make magnets in a reproducible manner, but that these magnets have a multipole structure that is wrong due to the shape for instance being slightly different than the shape for which the calculations were made. The result of these errors will be the appearance of sextupole and decapole terms plus perhaps some of the skew symmetric and normal harmonics that should vanish because of symmetry. If careful measurements are made of the magnetic field, it should be possible to calculate what changes are necessary in the coil angles in order to make the lower harmonics vanish as was the case for the desired perfect coil. Since the higher harmonics, i.e., 14 and above are determined only by the corners we have no control over these harmonics and hence, there is nothing that can be done. However, the other side of the coin should be that these harmonics very nearly have their calculated values. That this is actually the case will be demonstrated in the section on harmonic analysis that follows. In other words, all "near-by" shapes have a similar structure of field for multipoles of 14 and higher and in addition sextupole and decapole terms that can be adjusted by changing the key angles. The absolute shape is not important -- only its reproducibility.

Figure 1.3.1 then shows the possibility of controlling such a machine by means of feed back in order to produce accelerator quality magnets. In this feedback control system, there are two loops. The first is a room temperature measurement of the field just after the coil has been collared. This allows one to control slowly changing systematic errors such as wear of the tooling, change in the wire size, or change in the size of insulation used around the magnet coil. Since ultimately the magnet must be used in its superconducting mode, it must

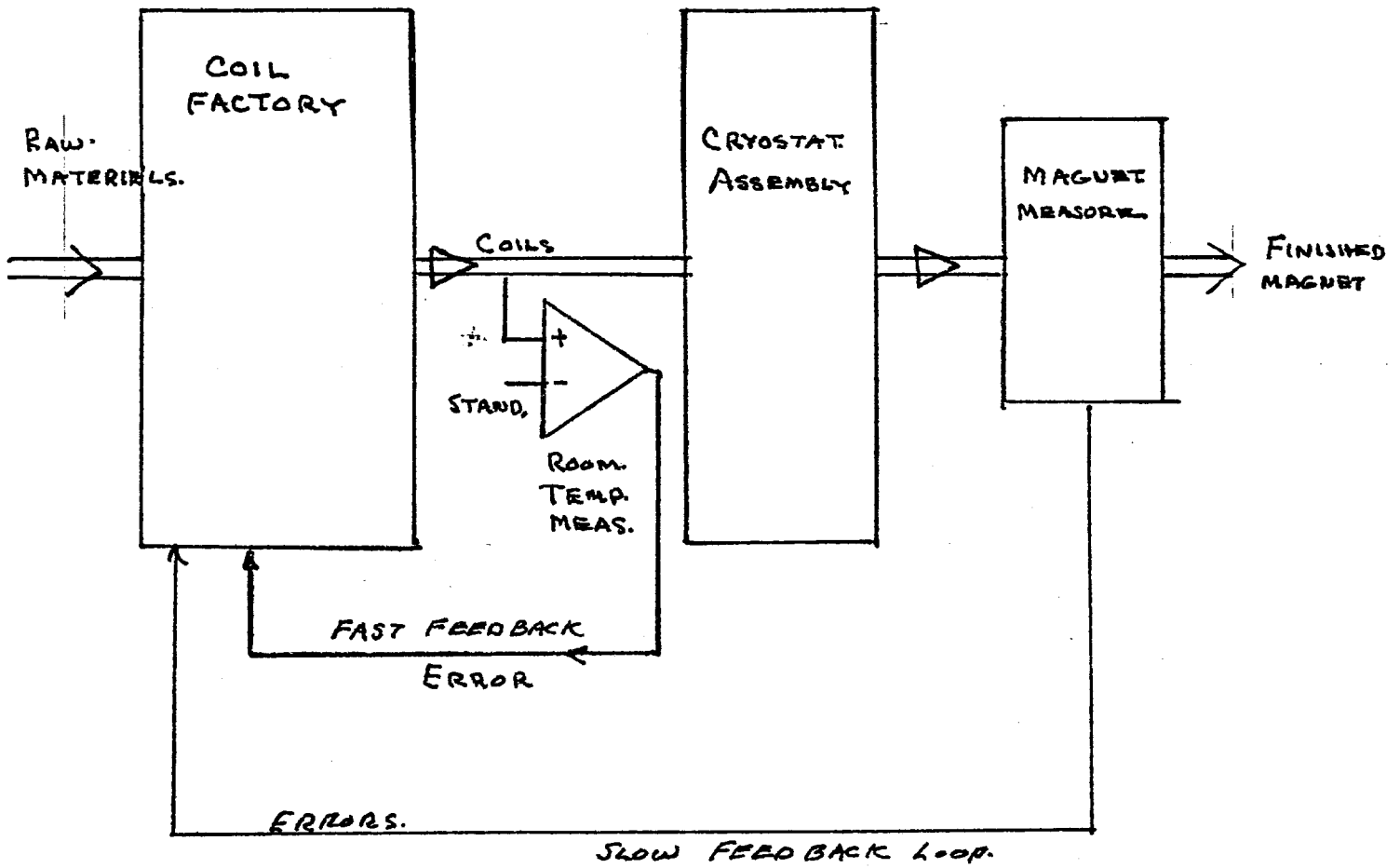


Figure 1.3.1

be measured in its own cryostat and inside an iron return yoke. These measurements provide the ultimate verification that the quality of the magnet is acceptable for use in the Doubler. They may take place as much as one or two weeks after the coil has been collared, and provide an absolute measurement of the field. Hence, one can see the crucial need for a rapid method of verifying the accuracy of the coil construction such as is provided by the room temperature measurement. We will discuss this in much more detail in Section 3.

1.4 Systematic Errors

In addition to the random errors due to conductor placement there are systematic errors that arise for at least three reasons:

- a. Motion of the coil from magnetic forces,
- b. persistent currents in the superconducting cable, and
- c. magnetization of the iron.

Motion of the coil results from the large magnetic forces present within the structure of the magnet. These forces are proportional to I^2 and if the magnet is well made are balanced by an elastic deformation of the coil collar. For instance, the magnet lengthens by 70 mils when it is magnetized to 4.5 tesla. This effect is negligible in its action on the beam, but does mean that the magnet has to be supported properly in its cryostat. The major diameter of the magnet also increases by about 2 mils during magnetization. This slightly alters the multipole structure of the magnet as it is excited.

Persistent currents in the superconductor are also present,

and mainly couple into the sextapole component. These fields tend to be constant in magnitude and hence are more important at injection than they are at full excitation. Their structure is displayed in Section 6. The iron in the magnet is mainly in its linear region, however, a small non-linearity is calculated due to saturation effects, and this will be different for the quadrupoles than it is for the dipoles. The effect as it has been measured in the dipoles is discussed in Section 4. The quadrupoles have not yet been measured and hence how well the two will track when they are connected in series is not known.

For all of the above reasons, a complete set of dynamic corrections must be made available. Unlike the iron magnets of the past, these corrections must be under program control in order to provide the proper correction at each point of the magnet excitation, from injection to full field.

1.5 Model for Error Analysis

In order to analyze the errors that various distortions in the magnet structure can give rise to, we have constructed a simple model for the magnet. This consists of line currents located at the centers of the busses in the real magnet. This model has the virtue that it represents the actual magnet quite well, and in the region inside of a radius of 1" allows us to make simple calculations for what various distortions in the wire placement will do to the magnetic field (these calculations were programmed by R. Flora).

We investigate here distortions of two types. The first type is distortions caused by the magnetic forces distorting the

coil support structure. There are two effects. One is that the collar becomes slightly elliptical and the wire moves both in azimuth and radius. These distortions will be proportional to the square of the current. Figure 1.5.1 shows the diameter of the magnet as a function of excitation current. The curve through this point is a fitted parabola and it can be seen from the curve that it fits the data nicely. Warren Young from the University of Wisconsin at Madison has made calculations of the elastic deflection expected through the collar. These distortions agree well with the values measured here. A second type of distortion that occurs under magnetic forces is a compaction of the wire in an azimuthal direction. The theory will be worked out in Section 6. The distortion that is calculated in that Section is used with the present model to calculate the perturbations to be expected in the field.

Another set of perturbations investigated here are those of a type that could be expected from various errors in the manufacturing process. For instance, the radius may be slightly wrong, the key angles could be wrong, the insulation of the parting plane could have fluctuations in its thickness, or finally there could be random fluctuations in the individual wires in the magnet. The error fields are highly correlated in so far as the error in the position of one wire will necessarily cause a displacement of nearby wires. However, correlations between the two sides of the magnet and between the top and bottom coil would not be expected. We will see later that the skew symmetric terms which should vanish under perfect symmetry

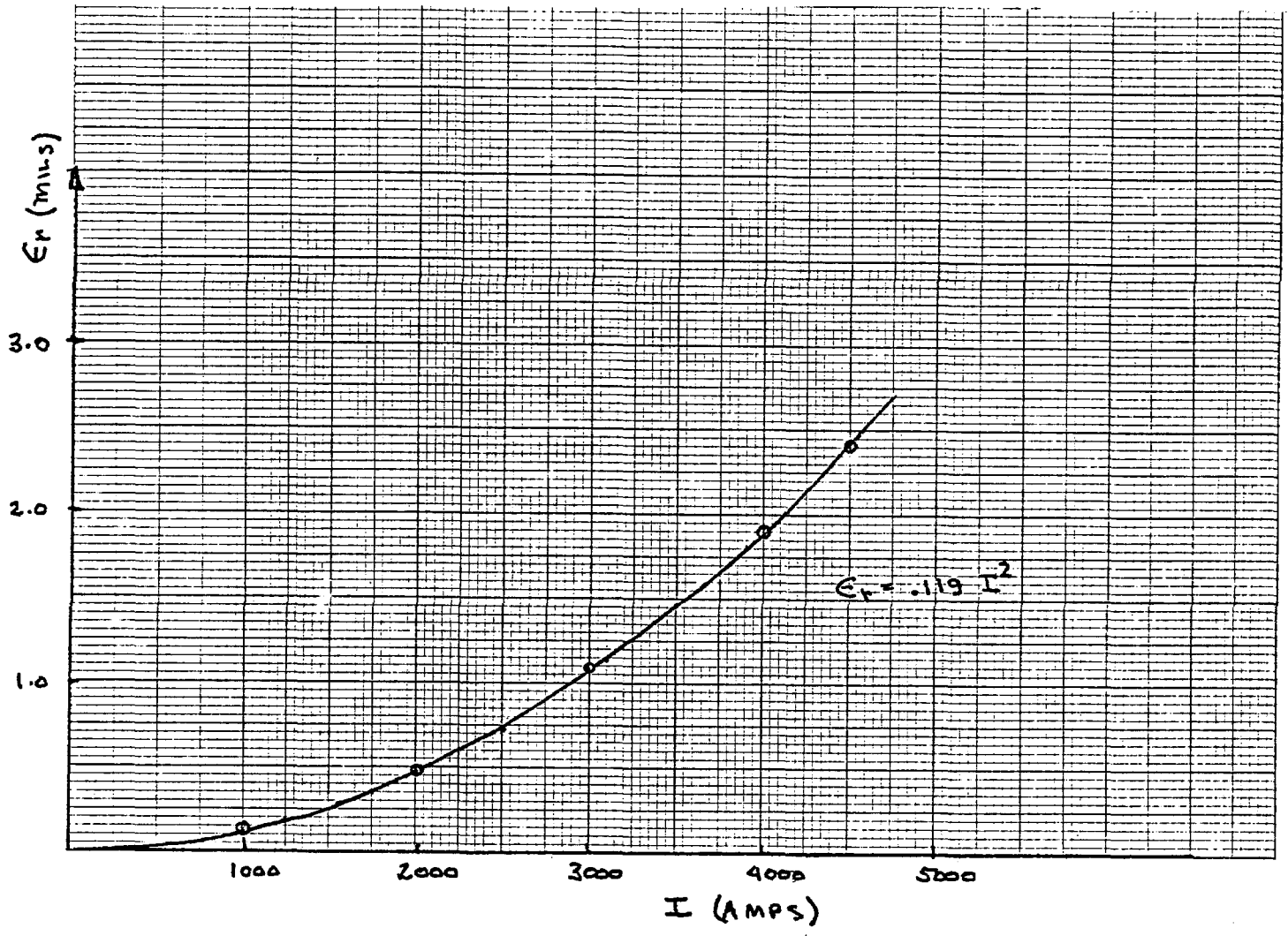


Figure 1.5.1

give us a sensitive measure of the various sorts of errors that we are discussing here. The following tables give the properties derived from this simple model.

Table 1.5.1 shows the calculated coefficients for a circular magnet with the wires equally spaced. This can be compared with the multipole structure given from S. Snowdon's calculations, (Table 1.1.1 and it is seen that there is a good deal of similarity. We now describe various perturbations that have been made on this basic structure. The following tables show in the first column the harmonic number where $K = 0$ is the dipole terms. The following four columns are the A_n and B_n for the inside and outside shell respectively. The units here as mentioned previously are in terms of $\frac{\Delta B}{B} \times 10^{-4}$ at 1".

Table 1.5.2: The distortion considered here is one that increases the inside radius of the magnet by 10 mils. All of the conductors maintain their same angles but move out in radius by this amount.

Table 1.5.3: The distortion given here is specified by the following equation:

$$r = r_0 + .01 \cos 2\phi$$

where R_0 is the original radius and ϕ is measured from the x axis. This is an elliptical distortion of the magnet and corresponds closely to the distortion caused by the magnetic forces. The amplitude of the distortion is .01".

Table 1.5.4: Considers the distortion that would arise if the collars are given an elliptical deformation. When a circle is distorted into an ellipse, the points on a circle move both radially and azimuthally. For a

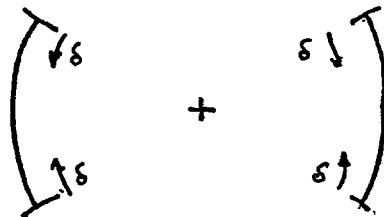
structure whose length is fixed, the peak radial motion is twice the peak azimuthal motion. The distortion is given by the following equation.

$$\epsilon_{\phi} = -.01 \sin 2\phi$$

The amplitude of the distortion corresponds to the wires at 45° moving an amount equal to .01". Combining on half of this distortion with the distortion in Table 1.5.3, would give the motion for an elliptical change in shape of the collar structure with a radial amplitude of .01".

Table 1.5.5: Considers the distortion caused by the elastic compression of the wires in an azimuthal direction due to the magnetic forces. This distortion is worked out in Section 6. The amplitude here corresponds to a maximum motion of the wires equal to 10 mils.

Table 1.5.6: This Table applies to the harmonics when the key angles are changed by 10 mils in a pattern shown below.

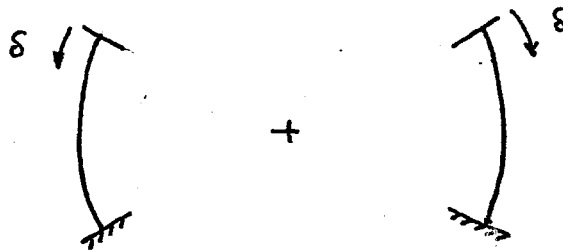


The median plane is assumed to stay fixed.

Table 1.5.8: Shows that if the key angles are symmetrically changed on only one side of the magnet, that then quadrupole and 12-pole terms come in to the B series of coefficients. Note that A coefficients are still all 0.

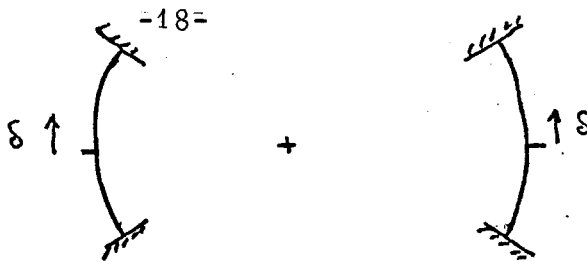
Table 1.5.9: Displays the results for a 10 mil gap inserted in the magnet at the parting plane on the right hand side. Note that this generates all of the B's, however, if a symmetrical 10 mil gap on the opposite side of the magnet were inserted then the even B's would be double in amplitude and the odd B's would go to zero. This table demonstrates that the transfer constant and the sextapole moment are very sensitive to symmetrical changes in the gap at the parting plane; and that in addition, strong quadrupole and octapole terms can come in if this gap is asymmetrical.

Table 1.5.10: Shows a distortion at the keys that is described in the following diagram.



The two top keys are assumed to move down by 10 mils, the bottom keys are fixed and the coil is assumed to be an elastic structure so that the parting plane would move down by 5 mils on each side. This distortion breaks the symmetry about the horizontal plane and induces skew quadrupole, octapole, etc., terms. Since it compacts the coil more on the sides, it also changes the normal sextapole, decapole, etc., terms in the B series.

Table 1.5.11: Shows the results of having a symmetrical raising or lowering of the parting plane. The table gives the values for a raising equal to 10 mils as shown in the following diagram.



In this distortion the keys are assumed fixed, hence, the top coil becomes more compressed and the bottom coil becomes less compressed. If the coils are molded in different sizes, this is the situation that would exist. Again the skew terms are strongly excited.

Table 1.5.12: Considers the displacement of only one of the keys. The other three are assumed fixed. This distortion completely breaks the symmetry of the magnet and generates all of the multipoles. The amplitude considered is 10 mils and it is depicted in the sketch shown below.

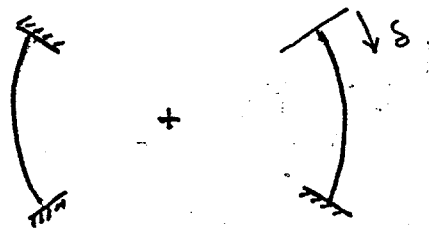


Table 1.5.13: Considers a case where the parting plane on the right hand side of the magnet is displaced upward by 10 mils, the keys are considered to be fixed. Again this distortion completely breaks the symmetry of the magnet and generates all terms, however, it can be seen that the effect on B is minimal. It is interesting to compare this case with the last one where the average current density was not changed, but it is changed in this case. This shows that the B's respond very strongly to right-left gross distortions in the current density.

Table 1.5.14: This Table shows the results of placing the coil inside of the yoke, but having the axis of the coil displaced from the axis of the yoke. The only effect of this displacement is to generate a quadrupole term in the amount that is shown in the table. The fact that only the quadrupole term is important is a result of the radius of the iron being very large compared to the radius of 1". Higher multipoles are clearly generated in the iron but their scale size is related to a radius equal to the image radius of the coil in the iron cylinder.

This completes the lists of distortions that will be considered here. In addition to these systematic distortions that can be expected during the manufacturing process, there are also random distortions due to fluctuations in the wire size, the insulation thickness, the details of the winding and so forth. An estimate of the magnitude of this type of error will be made later.

There is a second model that is useful for understanding the magnet. In this model, we replace the two individual windings by current sheets located at their individual centers. This model is useful because the coefficient can be written down in analytical form, and some insight can be obtained by studying the equations that result. We give below the equations for the A_n 's and B_n 's as an integral over the current sheet.

Table 1.5.1

K	B (IN)	B (OUT)	B (TOT)
0	5935.35	4064.65	10000.00
2	-410.36	417.34	6.98
4	11.64	-9.48	2.15
6	16.17	-13.27	2.90
8	-9.29	-1.45	-10.74
10	2.94	0.29	3.23
12	-0.77	0.08	-0.69
14	0.07	-0.01	0.07
16	0.02	-0.01	0.02
18	-0.03	-0.00	-0.03

Table 1.5.2

K	A (IN)	B (IN)	A (OUT)	B (OUT)
0	0.000	-23.971	0.000	-11.370
2	0.000	7.232	0.000	-3.946
4	0.000	-0.345	0.000	0.234
6	0.000	-0.667	0.000	0.457
8	0.000	0.490	0.000	0.064
10	0.000	-0.188	0.000	-0.015
12	0.000	0.058	0.000	-0.005
14	0.000	-0.006	0.000	0.001
16	0.000	-0.002	0.000	0.001
18	0.000	0.003	0.000	0.000

Table 1.5.3

K	A (IN)	B (IN)	A (OUT)	B (OUT)
0	0.000	-9.276	0.000	-3.596
2	0.000	-16.491	0.000	-5.555
4	0.000	1.651	0.000	-0.614
6	0.000	0.449	0.000	0.144
8	0.000	-0.339	0.000	0.049
10	0.000	0.188	0.000	0.001
12	-0.000	-0.052	0.000	-0.001
14	-0.000	0.010	0.000	0.000
16	-0.000	0.002	0.000	0.000
18	0.000	-0.002	0.000	0.000

Table 1.5.4

K	A (IN)	B (IN)	A (OUT)	B (OUT)
0	0.000	24.166	0.000	6.595
2	0.000	18.040	0.000	8.544
4	0.000	-3.135	0.000	2.622
6	0.000	0.677	0.000	0.094
8	0.000	-0.059	0.000	-0.133
10	0.000	-0.049	0.000	-0.026
12	0.000	0.038	0.000	0.004
14	0.000	-0.017	0.000	0.002
16	0.000	0.005	0.000	0.000
18	0.000	-0.001	0.000	-0.000

Table 1.5.5

K	A (IN)	B (IN)	A (OUT)	B (OUT)
0	0.000	18.830	0.000	4.834
2	0.000	17.383	0.000	6.850
4	0.000	-1.881	0.000	2.744
6	0.000	-0.139	0.000	0.489
8	0.000	0.182	0.000	-0.002
10	0.000	-0.074	0.000	-0.020
12	0.000	0.020	0.000	-0.003
14	0.000	-0.003	0.000	0.000
16	0.000	-0.000	0.000	0.000
18	0.000	0.001	0.000	0.000

Table 1.5.6

K	A (IN)	B (IN)	A (OUT)	B (OUT)
0	0.000	17.227	0.000	4.577
1	0.000	0.000	0.000	0.000
2	0.000	7.101	0.000	5.845
3	0.000	0.000	0.000	0.000
4	0.000	-4.117	0.000	1.702
5	0.000	0.000	0.000	0.000
6	0.000	1.415	0.000	0.005
7	0.000	0.000	0.000	0.000
8	0.000	-0.293	0.000	-0.105
9	0.000	0.000	0.000	0.000
10	0.000	-0.012	0.000	-0.018
11	0.000	0.000	0.000	0.000
12	0.000	0.046	0.000	0.004
13	0.000	0.000	0.000	0.000
14	0.000	-0.026	0.000	0.002
15	0.000	-0.000	0.000	0.000
16	0.000	0.009	0.000	0.000
17	0.000	0.000	0.000	0.000
18	0.000	-0.002	0.000	-0.000
19	0.000	0.000	0.000	0.000

Table 1.5.8

K	A(IN)	B(IN)	A(OUT)	B(OUT)
0	0.000	8.614	0.000	2.288
1	0.000	10.346	0.000	3.413
2	0.000	3.551	0.000	2.923
3	0.000	-1.923	0.000	1.824
4	0.000	-2.058	0.000	0.851
5	0.000	-0.106	0.000	0.260
6	0.000	0.707	0.000	0.003
7	0.000	0.302	0.000	-0.063
8	0.000	-0.147	0.000	-0.053
9	0.000	-0.164	0.000	-0.027
10	0.000	-0.006	0.000	-0.009
11	0.000	0.058	0.000	-0.000
12	0.000	0.023	0.000	0.002
13	0.000	-0.013	0.000	0.002
14	0.000	-0.013	0.000	0.001
15	0.000	0.000	0.000	0.000
16	0.000	0.005	0.000	0.000
17	0.000	0.002	0.000	-0.000
18	0.000	-0.001	0.000	-0.000
19	0.000	-0.001	0.000	-0.000

Table 1.5.9

K	A(IN)	B(IN)	A(OUT)	B(OUT)
0	0.000	-2.405	0.000	-0.606
1	-0.000	-3.943	-0.000	-0.962
2	0.000	-3.438	0.000	-0.927
3	0.000	-2.087	-0.000	-0.703
4	0.000	-1.048	-0.000	-0.453
5	-0.000	-0.559	0.000	-0.259
6	0.000	-0.366	-0.000	-0.135
7	0.000	-0.249	-0.000	-0.065
8	0.000	-0.151	-0.000	-0.030
9	0.000	-0.083	-0.000	-0.013
10	0.000	-0.047	0.000	-0.006
11	-0.000	-0.030	0.000	-0.003
12	0.000	-0.019	0.000	-0.001
13	-0.000	-0.012	0.000	-0.001
14	0.000	-0.007	0.000	-0.000
15	0.000	-0.004	0.000	-0.000
16	0.000	-0.002	0.000	-0.000
17	-0.000	-0.001	-0.000	-0.000
18	0.000	-0.001	-0.000	-0.000
19	0.000	-0.001	-0.000	-0.000

Table 1.5.10

K	A (IN)	B (IN)	A (OUT)	B (OUT)
0	0.000	8.636	-0.000	2.297
1	5.451	0.000	6.883	-0.000
2	0.000	3.582	0.000	2.936
3	-3.272	-0.000	0.856	-0.000
4	-0.000	-2.049	0.000	0.857
5	1.214	-0.000	-0.318	-0.000
6	-0.000	0.710	-0.000	0.004
7	-0.331	-0.000	-0.113	-0.000
8	-0.000	-0.145	-0.000	-0.052
9	0.023	0.000	-0.000	-0.000
10	-0.000	-0.006	-0.000	-0.009
11	0.023	0.000	0.006	0.000
12	0.000	0.023	0.000	0.002
13	-0.020	-0.000	0.000	-0.000
14	-0.000	-0.013	0.000	0.001
15	0.008	0.000	-0.000	-0.000
16	0.000	0.005	0.000	0.000
17	-0.003	0.000	-0.000	0.000
18	-0.000	-0.001	-0.000	-0.000
19	0.000	0.000	0.000	0.000

Table 1.5.11

K	A (IN)	B (IN)	A (OUT)	B (OUT)
0	-0.000	-0.044	0.000	-0.017
1	-14.007	-0.000	-7.854	0.000
2	-0.000	-0.063	-0.000	-0.026
3	-0.751	0.000	-2.301	0.000
4	0.000	-0.018	-0.000	-0.012
5	-0.219	0.000	-0.328	0.000
6	0.000	-0.006	0.000	-0.003
7	-0.130	0.000	-0.003	0.000
8	0.000	-0.002	0.000	-0.001
9	0.010	-0.000	0.007	0.000
10	0.000	-0.001	0.000	-0.000
11	-0.011	-0.000	0.000	-0.000
12	-0.000	-0.000	-0.000	-0.000
13	0.001	0.000	-0.000	0.000
14	0.000	-0.000	-0.000	-0.000
15	0.000	-0.000	0.000	0.000
16	0.000	-0.000	-0.000	-0.000
17	-0.000	-0.000	0.000	-0.000
18	0.000	-0.000	0.000	0.000
19	0.000	-0.000	0.000	-0.000

Table 1.5.12

K	A (IN)	B (IN)	A (OUT)	B (OUT)
0	8.965	4.318	5.104	1.148
1	2.724	5.191	3.441	1.713
2	-1.852	1.791	1.579	1.468
3	-1.636	-0.952	0.428	0.917
4	0.072	-1.025	-0.057	0.429
5	0.607	-0.051	-0.159	0.132
6	0.178	0.355	-0.117	0.002
7	-0.165	0.152	-0.056	-0.031
8	-0.129	-0.073	-0.017	-0.026
9	0.012	-0.082	-0.000	-0.014
10	0.049	-0.003	0.004	-0.004
11	0.012	0.029	0.003	-0.000
12	-0.015	0.012	0.001	0.001
13	-0.010	-0.006	0.000	0.001
14	0.001	-0.006	-0.000	0.000
15	0.004	0.000	-0.000	0.000
16	0.001	0.002	-0.000	0.000
17	-0.001	0.001	-0.000	-0.000
18	-0.001	-0.001	-0.000	-0.000
19	0.000	-0.001	0.000	-0.000

Table 1.5.13

K	A (IN)	B (IN)	A (OUT)	B (OUT)
0	-10.385	-0.022	-5.183	-0.009
1	-7.002	-0.036	-3.927	-0.014
2	-2.615	-0.031	-2.316	-0.013
3	-0.375	-0.019	-1.150	-0.010
4	0.030	-0.009	-0.482	-0.006
5	-0.109	-0.005	-0.164	-0.003
6	-0.143	-0.003	-0.039	-0.002
7	-0.065	-0.002	-0.001	-0.001
8	-0.005	-0.001	0.005	-0.000
9	0.005	-0.001	0.003	-0.000
10	-0.003	-0.000	0.001	-0.000
11	-0.005	-0.000	0.000	-0.000
12	-0.002	-0.000	-0.000	-0.000
13	0.000	-0.000	-0.000	-0.000
14	0.001	-0.000	-0.000	-0.000
15	0.000	-0.000	0.000	-0.000
16	-0.000	-0.000	0.000	-0.000
17	-0.000	-0.000	0.000	0.000
18	0.000	-0.000	0.000	0.000
19	0.000	-0.000	0.000	0.000

Table 1.5.14

$\Delta X = +.01''$	$\Delta Y = +.01''$
$\delta b_1 = +.27''$	$\delta a_1 = +.27''$

$$K_z(\phi) = \sum K_m^{(e)} \cos m\phi + K_m^{(o)} \sin m\phi$$

$$\begin{pmatrix} K_m^{(o)} \\ K_m^{(e)} \end{pmatrix} = -\frac{2B_0}{\mu_0} \frac{a}{b}^{n-1} \begin{pmatrix} -a_n - 1 \\ b_n - 1 \end{pmatrix}$$

The K_n even and K_n^0 stand for the even and odd Fourier components of the distribution. A properly constructed magnet will have a current distribution that is symmetrical about both the horizontal and vertical planes, and hence, one can see from these equations that all of the a_n 's will vanish and only the odd b_n 's will be present.

To complete this model we should include the effects of the iron. However, a separate study shows that to a very high degree of accuracy, the iron contributes only to the dipole field. This is an important effect which we will need when we discuss the ends of the magnet in more detail. Note, however, that since the a_n and b_n are all normalized to the field on the axis, that if the iron changes the dipole field, the a_n and b_n will be decreased by the amount the dipole field is enhanced. At 45 kilogauss Snowdon's calculations shows that 18.64% of this central field arises from iron.

1.6 We give here an outline of the following sections of this report:

2. Limits Set for Mechanical Tolerances
3. Room Temperature Measurements
4. DC Harmonic Analysis
5. AC Harmonic Analysis
6. Stability of Magnets
7. AC Losses
8. Short Sample Tests

3. Room Temperature Measurements

As we have discussed previously it is necessary to have some type of feed-back control on the coil assembly procedure. This feed-back is provided by means of the room temperature measurements that will be described here. We have developed the facility to make measurements of the gradient of the field in the coil at room temperature immediately after the coil is collared. These measurements will be shown to correlate well with the later measurements that are made when the coil is in its cryostat and yoke. We achieve two benefits from this measurement:

1. immediate knowledge is necessary in order to correct systematic errors in coil production,
2. quality control of the coil before it is completely finished.

The first allows us to monitor the effect of all of the errors that can creep into the coil production such as small systematic changes in wire size, the tooling aging, systematic changes in the insulation of the coil and so forth.

We emphasize here that a coil can not be corrected after it is manufactured, although, some thought has been given to a dynamic type of feedback that would correct individual coils as they are manufactured. This led to the invention of the so called key lock type of collar where a loose wedge is driven to set the key angle after the coil has been collared. We feel that such coil-by-coil correction will not be necessary and it needlessly complicates the manufacturing process, but the concept is interesting. If coils of much higher accuracy were required, it would be possible to collar the coil and then correct its field afterwards by slightly changing the key angle.

The second gain that we make by room temperature measurements is that we are able to predict whether a coil has such gross errors

that it will be unsatisfactory as a final product. Thus, if a coil does not come up to standards, it can be aborted at this point of the manufacturing process, and the costs involved in assembling it and the cryostat can be saved.

The techniques involve measuring the field gradient in the coil to less than one part in 10^4 at room temperature. The measuring system that has produced the results that we shall shortly discuss has been developed with enormous persistence by R. Peters, and the coils have been constructed by M. Kuchnir with great patience.

3.1 Method

Figure 3.1.1 shows the technique that is used to make these gradient measurements. Each coil is over 22' long and stretches completely through the magnet. There are 12 such coils, and their center-to-center spacing is .215". The difference in the voltage between coils is either integrated if the magnet is pulsed to about 100 amps, or alternatively a lock-in amplifier is used and the magnet is excited to about 10 amps at 11 hz. The later measurement technique has supplied all of the data in this report and seems to be the best technique.

These coils have been made by stretching thin tungsten wires over precision pins. A stainless steel tray is located very close under the wires and after the wires have been stretched, this tray is filled with a room-cure epoxy. It has been verified that the eddy currents in the tray do not effect the results. The whole coil is then inserted in an oval bore tube that can be slid in and out of the magnet bore. The clearances are rather small and the bore tube simply rests inside of the coil bore. The fit is such that its x position is probably determined to ± 50 mils and its y position to better than $\pm .1$ ".

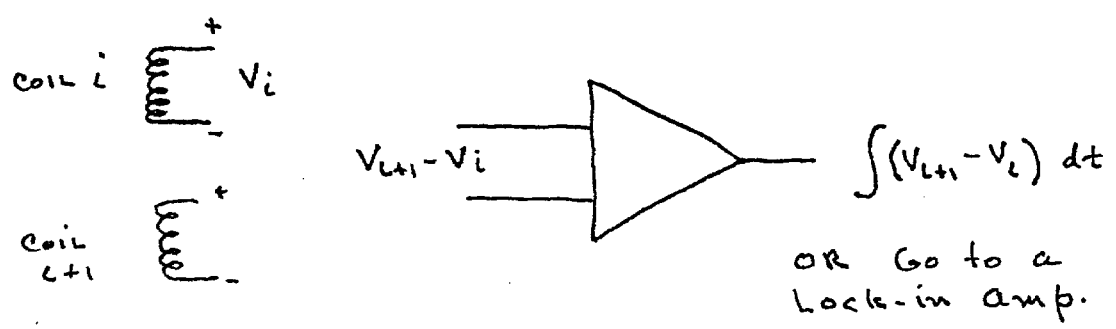
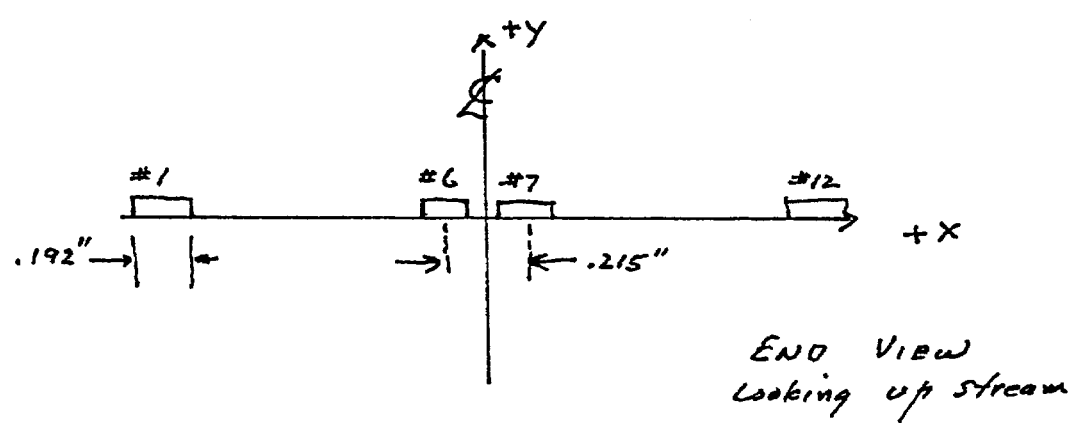
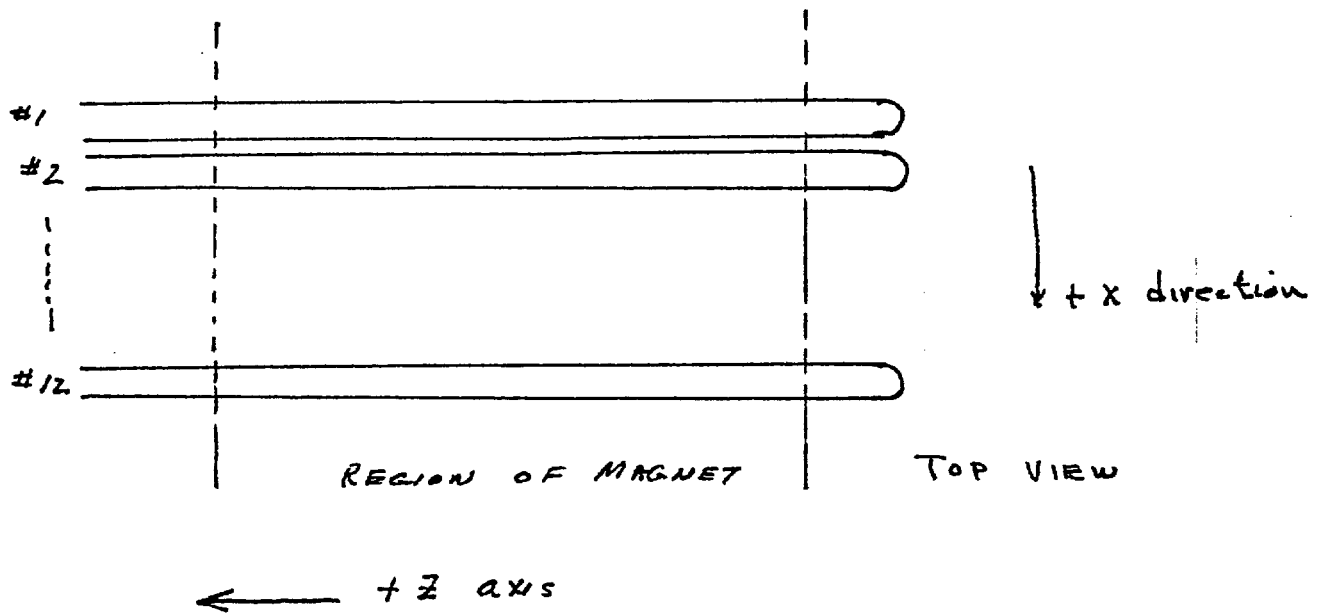


Figure 3.1.1

The ends of the coils are then collected together on twisted pairs and brought to a switch. The switch allows the difference voltage between any two adjacent coils to be applied to the input of a lock in amplifier that is operating at 11 cycles. The magnet coil is driven with about 10 amps of current at a frequency of 11 hz. If the coils were ideally perfect the difference voltage would be proportional to the gradient of the field inside of the magnet.

Consider now one of the harmonics of the field given by b_n using the diagram shown below.

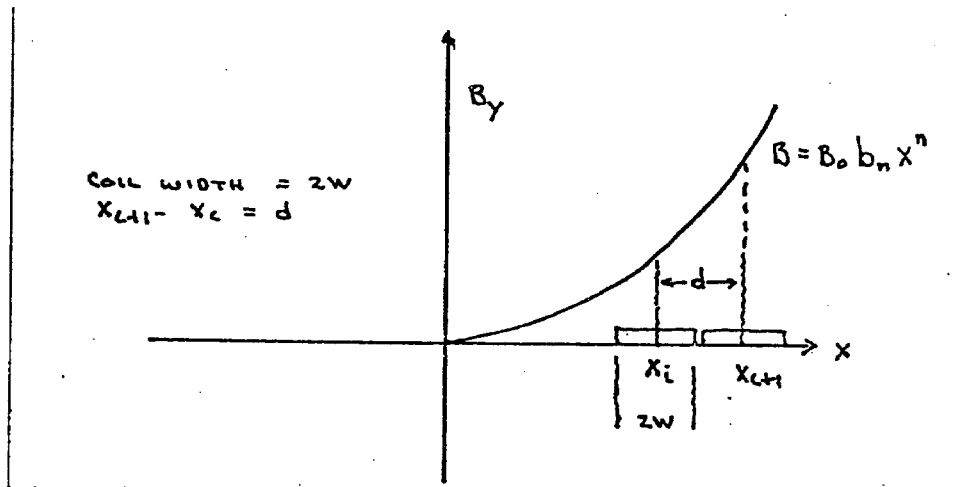


Figure 3.1.2

We can integrate the flux of this harmonic over a pair of coils and calculate its difference. The result is the following equation where the coordinates have been labeled in the diagram.

$$F(i) = \frac{B_0 b_n}{n+1} ((X + W)^{n+1} - (X - W)^{n+1})$$

$$F(i) = \text{Flux through } i^{\text{th}} \text{ coil from harmonic \#n}$$

If we choose one of the loops as a standard and divide by that voltage then we have an answer that is given in the following equation.

$$\frac{F(i+1) - F(i)}{2B_0 W} = \frac{.5b_n}{n+1} \{ (x_{i+1} + W)^{n+1} - (x_{i+1} - W)^{n+1} - (x_i + W)^{n+1} + (x_i - W)^{n+1} \}$$

We see in this equation the difficulty that arises with this type of measurement, and that is that although the induced voltage is proportional to the difference of the field at the centers of the two coils, it is also a function of the dimension of the coils. Thus, we can not distinguish between a gradient in the field and a difference in the area of adjacent coils. It was rapidly realized that one could not match the areas of the coils to one part in 10^4 which is a typical magnitude for the b_n 's that we wish to measure. As a result we decided that it would be necessary to calibrate the coils in a uniform field. As yet this has not been done. In fact, for the two primary goals of this measurement it is not necessary since even with a coil whose individual loops have various areas, we can monitor the constancy of the output of the factory, i.e., if all of the coils are stable, they will give the same pattern of the difference voltages. Many studies of repeatability and struggles to eliminate the noise in this system have resulted in measurements that are reproducible to the accuracy that we require. However, it was felt that some type of calibration of the instrument would be desirable. That is, if we see a deviation occurring, how big is it and does it correlate well with the field that will eventually be measured in the completed magnet?

3.2 Calibration

In order to make the room temperature measurements quantitative, we have attempted to calibrate them by means of using the fields of the magnets we measured in the MTF. The steps of this calibration are as follows.

1. Magnets #109 through #128 were selected as a set of normalization magnets (magnets #112, 122, and 125 were not included).
2. The room temperature measurements for this set of magnets was averaged.
3. The measurements made at the MTF on the same set of magnets were also averaged. The measurements used were those made at 2,000 amps and the values as integrated through the magnet were the ones selected.
4. The MTF values are corrected to what the reading would be with no iron and room temperature.
5. A comparison is made between the two averages so obtained, and a correction for each pair of coils is calculated.
6. This correction then effectively cancels the built-in differences of the coil areas and allows us to get absolute values of the gradient of the magnet.

The last two steps need to be discussed. First of all, as mentioned in Section 1, the multipole fields in gauss except for the sextapole, are the same with and without iron. The iron changes the dipole field by a factor of 1.23. However, since all of the multipole coefficients are normalized to the central field, when iron is placed around the magnet all of the coefficients will be decreased by a factor of 1.23. Thus, the room temperature measurements and the MTF measurements must be corrected by this ratio. In addition, the iron adds a sextapole component to the field. The relation between the cold and room temperature coefficient is:

$$\begin{aligned} b_n \text{ (cold)} &= b_n \text{ (room temp)} / 1.23 & n \neq 2 \\ &= (b_2 \text{ (room temp)} / 1.23) + 6.22 & n = 2. \end{aligned}$$

There are some other discrepancies that the calibration procedure covers up. The first is that the room temperature measurements are made without iron, and if the iron is off axis, it can induce a quadrupole moment (See Table 1.5.14). This quadrupole error will be built into the calibration of the room temperature measurements. However, the effect is probably small since the induced quadrupole moment from an off axis displacement of 1 mil is only 0.2 units, and we have normalized to an average over 14 different magnets. If there is a systematic effect from the yoke it will show up as an error in the RT calibration.

Two other effects are the preresistant currents in the superconductor and distortion of the coils where they are energized. For both of the reasons we have chosen 2,000 amps as our appropriate comparison point. At this level the preresistant currents change the sextapole moment by less than 1.2 (decrease) and the forces which are proportional to I^2 are only 1/4 their final value and, therefore, have made negligible distortion of the coil package.

We now display in Figures 3.2.1 to 3.2.2 a set of representative room temperature measurements. The first figure shows representative sets of magnets included in the range of #110 to #128 that were used for calibrating the measuring coil. It should be emphasized that the comparison only required that these curves agree in an average sense. The fact that fluctuations are well reproduced is an indication that the measurement is working well. The last Figure includes magnets outside of the calibration range and it is seen that the rather large changes in sextapole moments of these magnets which are

picked past #130 is well represented by the measurements. In these curves the circle is the result of the room temperature measurement and the asterisk is the predicted number as measured at MIT for the completed magnet.

The room temperature measurements were the first to show up an error in magnet construction near magnet #130, and this case represents a nice example of the way that room temperature measurements will be able to monitor the quality of the coil assembly. As we will see in Section 4 some place around magnet #125 we suffered from a defective shim in the magnet. Due to the time lag between when the coil was formed and when the magnet was completed and assembled in a cryostat, this defect was not discovered immediately. However, we had at this time, started the program of making room temperature measurements. Figures 3.2.3 and 3.2.4 show a pair of coils, one suffering from a crushed key and the other properly assembled. It is seen that the room temperature measurements indicated that a trouble existed in the coil. If we had understood the room temperature measurements well enough at the time, this would have enabled us to eliminate the defect immediately. Instead, the defective part has probably been built in to about 15 coils.

In order to use the room temperature measurements in a quality control program, it is necessary that we place limits on what is acceptable in a measurement. We will see in Section 4 the only harmonics that vary with magnet construction are the ones up to decapole, and since the only terms to which the room temperature measurement is sensitive are the normal series of b_n 's. We see that the room temperature measurements is

monitoring the four coefficients $b_1, b_2, b_3,$ and b_4 . However, an examination of the shape of the curves in Figures 3.2.1 to 3.2.4 shows a rapid change at the outer coil due to the higher multipoles that are being measured. Since these higher multipoles do not change, it would be useful to subtract their calculated values out of the measurement in order to display the lower order harmonics more clearly.

To do this, we chose the field given by:

n	b_n
6	3.69
8	-12.79
10	4.56
12	- 1.24

The calculated response of the RT coils to this field is subtracted from the actual measurement and some typical results are given in Figure 3.2.5. Comparison with figures 3.2.1 shows that the subtractions is at least a qualitative success.

In order to investigate the success of this procedure, we have analyzed all of the magnets measured at both room temperature and at the MTF. The RT measurements are treated in the following fashion. First the two sums are formed.

$$E(X) = 1/2 (F(X) + F(-X)) \quad 6 \text{ points}$$

$$O(X) = 1/2 (F(X) - F(-X)) \quad 5 \text{ points}$$

A least squares fit is the mode using:

$$E_F(X) = B_1 + B_3X^2$$

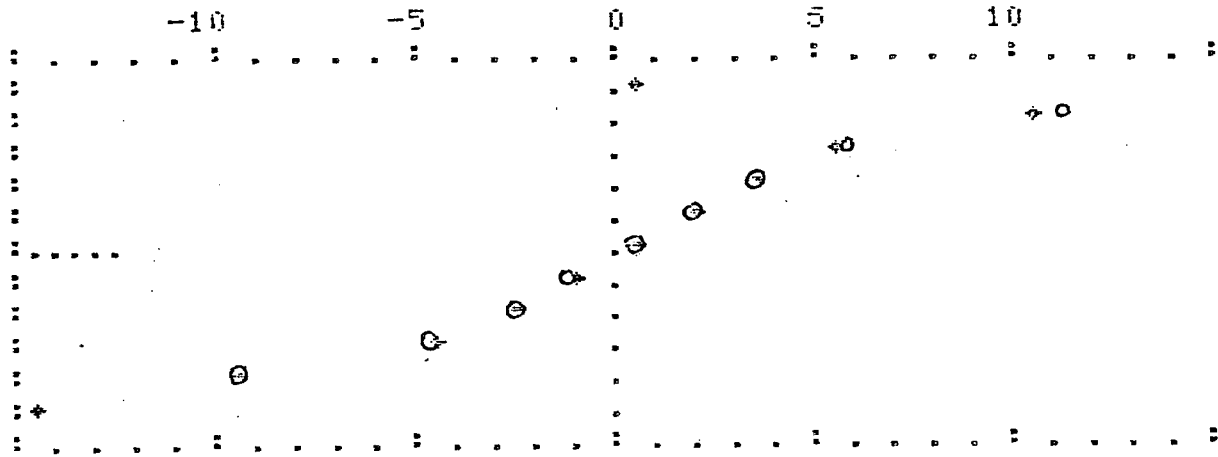
$$O_F(X) = B_2X + B_4X^3$$

B_1, B_2, B_3 and B_4 are directly related to b_1, b_2, b_3, b_4 .

MAGNET#RHA111 2000

COLD PREDICTIONS

26.12	10.40	5.36	3.41	1.89	0.34
-1.18	-2.63	-4.48	-9.59	-27.18	



MAGNET#PBA123 2000

COLD PREDICTIONS

18.61	5.39	1.83	0.96	0.27	-0.57
-1.39	-2.01	-2.67	-5.63	-18.48	

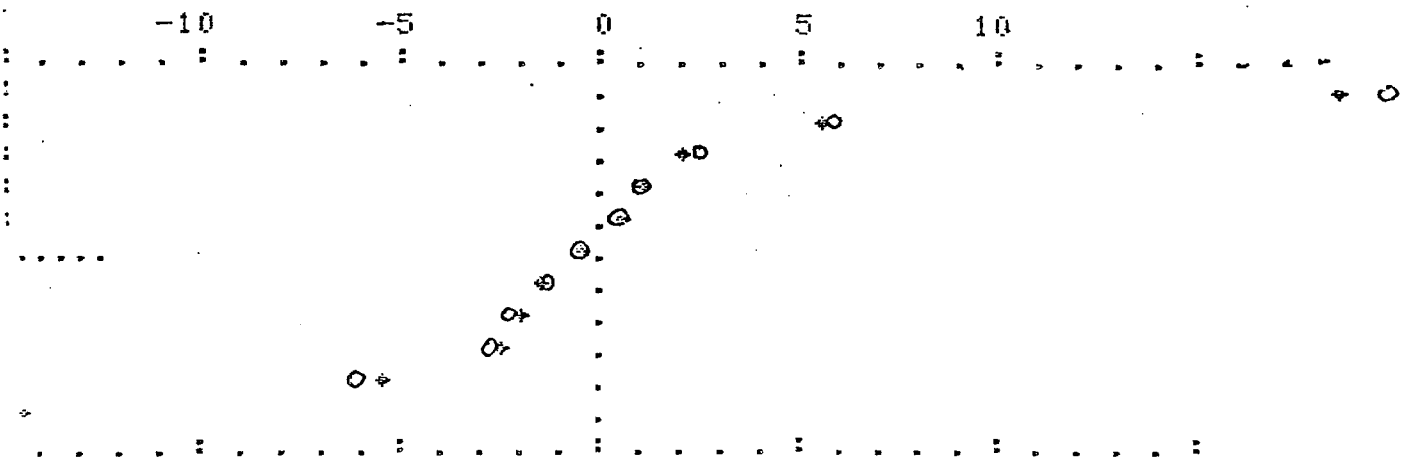
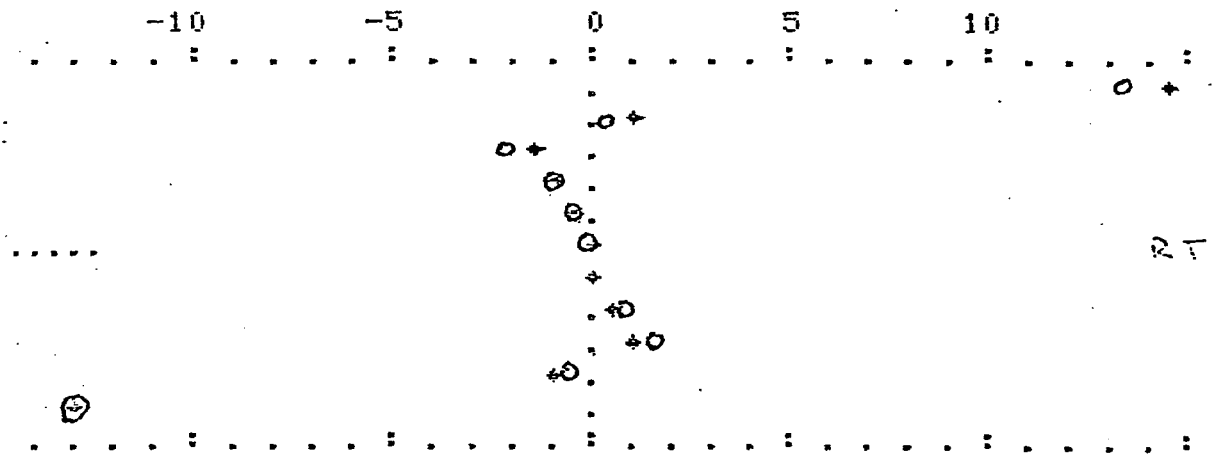


Figure 3.2.1

MAGNET#PCA148 2000 *05*
 OLD PREDICTIONS
 14.69 1.04 -1.31 -0.98 -0.53 -0.25
 0.06 0.60 1.13 -0.30 -13.23



 MAGNET#PCA131 2000
 OLD PREDICTIONS
 14.31 2.07 0.03 0.29 0.46 0.38
 0.39 0.82 1.60 0.65 -8.45

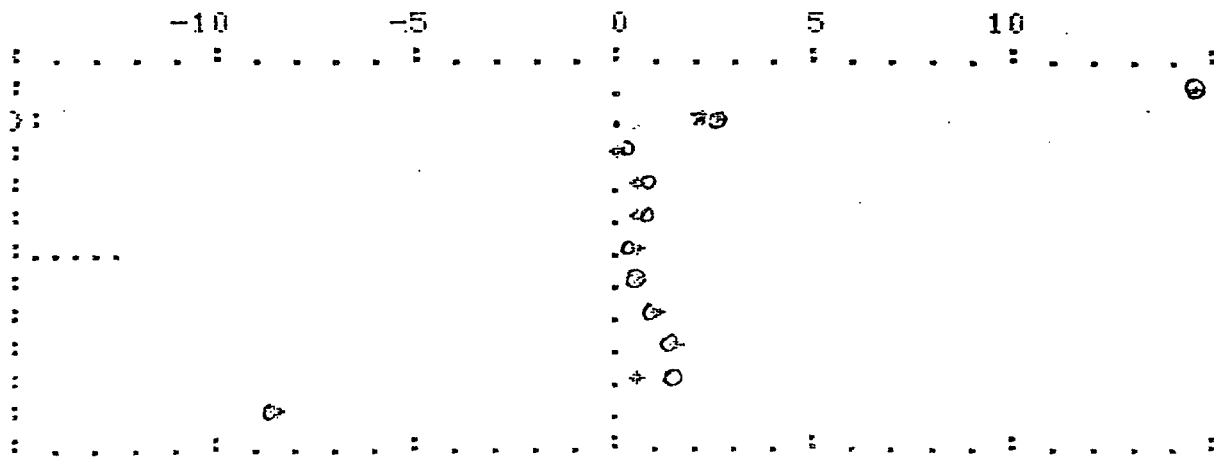


Figure 3.2.2

MAG.# 142

C

12.18	-0.15	-2.45	-1.42	-0.50	-0.02
0.80	2.11	2.88	0.73	-12.47	

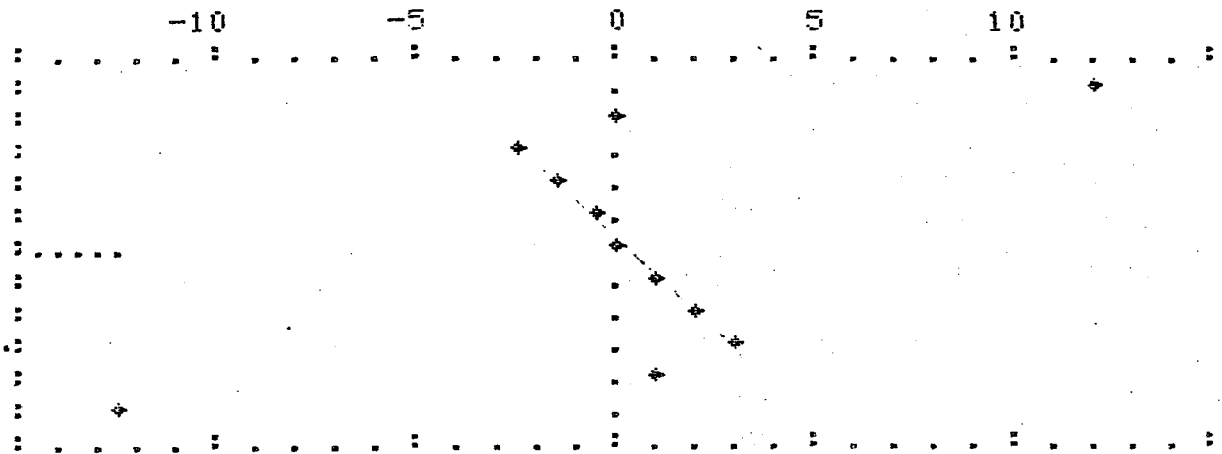


Figure 3.2.3: Normal Irrigation Channel.

MAG.# 143

C

14.27	3.65	0.97	1.59	0.75	0.63
-0.13	-0.17	-0.09	-1.85	-14.83	

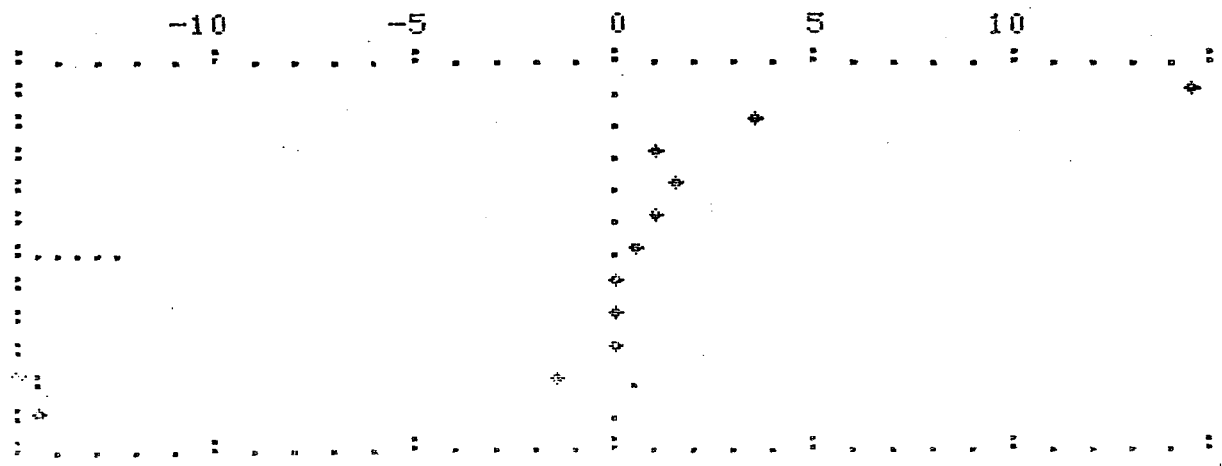
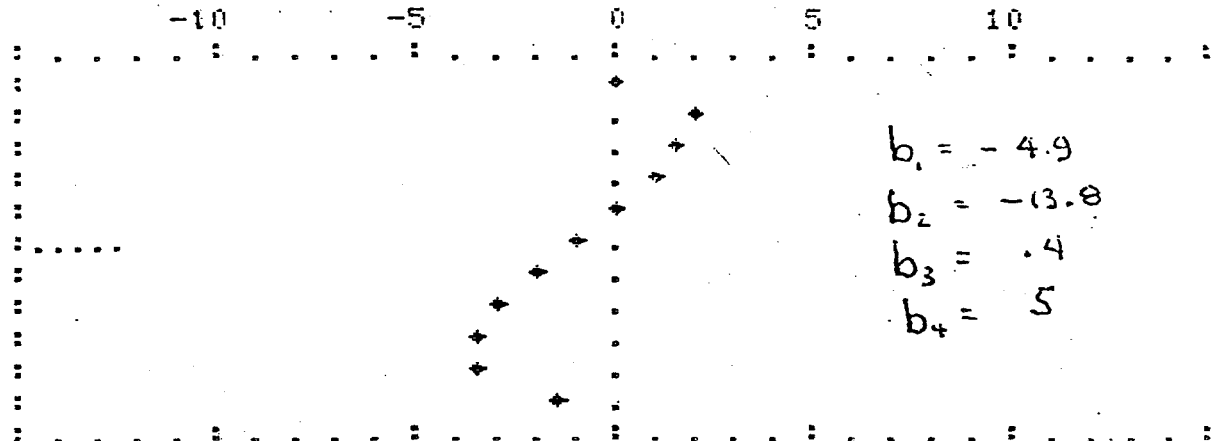


Figure 3.2.4: Crushed Irrigation Channel.

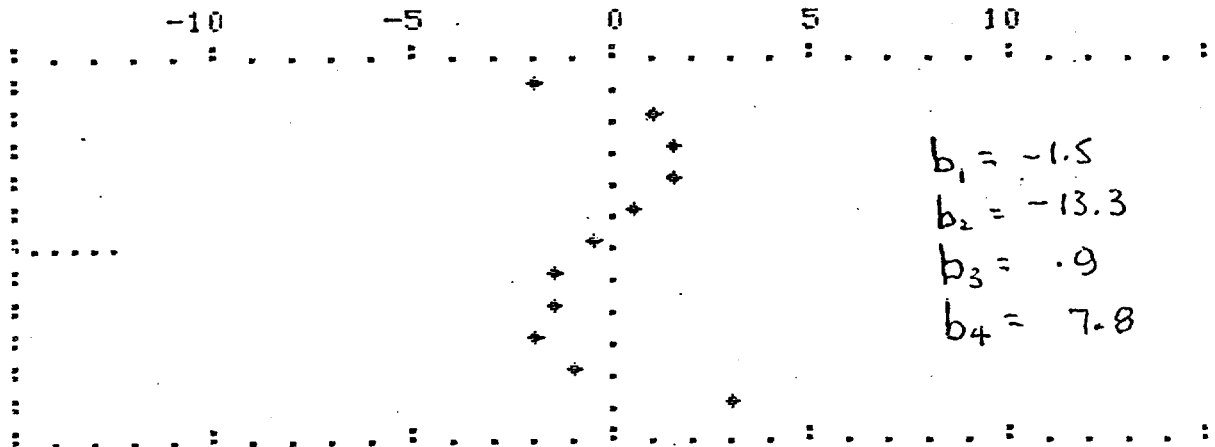
MAG.# 129

0	0.00	2.02	1.40	1.16	-0.01	-1.02
	-2.09	-3.20	-3.43	-3.44	-1.66	



MAG.# 130

0	-2.03	1.08	1.57	1.55	0.70	-0.25
	-1.51	-1.50	-2.07	-1.14	2.90	



MAG.# 104

0	7.46	6.78	5.04	3.46	1.95	0.47
	-1.40	-2.82	-4.61	-5.87	-9.60	

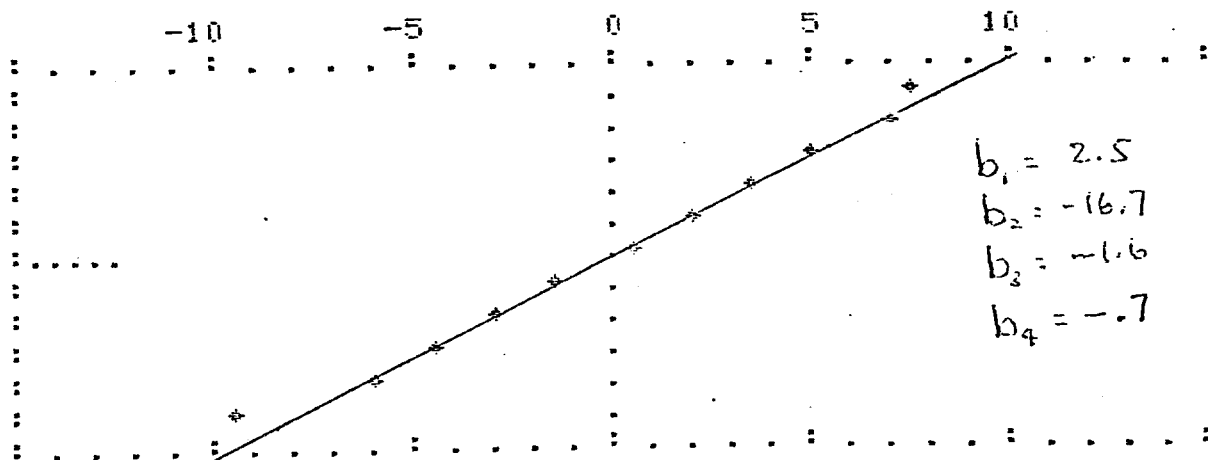


Figure 3.2.5

If the RT measurements are correct, we should be able to compare with the same coefficients as measured at MTF. Figures 3.2.6 through 3.2.9 show the comparison on magnets #101 to #149 of the first four b_n .

First, lets consider b_1 . There is clearly a correlation of the two numbers, but there is also a spread outside of the measurement errors. Remember that the normalization only requires that the average b_1 of magnets #110 to #128 agree for the two measurements. Correlations between the two sets of numbers are significant and not the result of normalization. However, also we must take into account that the RT b_1 is measured without iron and that the MTF b_1 is with iron. If we assume that the measurement errors are small, then we have discovered a measurement that is sensitive to the accuracy with which the magnet coil is centered in the yoke. The two displaced 45° lines contain most of the magnets. These lines correspond to a displacement of ± 5 mils of the coil axis from the yoke axis and give roughly a one σ effect.

Next, we examine b_2 , b_3 , and b_4 . The agreement of b_2 is quite nice, and will serve well to control the sextapole moment. The correlation plot for b_4 is some what worse and b_3 looks pretty rough. I have not yet examined the least squares program to see why there is so much difficulty. However, it is worth noting that the RT coils is merely placed in the bore of the magnet. Figure 3.2.10 shows the results of a calculation by R. Peters of the effect of the coil being misplaced by $\pm .1$ " and $\pm .05$ ". This error would upset the measurement of b_4 . Similarly x displacements would undermine the determination of b_3 although averaging the values for positive and negative x

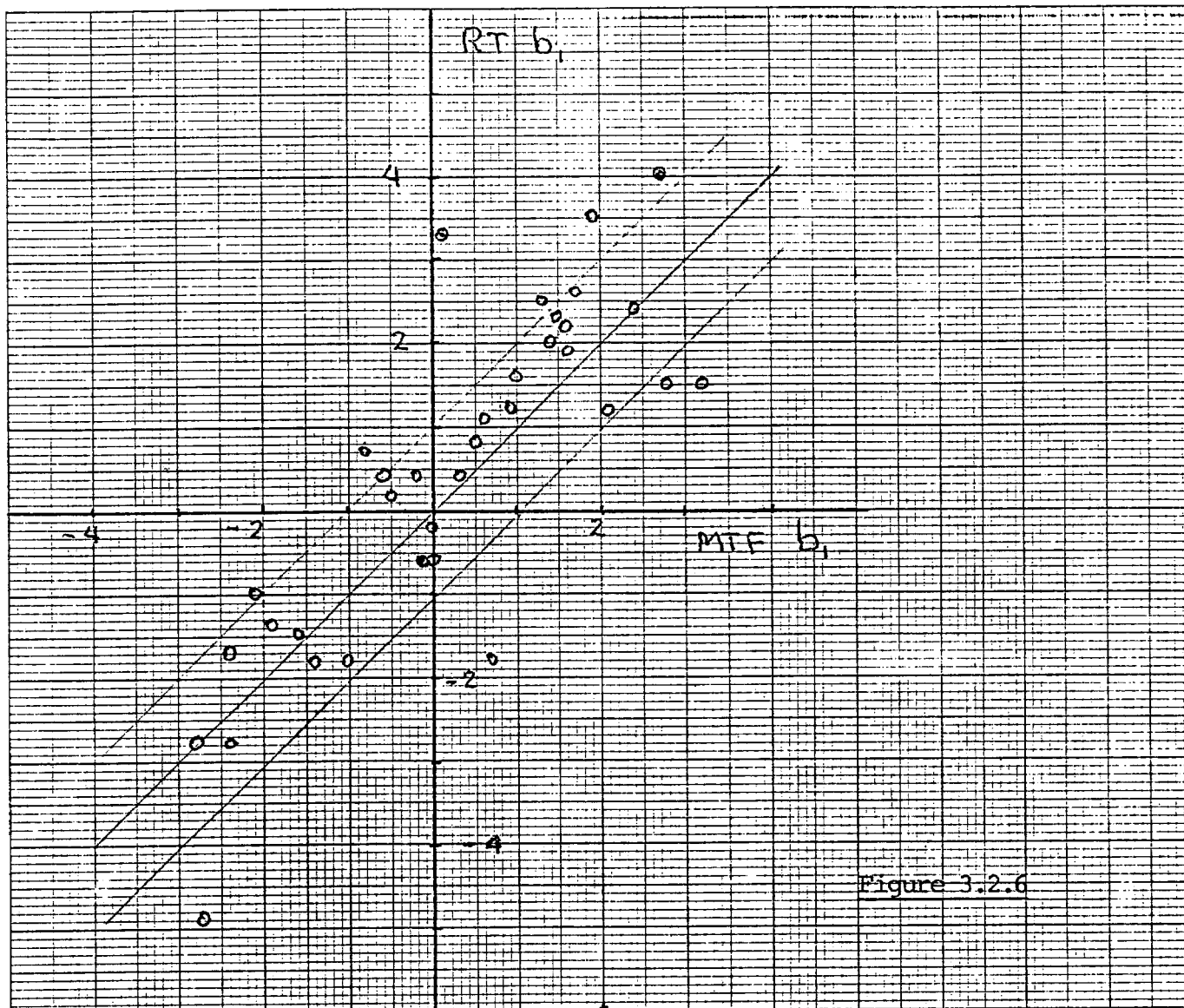


Figure 3.2.6

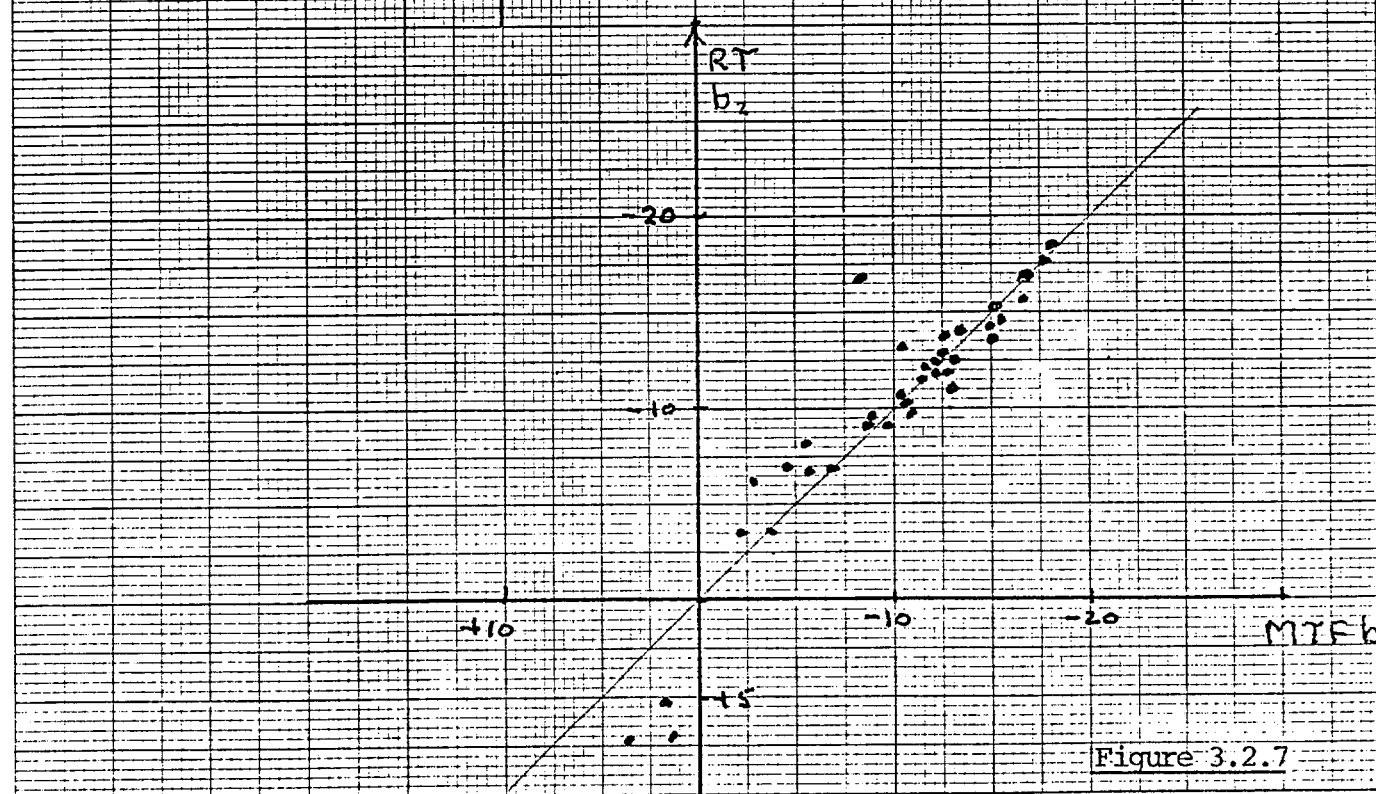


Figure 3.2.7

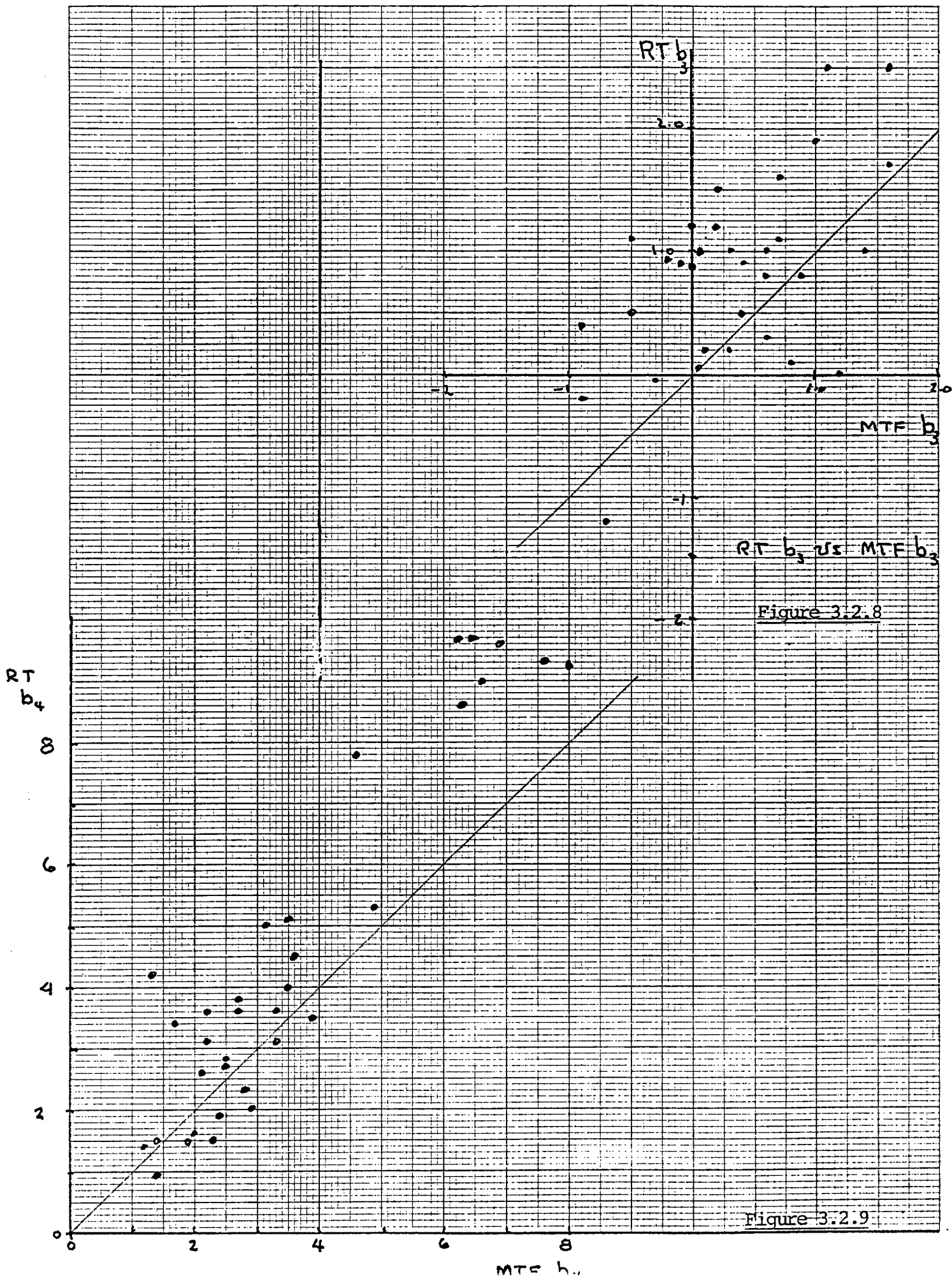


Figure 3.2.8

Figure 3.2.9

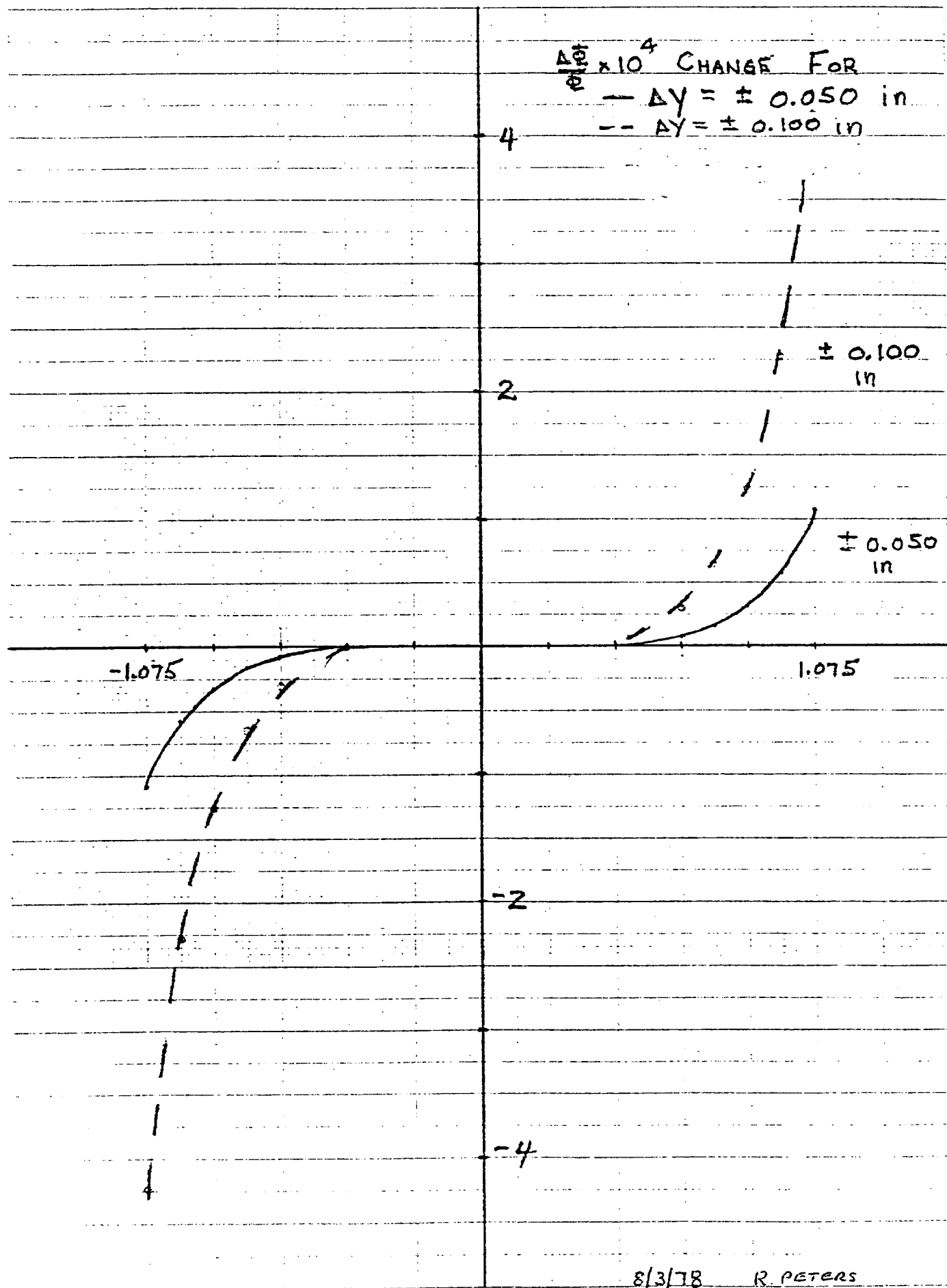


Figure 3.2.10

reduces the impact of such displacements. More work is needed here. One additional source of noise is an unexplained fluctuation of the differences of coils #7, #8, and #9. The smoothness of the curve is always better for the -x coils. A new measuring coil is being constructed to try and eliminate this effect.

In the next subsection we will propose limits for an acceptable magnet when it has a RT measurement made.

4. DC Harmonic Analysis

After the magnet is completed and assembled in its cryostat, it is moved to the Magnet Test Facility (MTF) where it is connected to a 1,500 watt refrigerator and cooled for its final verification. We will discuss here the DC harmonic analysis that is carried out. This measurement is made by means of an 8 foot long coil. The coil consists of two planar loops located at different radii. The magnet current is held at a constant value and the coil is rotated. The two loops which have nearly the same area are balanced against each other to cancel out the dipole component. A Fourier analysis is made of the difference of the induced voltage between the two coils. Since the coils are located at different radii, the difference in induced voltage is a measure of the higher harmonic content of the magnet. Since the coils measure out to about 1", the field every place within the useful aperture is determined.

It should be noted that it is dangerous to extrapolate to radii much larger than 1". This is because these higher harmonics are multiplied by large powers of x^n , and hence, for instance, the 30th pole which is rather poorly determined can rapidly become very much more important in its influence than any of the remaining terms, which are accurately measured. For instance at 1.2", $x^{14} = 12.8!$ However, remembering the theorems on multipoles that were mentioned

in Section 1 and that the 30th pole is only a fraction of a gauss at 1" while the central field is 45 kilogauss, it is clear that we have a very well determined field within the aperture that the beam will occupy. If it is necessary to use fields outside of the 1" radius in order to follow beam trajectories during extraction or injection it would undoubtedly be wise to use the calculated values for the multipoles above the 22-pole rather than the measured values. There is no reason to believe that these harmonics have other than their calculated values.

Since the coil that measures the field is only 94" long and the magnet has an effective length of 254", it is necessary to make three measurements in order to measure the field through the whole magnet.

In Section 4.1 we will discuss in detail how these three measurements are joined together in order to get this integrated structure for the whole magnet.

4.1 When the magnet is measured a warm bore is inserted into the beam tube, and the measuring coil rides within this tube. Its position is difficult to survey in an absolute sense. We therefore, had to develop a means of locating this coil without trying to survey it by some optical technique. We can explain this technique by means of the following simple example: Suppose there is only an 18-pole term present and suppose that the origin is displaced by an amount Δx . We can then expand the new multipole structure as is indicated in the following equation:

$$b_y(x) = b_8(x + \Delta)^8 \approx X^8 + 8\Delta b_8 X^7 + b_8 \Delta^8$$

We see that a displacement in the x direction has generated a

complete set of multipoles from 18-pole down to dipole. However, to first order in Δx , we have only generated a 16-pole term. We now invert this procedure and instead of calculating the 16-pole from the displacement, calculate Δx by assuming that the entire 16-pole measured is generated by a displacement coupled with the strong 18-pole naturally present in the magnet. This would then give the following first approximation for displacement.

$$\Delta x = \frac{b_7}{8b_8}$$

A similar equation exists for Δy , i.e., the 16-pole skew term a_7 can be generated by a displacement in y from the normal term.

We have pursued this line of reasoning and have investigated determining the center from measurements by using the 18-pole and as a first approximation setting the 16-pole skew and normal terms equal to 0 in order to generate a Δx and a Δy . We have also examined using as a driving term the 22-pole and setting to zero the 20-pole terms.

Δx and Δy are generated in the linear approximation, however, the transformation for the set of multipoles by Δx and Δy is done in an exact manner except for the fact that one has to neglect all of those multipoles above 30 which have not been measured. Since the calculated values for these multipoles are negligible within the region that we are working, we feel that this is a valid approximation.

In order to correct for the probe centering then the following program is carried out:

1. The Δx and Δy are calculated using the 18-pole normal component as a driving term and setting the 16-pole normal and skew terms equal to zero. The values for these terms at 4,000 amps are the ones that determine Δx and Δy .

2. Keeping Δx and Δy fixed at the above value the whole set of harmonics at all of the measured currents are translated to the new coordinate center making an exact transformation neglecting only those multipoles above 30. (See a note by S. Ohnuma for a description of the program used.)

Note that this gives a set of measurements that is basically centered on the sharp corners of the coil as determined by the collars and not necessarily the point in the magnet where the slope of the field is zero. This is determined by the quadrupole and octupole components and may or may not coincide with the center as we have just determined it.

The same x and y value is used for all of the currents at one z location since the coil has not moved between these measurements. However, the coil is moved when different z positions are measured and hence Δx and Δy may be different for these other positions. There are three sets of data to be corrected as described above; two for the ends, plus a center measurement. When the corrections have been made, a proper weighted integral through the magnet is generated for each harmonic and each current. As the coil positions slightly overlap, a complete integral for the magnet is accurately generated. Since we have measurements of the two ends and the center separately we can abstract the behavior of the end fields as differentiated from the body field of the magnet. These measurements will be discussed in a section on ends below. The amount that the measuring coil is inserted in the magnet is recorded automatically in terms of the voltage induced in it by the dipole component field as it is rotated, and these numbers are used to make the weighted integral.

We can now examine the effects of shifting the coordinates. Figures 4.1.1 and 4.1.2 display the consistency of Δx and Δy

as generated by the 18-pole term and the horizontal axis displays Δx and Δy as calculated using the 22-pole. It is seen that within about ± 15 mils these measurements are consistent with each other. It should be noted that the underlying assumption made is that there is no natural 16-pole or 20-pole component in the magnet when we calculated Δx and Δy . Hence, the fact that these two methods of calculation do not agree is a reflection of the fact that there is some natural 16- and 20-pole component present in the coil structure due to small asymmetries in the construction process. The spread in x and y from these two measurements is consistent with the 16- and 20-pole terms being an order of .1 to .2 in value.

Let us now examine what effects these shifts have on the multipoles. Figure 4.1.3 shows the a_n as a function of N as measured in the raw data. A very strong 16-pole term at $N = 7$ is seen as well as terms at $N = 5$ and $N = 9$. The data in this curve and the following curves are for the central field at 2,000 amps. The shift in this particular case was calculated from the 3,000 amp data, although the normal procedure is to use the 4,000 amp numbers. Also the coefficients displayed have been averaged over a set of magnets from number 110 to number 128. There are 16 magnets in this set with number 112 and 125 missing. During this period of construction the assembly of the magnet was kept fixed, no intentional changes were made. Hence, this data set can be used to estimate what the random errors are in the construction process. The same set will be used as a control in the rest of this study. The error bars in Figure 4.1.3 indicate the rms spread generated by averaging over the set of 16 magnets. Figure 4.1.4 shows the corresponding set of b_n

as measured also at 2,000 amps. Here the very strong 18-pole at $N = 8$ is evident as are also the decapole 14-pole and 22-pole terms at $N = 4, 6,$ and 10 . We next look at Figure 4.1.5 which shows the values of a_n after they have been shifted using either the 18-pole term as a driver or using the 22-pole terms as a driver. This data is shown in Figure 4.1.5. One can see that there has been a dramatic reduction in the set of errors driven by the larger multipoles in the normal expansion. Except for the skew quadrupole and octapole all of the terms are small and, in general, above the decapole have a value consistent with zero for an average and a spread of $\pm .5$. This curve then represents one of our first important results, namely, it gives the noise spectrum of the skew symmetric harmonics of the magnet. Since the error bars are all large compared to the average value of the terms, we assume that there is no systematic skew error being made in the manufacturing process. This statement does not apply to the skew quadrupole and sextapole terms, and we will discuss these separately.

Figure 4.1.6 gives the average over the 16 magnets for the shifted b_n . The terms $b_1, b_3, b_5,$ etc., should be missing. By symmetry the errors of these terms are comparable to that for the a_n for $n \leq 5$. The black squares are the values that are calculated by S. Snowdon. Except for the sextapole, the values agree well. As will be explained later, the geometry of the key angles was incorrect, and hence, the sextapole is wrong. It is seen that the major fluctuations occur in $n = 1$ to 3 as was the case for the a_n . Our major concern will be with these low harmonics.

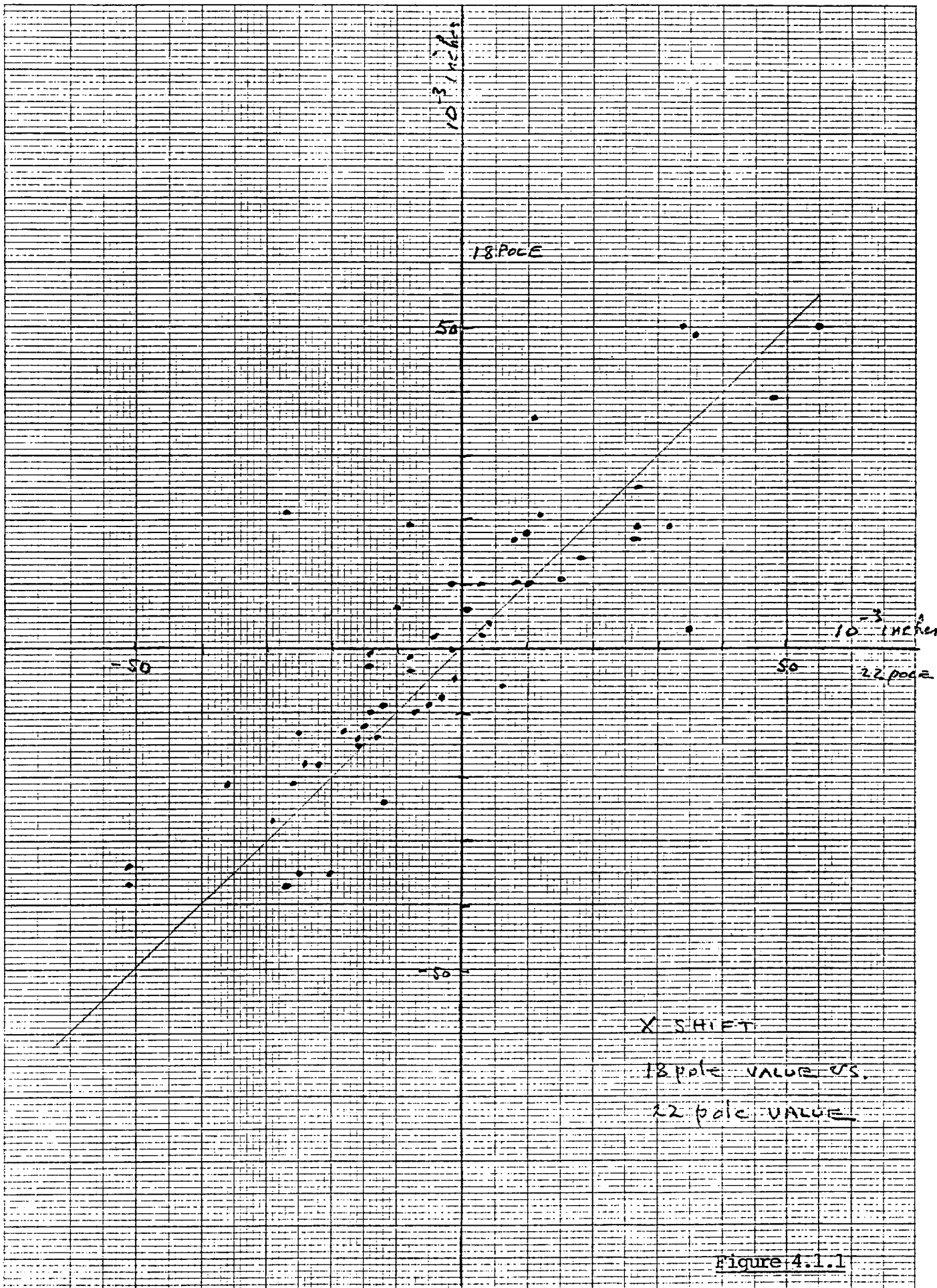
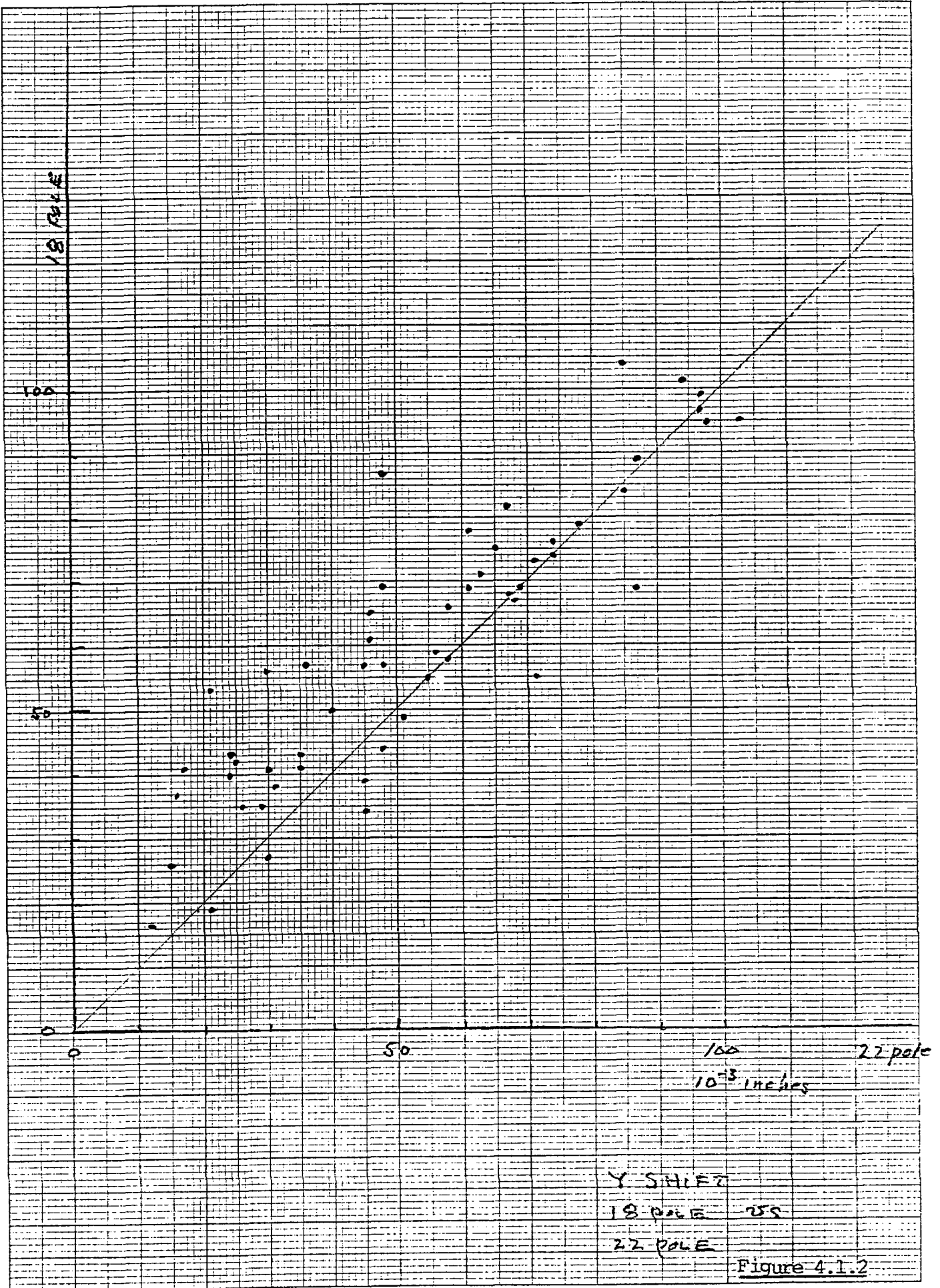


Figure 4.1.1



UNSHIFTED A_n vs n .

$I = 2000$ Amcs

$\frac{SB}{B} \times 10^4$

5

0

-5

n

15

A_n

$$B_x(x) = B_0 \sum A_n x^n$$

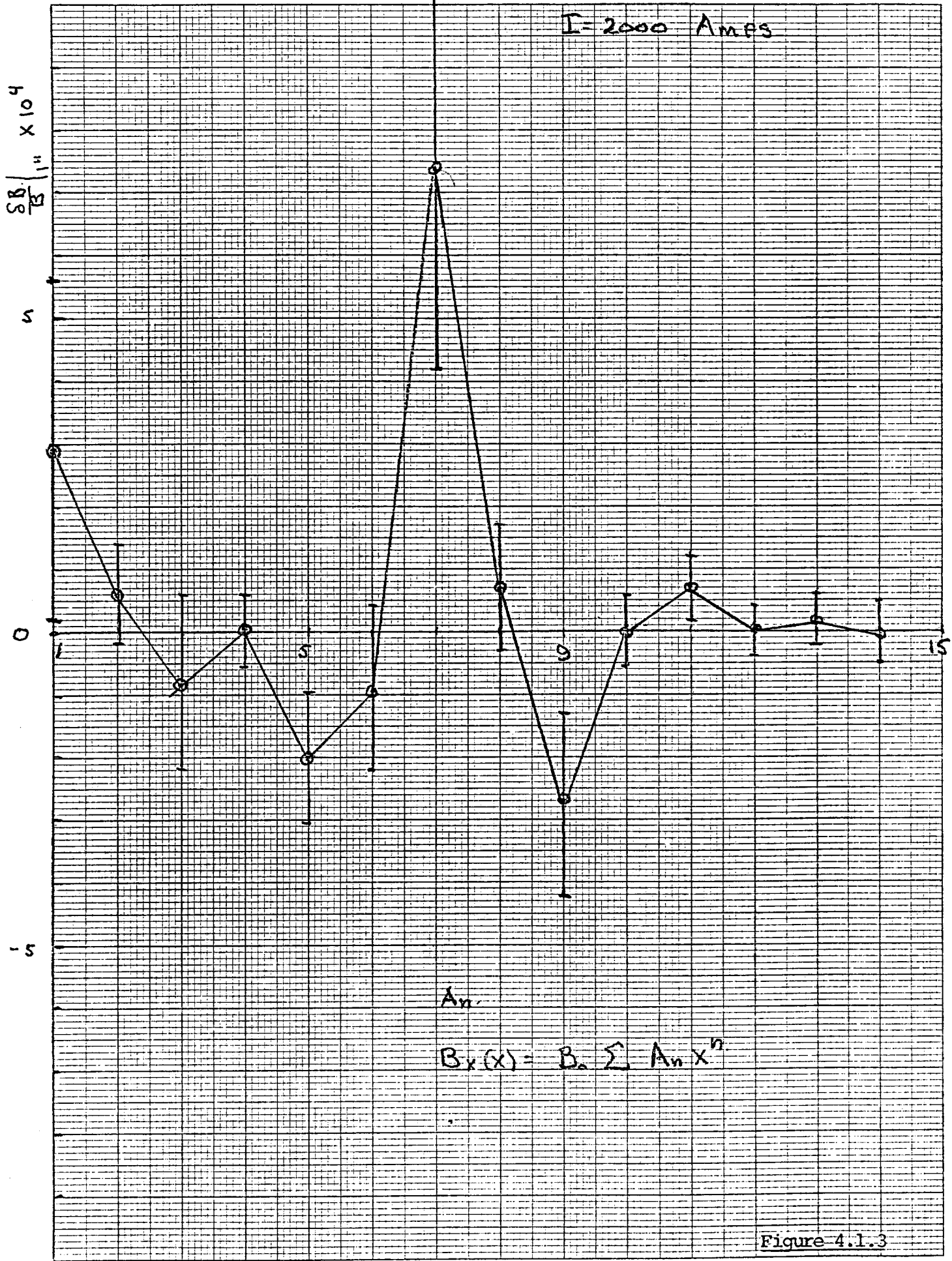
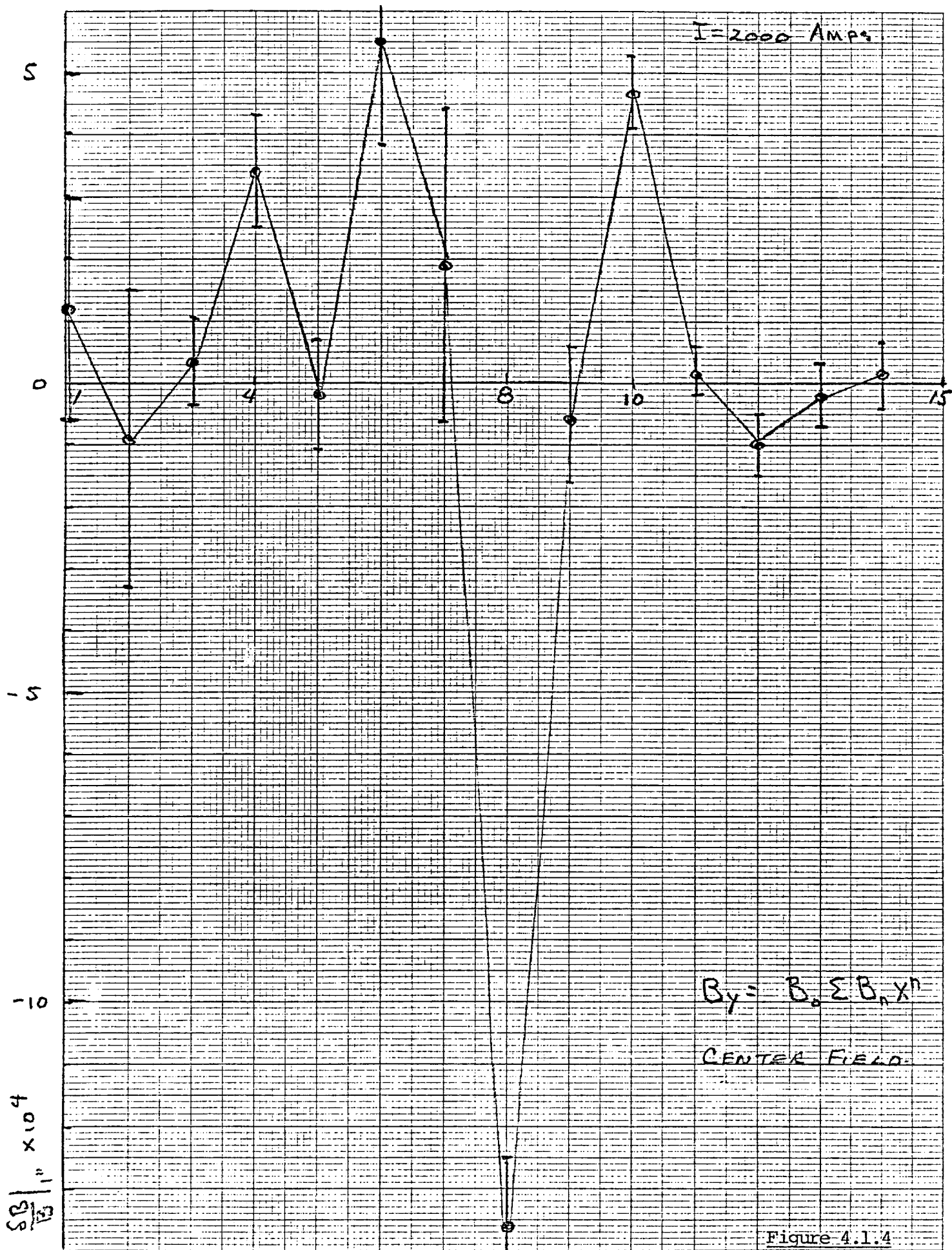


Figure 4.1.3



$I = 2000 \text{ AMPS}$

$$B_y = B_0 \sum B_n X^n$$

CENTER FIELD

Figure 4.1.4

A_n SHIFTED

18 POLE DRIVER
FOR S_x, S_y

22 POLE DRIVER
FOR S_x, S_y

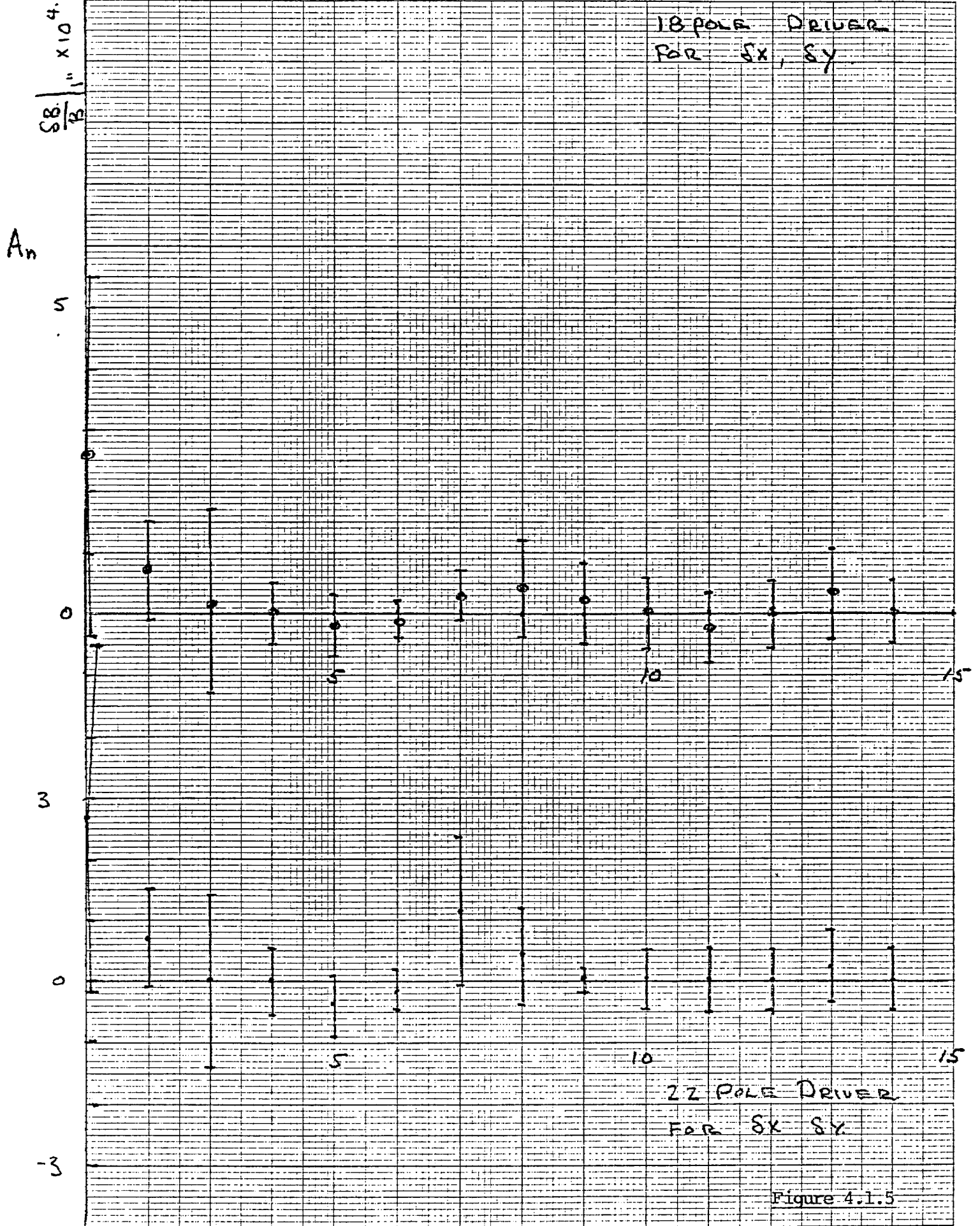


Figure 4.1.5

I = 2000 AMPS

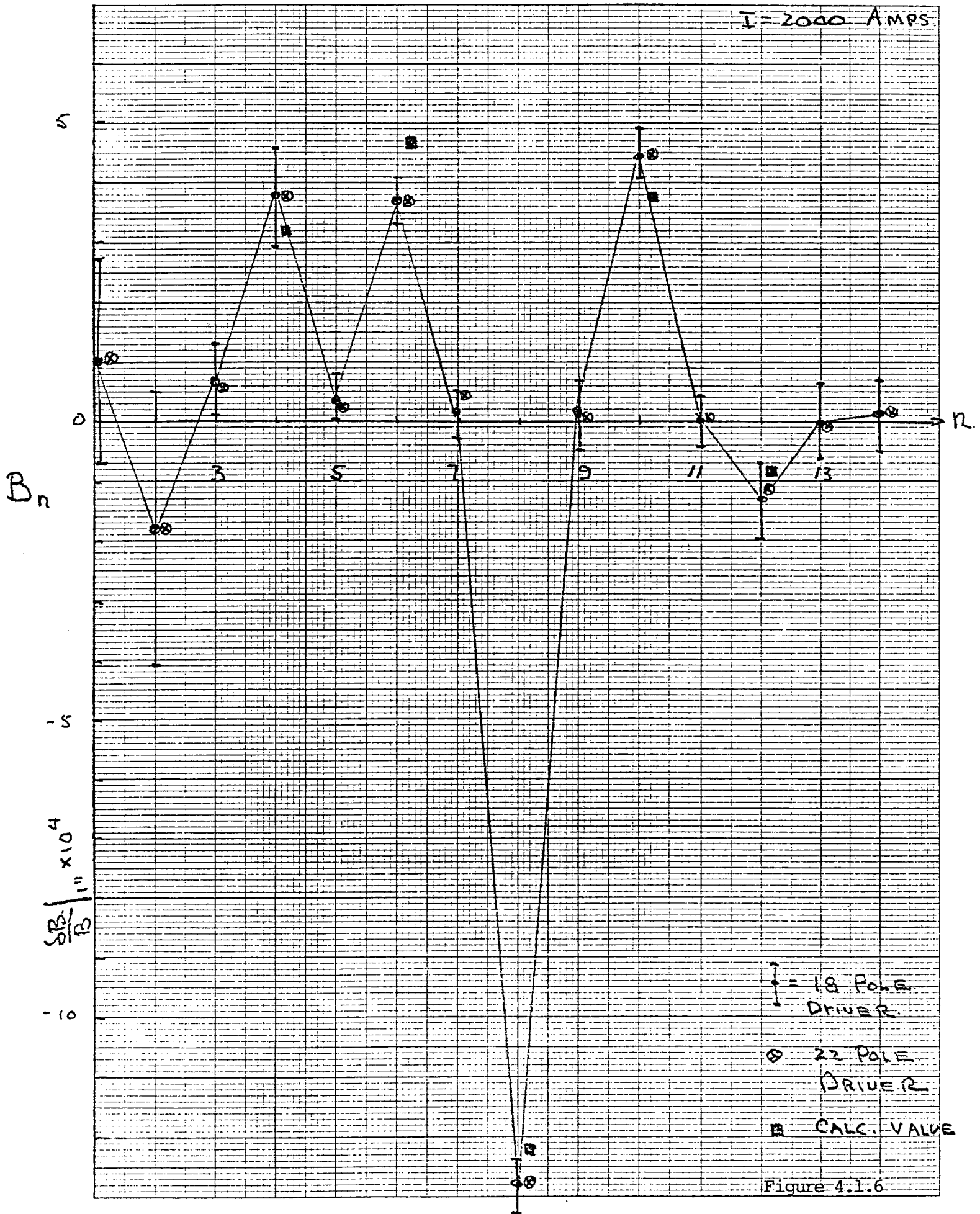


Figure 4.1.6

4.2 Since the centering process is applied to all of the measurements it is important to understand whether we disguise or eliminate certain errors in the fields through this process. It should be noted that the transformation equations are exact and the only approximation made is that we neglect multipoles above the 30-pole term. Since calculations show that these have magnitudes of less than 1/3 of a gauss inside of a 1" circle, we can rest assured that if the displacements are small, the transformation will accurately preserve the field shape. However, the question remains, are we finding the same center for the middle of the magnet as we are for the ends, and are we disguising or covering up errors in the magnet structure that we need to discover? To address this problem I have considered the centering process as applied to a model magnet with errors induced it by the distortions discussed in Section 1.5.

It is recalled that the model replaces the conductors with current filaments located at the center of each conductor. These are then displaced in a known manner and the exact field is generated. We consider here several of the distortions as generated in this model, and we use the prescription in the last Section to relocate the center of the field.

Consider, for instance, the distortion discussed in Table 1.5.8 where the coils on the right hand side of the magnet are pinched together and, hence, there is a normal series of quadrupole, octapole, etc., terms generated. Since no asymmetry about the horizontal plane is generated by this distortion, there will only be an x displacement generated by our centering procedure. Table 4.2.1 shows the results of calculating DX by means of the following simple equation:

$$DX = \frac{b_n - 1}{n b_n}$$

The first line shows how far the X displacement would have to be in order to eliminate the quadrupole moment due to this distortion by cancelling it against the normal sextapole moment of the magnet. The answers are in inches and the distortion assumed is 100 mils instead of 10 mils as it was in Table 1.5.8. Normal centering procedures would use $K = 7$ which corresponds to the 16-pole term being reduced to 0 and the 18 pole term being a driving source. It is seen that the procedure would yield a DX of .029". Other multipoles considered as drivers and other terms considered as pairs are shown in the column under DX. A point to note here is that for the lower order terms, i.e., quadrupole, octapole, etc., the shift calculated from the 16-pole is only 1% of the shift that would be necessary to reduce the lower order terms to 0. Hence, real magnet with a skew asymmetry of .100" (enormous!) subjected to our centering operation would have a shift of .029", and this would leave the real errors in the lower b_n ' essentially unchanged.

Table 4.2.2 shows the corresponding calculations for this distortion considered in Table 1.5.13, i.e., an upward displacement of the right hand median plane by 10 mils. This table yields because of the asymmetry of the distortion both of DX and DY. Table 4.2.3 shows the results for the distortion considered in Table 1.5.11 which is an upward shift of the parting plane on both sides of the magnet by 10 mils. This effects only the skew symmetric terms and hence only yields a DY. Table 4.2.4 shows the results expected for a displacement of the upper right hand key by 10 mils while keeping the median plane fixed. This distortion has not been considered in the previous tables. Again it breaks all of the symmetry so it yields a DX and a DY.

In all of these tables it is observed that the shift necessary to restore the center as measured by the 16-pole is very small compared to the shifts that would be necessary to eliminate the lower order multipoles. In fact, we can say roughly in this linear approximation that the effect of the shift on the lower order terms is in the ratio of the DX calculated for the two different values of K. The results of this study then give us some confidence that for a real magnet when the origin of the measurements are shifted by the prescription described in Section 4.1 that we are not eliminating lower order errors. Small effects in the higher order terms, of course, are not independent of the shifting procedure, and in some sense we can only arrive at a feeling for the magnitude of these terms by seeing what fluctuations exist over a large series of magnets where we make a shift at one current and study the field at other currents.

This study can be turned around and another conclusion drawn. When one makes a distortion of a field it is never clear whether the shape of the field has been changed in a fundamental way or whether one would find an equally good field by moving the coordinate system slightly. For the distortions considered here this study shows that no trivial translation of the coordinate center can restore the field. The terms that are induced by these changes are fundamental and deleterious to the field desired. We will now proceed with a detailed discussion of the multipoles as they have been measured.

Table 4.2.1

K	DY	DX	DY	DX
1	-0.000	-2.325	-0.000	-0.690
3	0.000	-2.423	-0.000	-0.815
5	-0.000	-0.321	0.000	-0.143
7	0.000	0.029	0.000	0.008
9	0.000	-0.026	-0.000	-0.004
11	0.000	0.036	-0.000	0.003
13	-0.000	-0.126	0.000	-0.008
15	0.000	-0.143	0.000	-0.008
17	0.000	0.031	0.000	0.001

Table 4.2.2

K	DY	DX	DY	DX
1	-0.502	-0.003	-0.281	-0.001
3	-0.044	-0.002	-0.134	-0.001
5	-0.006	-0.000	-0.009	-0.000
7	0.001	0.000	0.000	0.000
9	0.000	-0.000	0.000	-0.000
11	0.001	0.000	-0.000	0.000
13	0.000	-0.000	-0.000	-0.000
15	0.000	-0.000	0.000	-0.000
17	0.000	0.000	-0.000	-0.000

Table 4.2.3

K	DY	DX	DY	DX
1	-1.064	-0.000	-0.563	0.000
3	-0.087	0.000	-0.267	0.000
5	-0.013	0.000	-0.019	0.000
7	0.002	-0.000	0.000	-0.000
9	0.000	-0.000	0.000	0.000
11	0.001	0.000	-0.000	0.000
13	0.001	0.000	-0.000	0.000
15	0.000	-0.000	0.000	0.000
17	0.000	0.000	-0.000	0.000

Table 4.2.4

K	DY	DX	DY	DX
1	-0.056	0.371	0.106	0.122
3	-0.212	-0.112	-0.017	0.106
5	0.032	-0.003	-0.014	0.007
7	0.002	-0.002	0.001	0.000
9	0.000	-0.003	0.000	-0.000
11	-0.001	-0.003	-0.000	0.000
13	-0.011	-0.007	0.000	0.001
15	0.015	0.000	-0.001	0.001
17	0.003	-0.002	0.000	0.000

4.3 Multipoles as a Function of Magnet Member

The primary goal of the magnet development program is to set up the machinery to construct magnet coils with acceptably small errors. In the last section, we have been examining the size of these errors for a group of magnets that have been made for the past year. We will now consider the variations of the multipole structure with magnet member. To anticipate the conclusion, this section will show that the low order multipoles i.e., up through the decapole, are subject to fluctuations in the magnet structure itself. The higher order multipoles are not influenced by small changes in this structure.

We will consider magnet members starting with magnet #100 and proceeding up through magnet #150. During this time various structural changes were made in the magnet, and as we shall see, these changes resulted in a change of the multipole structure. In addition, as we shall see, unintended things were happening inside of the magnet structure that resulted in undesired mechanical changes. We show here how these mechanical fluctuations can be detected by means of the magnetic measurements and make some attempt to identify their source.

First, consider the harmonics as measured in the central region of the magnet and the end fields will be examined later. The central fields are a function of the two dimensional cross section of the magnet and studying the fluctuations in these fields should give us some indication of the dimensional accuracy of this cross section.

Figures 4.3.1 through Figures 4.3.28 gives a complete set of multipoles as measured at MTF for the magnet series between 101 and 149. The horizontal scale is such that the smallest unit put out by the teletype is 0.2×10^{-4} and the

divisions labeled 1, 2, 3, are in units of 1×10^{-4} .

First, let's examine the b_n 's shown in Figure 4.3.1 to 4.3.14. One notices immediately that there is a large apparently random fluctuation in the normal quadrupole moment. This quadrupole term is driven by errors in centering the coil in the yoke and by right-left asymmetries in the coil structure. Next, we observe in Figure 4.3.2 that the sextapole moment is also fluctuating badly, but that there are also systematic changes occurring in it. There is a drop from positive values to negative values that takes place at magnet #110. The values then fluctuate in the negative region up through magnet #129 at which point they go positive and then there is a second jump in the positive direction at magnets in the 140 series. These changes are a result of physical changes in the coil. For future reference, a short history is given here:

Magnet #103: Type V collars and an outer coil size that has been increased by .007".

Magnet #109: At this point we discovered that the collars had not been completely closing around the coils. From this point on, all collars are Type V and are tightly closed.

Magnet #126: Outer coils were to have been decreased in size by .007".

Magnet #130: Reduced inner coil size .005", outer coil size .008".

The effect of the collar closing on the magnet can be seen in the big change of sextapole moments from positive values to negative values at magnet #109. These changes before magnet #109 are complicated in that the collar type was changed, the shims on the outer coil were being changed, and an undiscovered gap existed in the collar structure. From magnet #110 to

to magnet #128 no intentional changes were made in the magnet structure. The change in the shims at magnet #130 came about because the magnets were discovered to have a sextapole moment from the ends that was much more negative than calculated. Hence, the change in magnet #130 was intended to correct for this end sextapole moment.

Lets now examine the rest of the multipoles. Figures 4.3.3 and 4.3.5, etc., shows the octapole, 12-pole etc., and these terms it is noted, do not react to any of the changes in the structure that are exhibited by the sextapole. However, an examination of Figure 4.3.4 shows that the decapole has changes at magnet 108 and at magnet 130, and 148 and these changes are systematic rather than random. Again we will show that these are correlated with changes in the magnet structure.

The examination of Figures 4.3.8, 4.3.10, 4.3.12 shows that the series of multipoles 14, 18, 22, and 26 are essentially stable and exhibit none of the fluctuations that the sextapole and decapole do. Thus we conclude that the magnet structure itself is mainly active in influencing the multipoles up through the decapole in the normal series of multipoles.

Lets now examine the skew terms. Figure 4.3.15 shows large and uncontrolled fluctuations in the quadrupole moment. This term is driven by asymmetries in the magnet structure about the parting plane, i.e., the top is different than the bottom. The skew terms can further be divided into terms that are symmetric about the vertical axis and asymmetrical about the vertical axis. The quadrupole is an example of one type and the sextapole an example of the other. Fig. 4.3.16 shows the skew sextapole. A comparison of the following figures show

Figure 4.3.2
B(2)/2

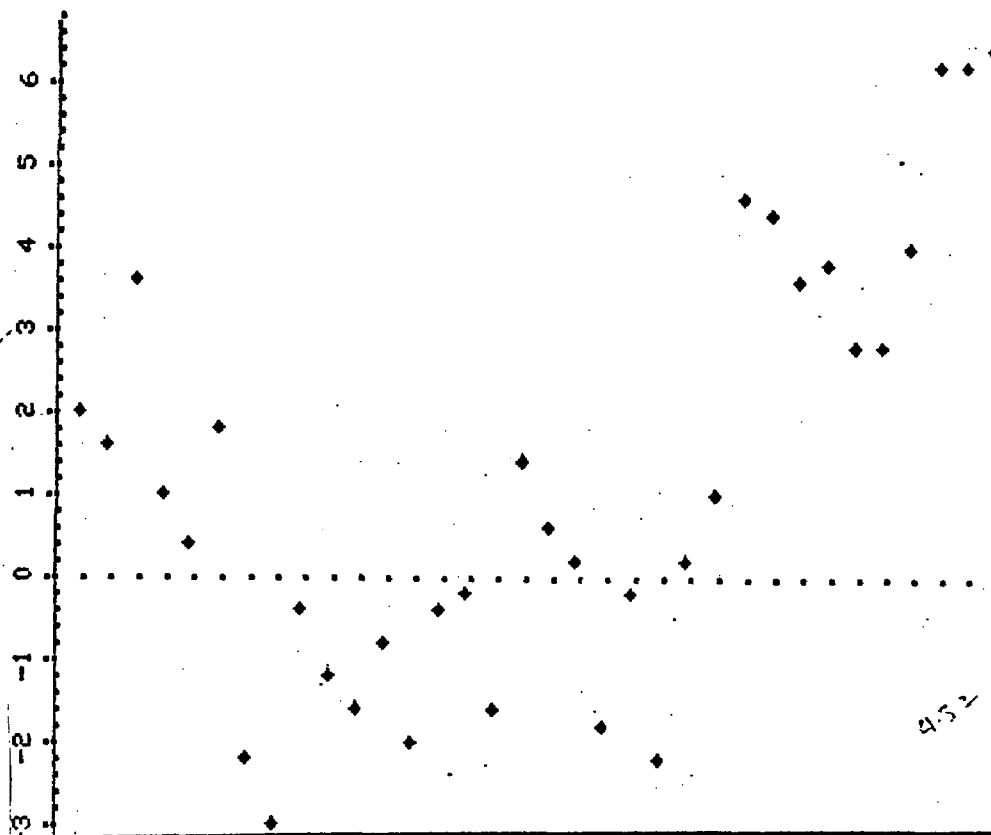
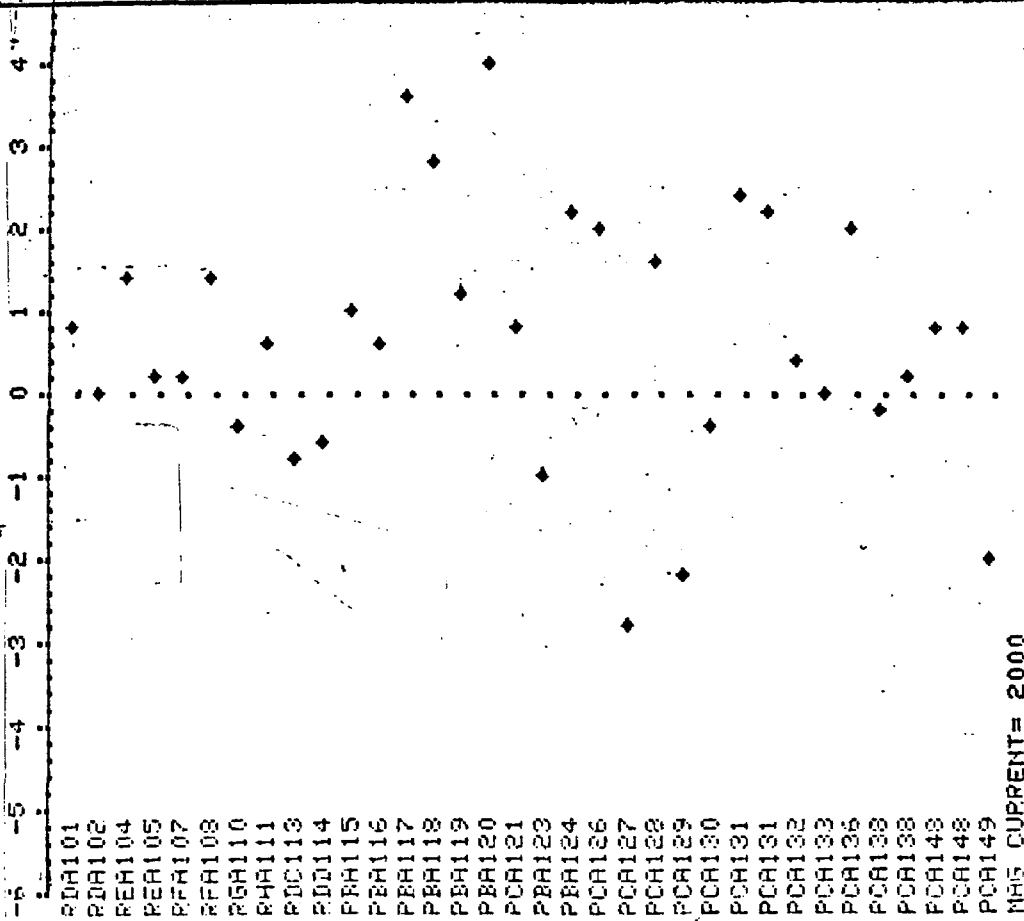


Figure 4.3.1
B(1)



MMS CURRENT= 2000

Figure 4.3.7
B(7)

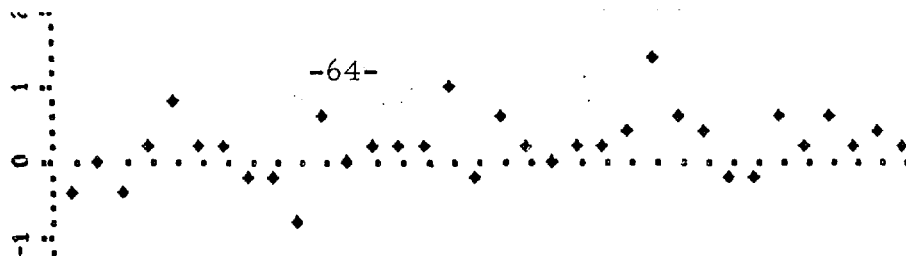


Figure 4.3.6
B(6)



Figure 4.3.5
B(5)

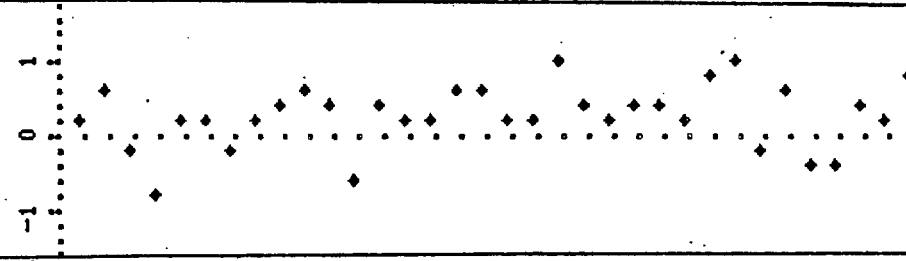


Figure 4.3.4
B(4)/2

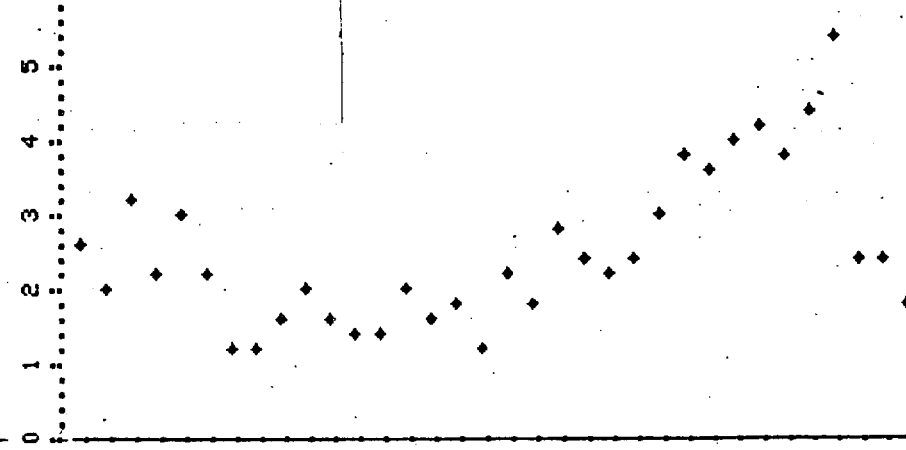
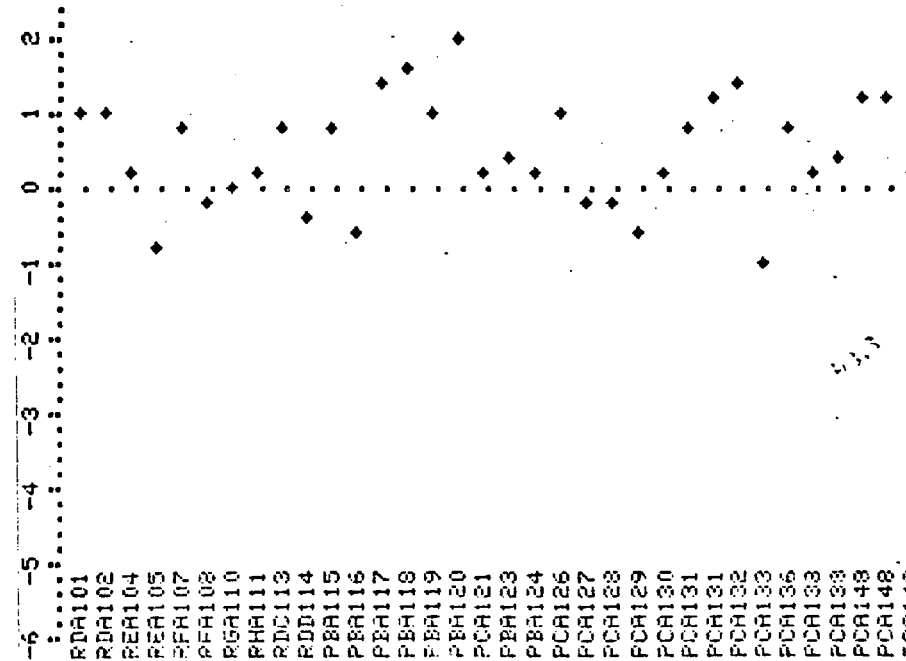


Figure 4.3.3
B(3)



RDA101
 RDA102
 REA104
 REA105
 RFA107
 RFA108
 RGA110
 RHA111
 RDC113
 RDD114
 PEA115
 PEA116
 PEA117
 PEA118
 PEA119
 PEA120
 PCA121
 PCA123
 PCA124
 PCA126
 PCA127
 PCA128
 PCA129
 PCA130
 PCA131
 PCA132
 PCA133
 PCA136
 PCA138
 PCA139
 PCA148
 PCA149
 NMS CURRENT= 2000

Figure 4.3.14
B(14)

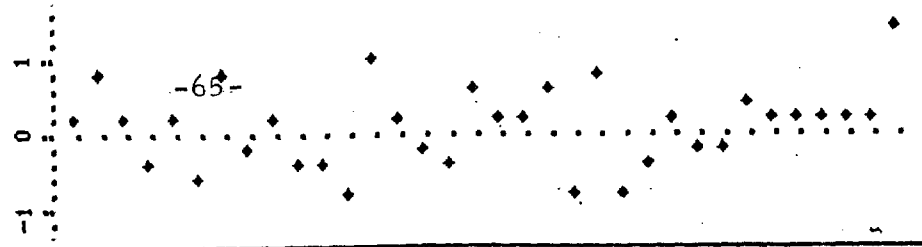


Figure 4.3.13
B(13)

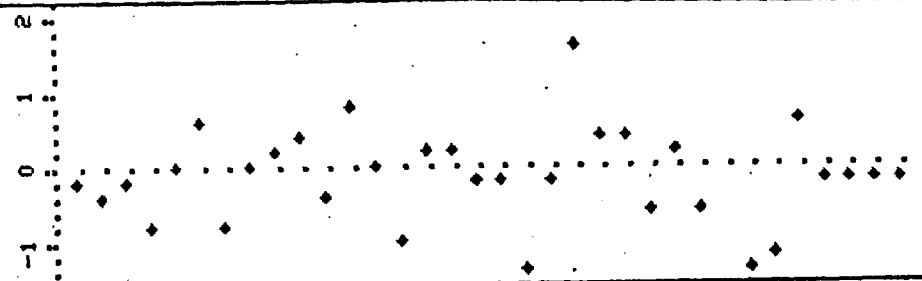


Figure 4.3.12
B(12)

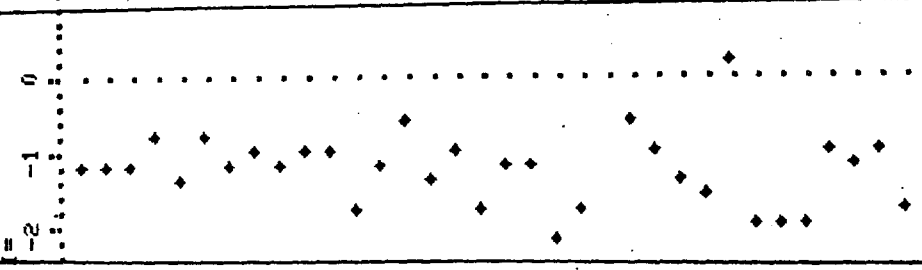


Figure 4.3.11
B(11)

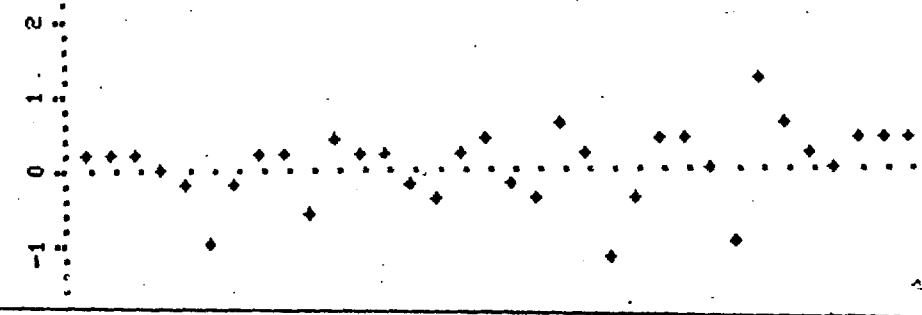


Figure 4.3.10
B(10)

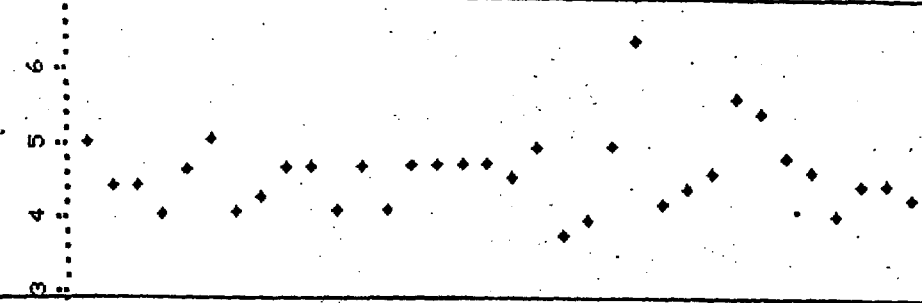


Figure 4.3.9
B(9)

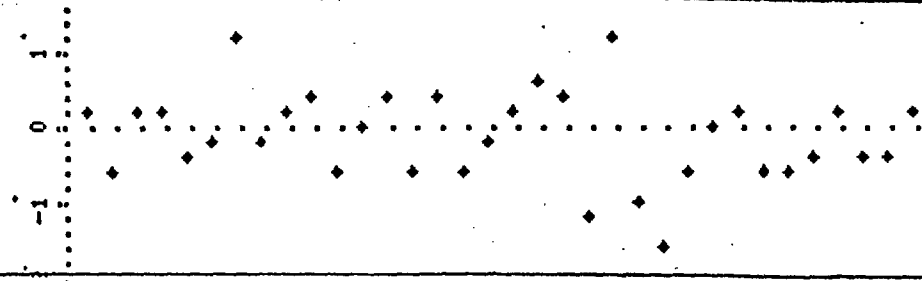
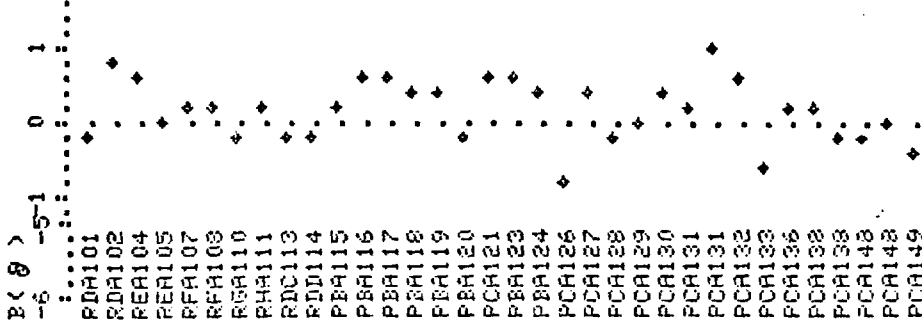


Figure 4.3.8
B(8)



♦♦♦♦♦
 B(8) > -6
 RDA101
 RDA102
 REA104
 REA105
 REA107
 REA108
 REA110
 REA111
 RDC113
 RDD114
 PEA115
 PEA116
 PEA117
 PEA118
 PEA119
 PEA120
 PCA121
 PCA123
 PCA124
 PCA126
 PCA127
 PCA128
 PCA129
 PCA130
 PCA131
 PCA131
 PCA132
 PCA133
 PCA136
 PCA138
 PCA138
 PCA143
 PCA148
 PCA148
 PCA149
 NMS CUR1

Figure 4.3.22
A(8)

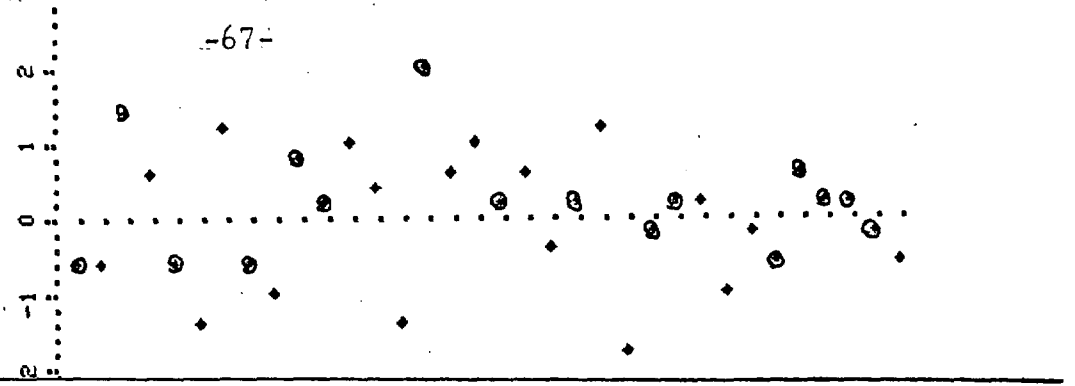


Figure 4.3.21
A(7)

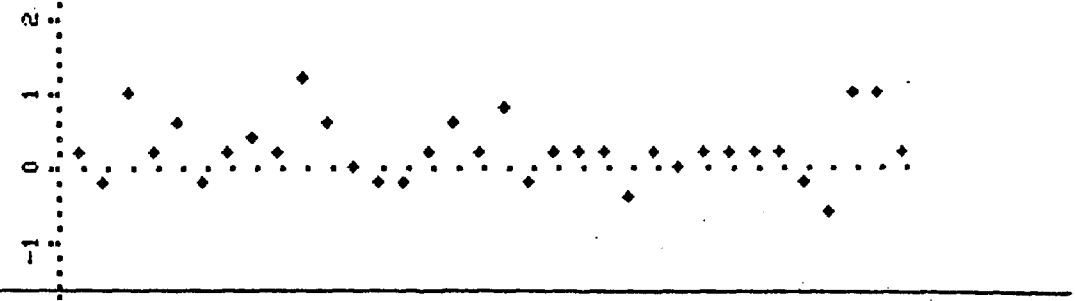


Figure 4.3.20
A(6)

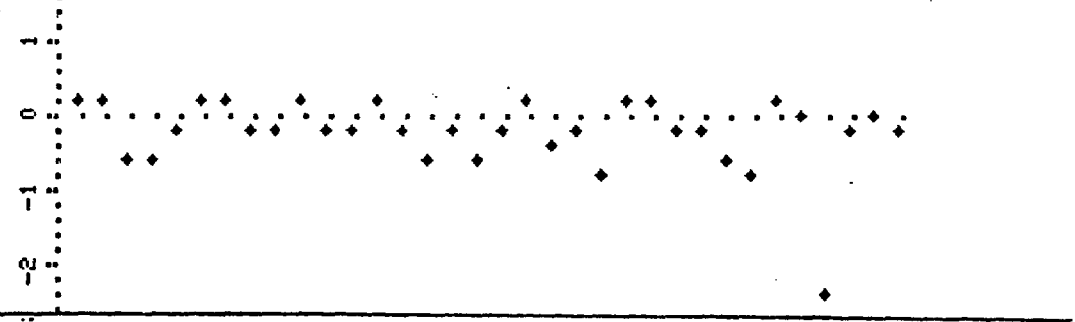
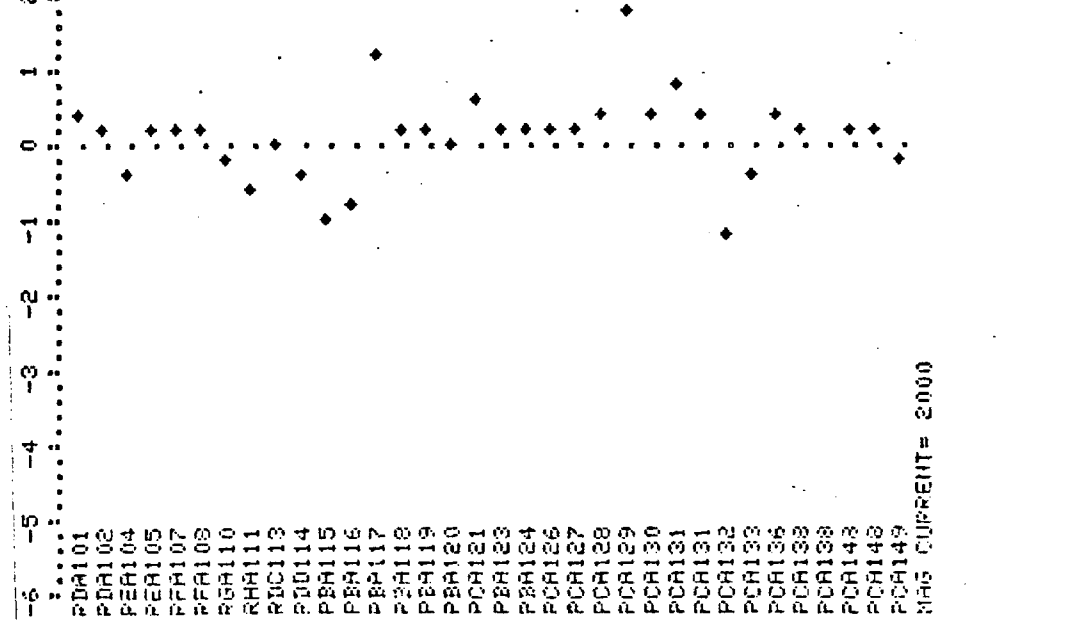


Figure 4.3.19
A(5)



Figure 4.3.18
A(4)



PDA101
 PDA102
 PEA104
 PEA105
 PEA107
 PEA108
 PEA110
 PEA111
 PEA113
 PEA114
 PEA115
 PEA116
 PEA117
 PEA118
 PEA119
 PEA120
 PEA121
 PEA123
 PEA124
 PEA126
 PEA127
 PEA128
 PEA129
 PEA130
 PEA131
 PEA131
 PEA132
 PEA133
 PEA136
 PEA138
 PEA138
 PEA143
 PEA143
 PEA149
 PEA149

MAX CURRENT = 2000

Figure 4.3.28
A(14)

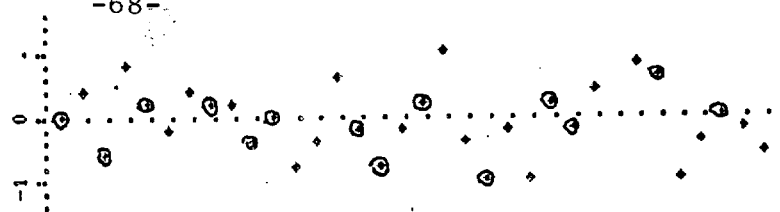


Figure 4.3.27
A(13)

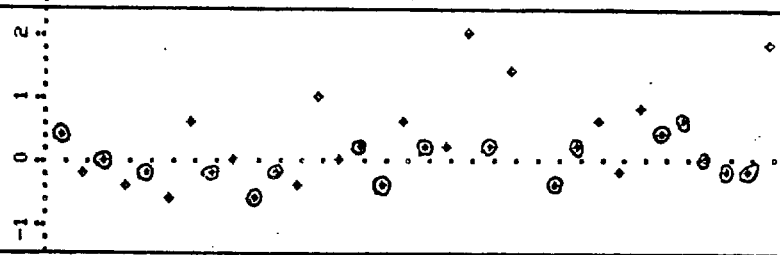


Figure 4.3.26
A(12)

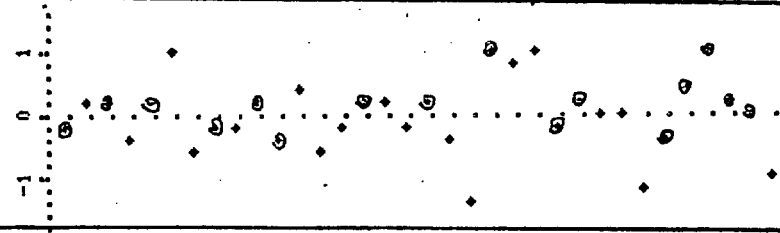


Figure 4.3.25
A(11)

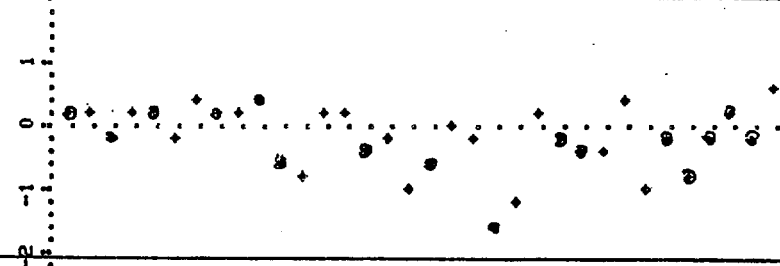


Figure 4.3.24
A(10)

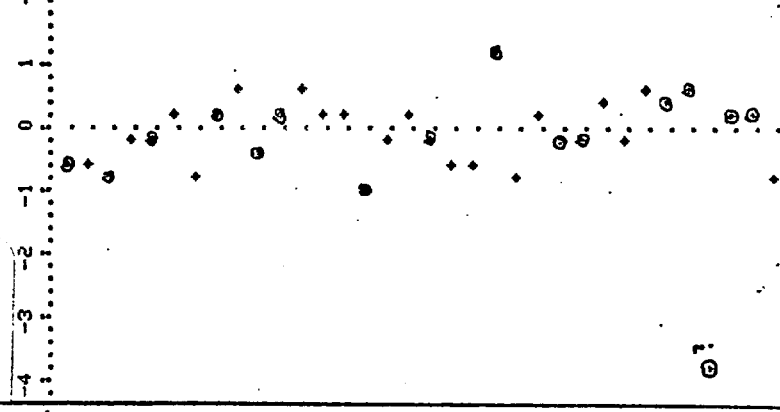
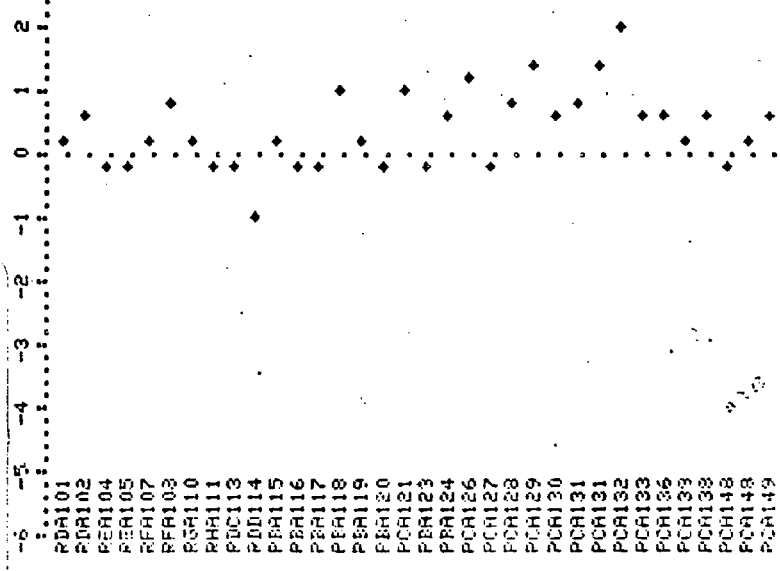


Figure 4.3.23
A(9)



RD101
RD102
PER104
PER105
RF107
RF108
RG110
RH111
PDC113
RDI114
PE115
PE116
PE117
PE118
PE119
PE120
PC121
PC123
PC124
PC126
PC127
PC128
PC129
PC130
PC131
PC132
PC133
PC135
PC136
PC138
PC143
PC148
PC149

IT= 2000

MAX CURRENT= 2000

that the sextapole and decapole have smaller fluctuations than the quadrupole and octopole do. Again there is no obvious association between these terms and the big changes that were taking place in the sextapole. This shows that to a fairly good accuracy the collaring operation is not introducing vertical asymmetries into the coil structure. We will examine this in more detail shortly.

4.4 Model for Construction Errors

In principle, a careful measurement of the magnetic structure of the field will enable us to reconstruct the current distribution exactly. However, the limited accuracy of the measurements prohibits this in practice. Hence, we must find a way of analyzing the field in terms of the most likely errors that could occur in the magnet manufacturing. It must be emphasized at this point that the analysis model presented here is not unique and, in fact, some of the assumed errors may not be present in actual fact. Their appearance in the following analysis may only be mirroring some other error that we have not identified. However, our main effort will be to categorize these various distortions in terms of symmetry and hence they should be rather general in their ability to point at least in the direction of the trouble.

We use now the tables given in Section 1.5 in order to make an analysis of the various natural symmetries of the magnet structure. First of all, we note that theoretically the coil is symmetrical right and left and up and down. Errors have symmetries that couple naturally into the even and odd A_n 's and into the even and odd b_n 's. We identify five of these possible types of distortions. Each distortion

is divided into a symmetrical and asymmetrical component. The even terms are designated in the label with a 2 and the odd terms are designated with a 1. Thus, we will consider distortions designated by A, B, C, and D of type symmetries 1 and 2 making a total of 8 distortions in all. However, in addition to this division, there are two coils in the magnets, an inside one and an outside one. Hence, if we apply these distortions differently to the inside and outside coil, we are considering a total of 16 possible errors.

The diagram below shows a coil and its four corners labeled Y1, Y2, Y3, and Y4. If we consider that the coils

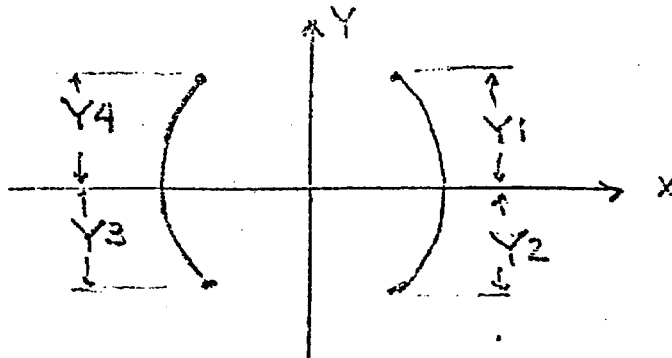


Figure 4.4.1

is constrained to lie on a circle then the four coordinates will completely describe the coil. We could consider the harmonics generated by an arbitrary displacement of any combination of these corners from their correct position. However, it is best to use our knowledge of symmetry of the harmonics in order to pick sets of displacements that correspond to the natural symmetries of the magnetic fields. Since there are four corners, we can replace these four coordinates with four sets of new coordinates that remind us of normal coordinates in a mechanical oscillator problem. These four coordinates are shown in a small diagram in the figure below. In all of these

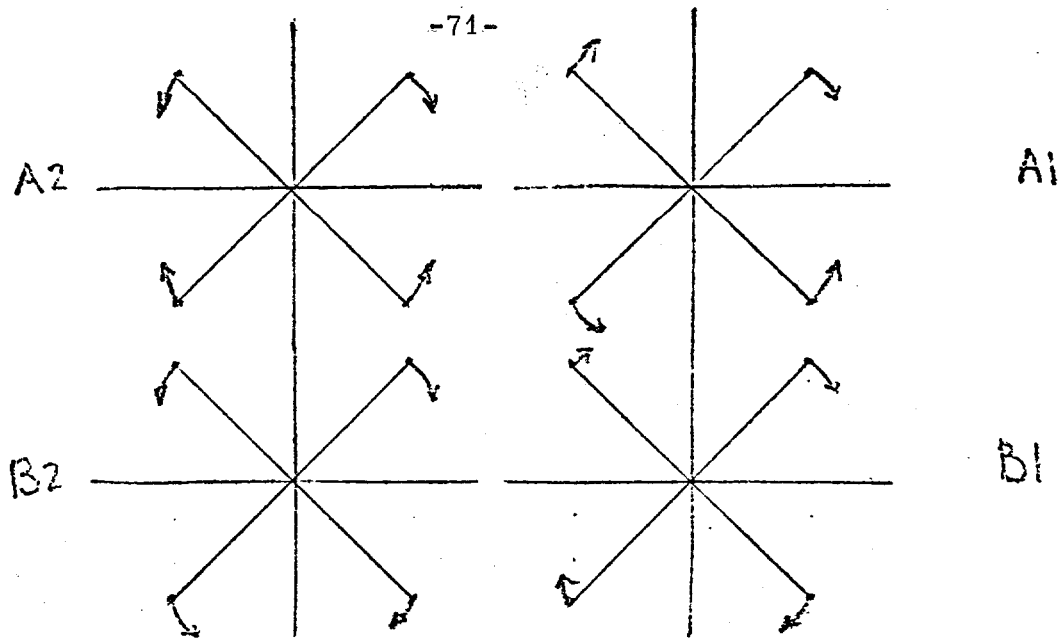


Figure 4.4.2

cases we consider the coil as an elastic member whose length is only determined by where the corners are located. The matrices that give the field for these displacements can be generated from the Tables given in Section 1.5. Of the four distortion types shown, only three result in a real field distortion. B1 is simply a rotation of the magnet as a unit. Table 4.4.1, 4.4.2, 4.4.3, and 4.4.4 gives the matrices, which are normalized to an azimuthal displacement of the corners equal to .01". A2 and A1 come about when the coils in a collared condition are bigger or smaller than their design value. B2 results from a displacement of each side of the coil as a rigid unit.

The above four distortions do not redistribute the current density within the coil, however, since the coil is molded in a top half and a bottom half separately, it is possible that the size of the top coil is different than the size of the bottom coil. Since, the wire carries the same current through the

whole magnet the expected current density in half of the coil can be different than it is in the other half of the coil. It, therefore, is necessary to have a distortion that describes such an error in the manufacturing process. This distortion is shown below. Here it is assumed that the corners of the

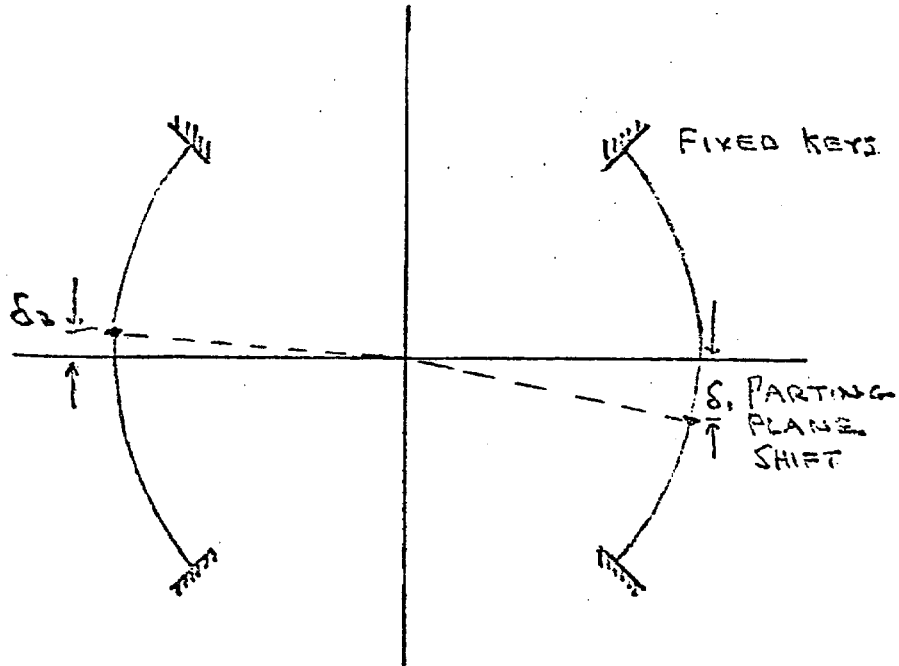


Figure 4.4.3

coil are in contact with the corners of the collar and that the collars are correctly dimensioned, but that either the size of the coil or its elastic constant is different above and below the median plane. This results in a vertical shift in the parting line of the two sections of the coil. Clearly we can break this displacement up into a symmetrical and anti-symmetrical term shown below as C2 and C1.

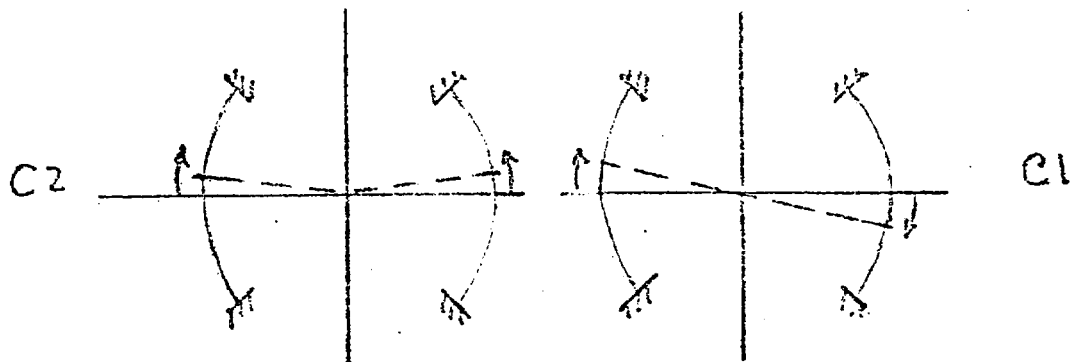


Figure 4.4.4

Again we may use Section 1.5 to manufacture the error matrices and these are given for C2 in Table 4.4.5 and for C1 in Table 4.4.6. The displacements are normalized to .01".

We have now described a shift of the centroid of the current block and in a crude sense the distribution of current density within the coil. This set of distortions will generate all of the harmonics that are seen. Never the less, we will add one more error term that could naturally arise. Because of the extra insulation placed around the return buss and the necessity of insulating the top and bottom half of the coils from each other due to the fairly large voltage difference at this point, it is possible that a gap variation can take place at a median plane. This is shown below. Again we

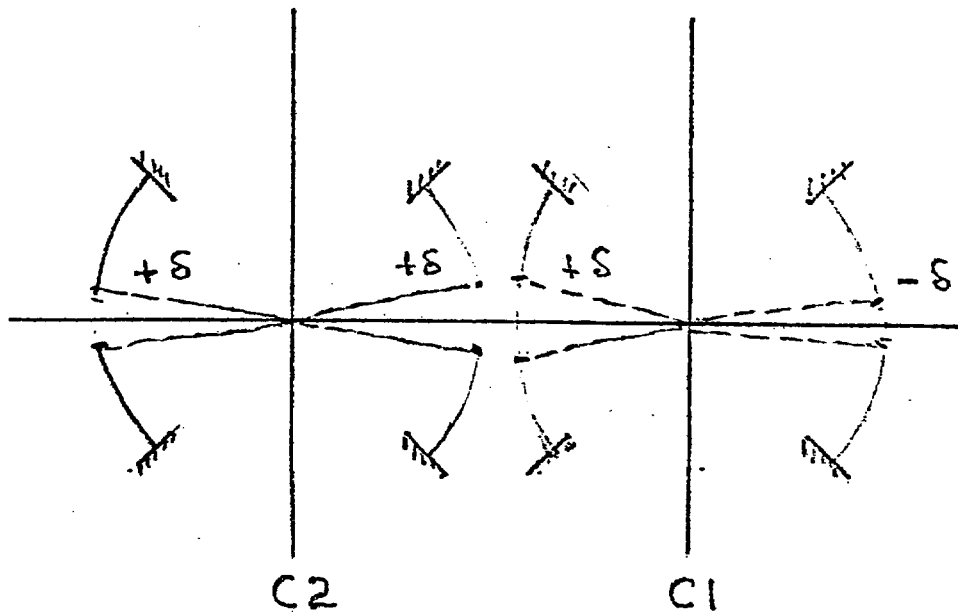


Figure 4.4.5

can break this type of error up into a symmetrical and anti-symmetrical gap fluctuation. Table 1.5.9 can be used to generate the error matrices for this case.

There are two more errors that have a strong influence on the harmonics. The first is a change in radius of the magnet.

Table 1.5.2 gives the matrix for this error. It is seen that for a change of 10 mils this error has a big influence on the transfer constant and rather negligible influence on the rest of the field harmonics. It should be noted that this would not be the case if the change of radius were different for the inside and outside coils. This is because the two individual coils have very large sextapole moments of opposite sign that cancel against each other. Hence, the sextapole moments will fluctuate more if the radii of the two coils are independently changed than if the whole coil suffers a radial distortion.

One last error that we must consider is caused by the coil being placed off-axis within the yoke. This has been analyzed in Section 3.2.

We now have completed the description of a model of the construction errors. Altogether there are 16 coordinates that come in from the distortions A, B, C, D when applied to the two separate coils. If we consider that the radius of the whole coil package may change and that it may be placed off-center in the iron yoke then there are a total 19 independent coordinates that describe the errors that we have considered here. In MIF a total of 14 normal and 14 skew harmonics are measured as well as the transfer constant, giving us 29 independent measurement. Thus, it would seem at first glance that we have a set of overdetermined equations for the coordinates that we are considering. The falacy of this remark can be seen by considering the size of the errors displayed in Figure 4.1.4 and 4.1.5 for the a_n and the b_n . It is seen that typical errors in the higher harmonics are $\pm .5$, and an examination

of the Tables 4.4.1 through 4.4.8 show that the distortions would have to be enormous to generate higher harmonics of this magnitude. Hence, it must be concluded that these higher harmonics either come in through errors in the measuring process and are not real, or they come from random fluctuations in the positions of the individual conductors; and hence, are not described by the distortions that we have considered here. This remark can be further verified by examining Figures 4.3.2 and 4.3.4 that show the sextapole and decapole as a function of magnet number. Clearly, structural effects are important in determining the magnitude of the b_2 and b_4 . However, as we have noted previously, harmonics above the decapole are not influenced by the type of structural errors that we are considering here. This is also shown theoretically in Tables 4.4.1 through 4.4.8. Therefore, we are reduced to using a set of numbers up through the decapole to try to discover the errors. That means we have only a quadrupole, octopole, sextapole, and decapole terms to work with. Using these for the normal and skew components gives us 8 measurements. In addition to this, the transfer constant is measured which gives us 9. We thus see that our set of unknowns is enormously undetermined.

There is one additional fact that tends to make the analysis very difficult and that is that the error matrices for the various errors are not sufficiently different, and, in some cases, are almost degenerate with one another. In Table 4.4.9 below we list the distortions and the harmonics that each one couples into. (k is the transfer constant, gauss/amp.)

Table 4.4.1

		A2	
		<u>Inner</u>	<u>Outer</u>
k	b_k	b_k	b_k
0	17.229		4.578
2	7.102		5.845
4	- 4.116		1.701
6	1.415		.005
8	- .293		- .105
10	- .012		- .018
12	.046		.004
14	- .026		.002

Table 4.4.2

		A1	
		<u>Inner</u>	<u>Outer</u>
k	b_k	b_k	b_k
1	20.692		6.826
3	- 3.846		3.648
5	- .212		.521
7	.604		- .127
9	- .327		- .054
11	.115		- .001
13	- .026		.003

Table 4.4.3

		B2	
		<u>Inner</u>	<u>Outer</u>
k	a_k	a_k	a_k
1	10.901		13.765
3	- 6.543		1.712
5	2.429		- .635
7	- .662		- .226
9	.046		- .001
11	.046		.012
13	- .040		.001

Table 4.4.4

		B1	
		<u>Inner</u>	<u>Outer</u>
k	a_k	a_k	a_k
0	35.858		20.413
2	- 7.408		6.314
4	.290		- .226
6	.714		- .469
8	- .514		- .068
10	.195		.015
12	- .059		.005
14	.006		- .001

Table 4.4.5

C2		
	<u>Inner</u>	<u>Outer</u>
k	a_k	a_k
1	-14.007	-7.854
3	- .751	-2.301
5	- .219	- .328
7	- .130	- .003
9	.010	.007
11	- .011	0.
13	.001	0.

Table 4.4.6

C1		
	<u>Inner</u>	<u>Outer</u>
k	a_k	a_k
0	-20.77	-10.364
2	- 5.230	- 4.632
4	.06	- .964
6	- .287	- .079
8	- .010	.01
10	- .006	.003
12	- .004	0.0
14	.001	0.0

Table 4.4.7

D2		
	<u>Inner</u>	<u>Outer</u>
k	b_k	b_k
0	-4.811	-1.212
2	-6.876	-1.854
4	-2.094	- .907
6	- .731	- .269
8	- .301	- .059
10	- .094	- .012
12	- .038	- .003
14	- .013	- .001

Table 4.4.8

D1		
	<u>Inner</u>	<u>Outer</u>
k	b_k	b_k
1	-7.885	-1.925
3	-4.174	-1.405
5	-1.117	- .518
7	- .497	- .129
9	- .166	- .026
11	- .059	- .006
13	- .023	- .002

A2 + D2	B1 + C1	A1 + D1	B2 + C2
k	(a ₀ = 0)	b ₁	a ₁
b ₂	a ₂	b ₃	a ₃
b ₄	a ₄	b ₅	a ₅
b ₆	a ₆	b ₇	a ₇
b ₈	a ₈	b ₉	a ₉

We will find in the following Section that, for instance, error of the type D2 are covered up by errors of the type A2. Similarly A1 and D1 get confused as do B2 and C2. Hence, we must look for rather subtle effects in trying to separate these various kinds of errors. So lets get on with the struggle.

4.5 Consideration of A2 and D2

We consider first the distortions A2 and D2. A2 errors pop up naturally because of the insulation, the shimming, and the irrigation channel that is inserted at the key, and error D2 arises quite naturally through the additional insulation that is placed on the parting plane. As an examination of Table 4.4.9 will show these two distortions couple into the sequence of harmonics given by b₂, b₄, b₆, b₈, b₁₀, etc., i.e., these are the permitted harmonics in a normal magnet. The effect of errors then is to shift these harmonics away from their calculated and desired values. An examination

of Figure 4.2.3 shows that the sextapole and decapole are fluctuating rather badly. If we consider the two errors together, there are altogether 4 unknowns, hence, one might think that we could use k , b_2 , b_4 , and b_6 in order to uniquely determine the amplitude of the inner and outer key errors and the inner and outer parting plane errors. However, as has been mentioned previously, k is too sensitive to the radius to be used in this manner. In other words, the fluctuation in k as will be shown later is determined by almost entirely radial fluctuations and very little by the shim or the parting plane fluctuations. This reduces the available variables to b_2 , b_4 , b_6 , and b_8 . But now we are in the situation where b_6 and b_8 are fluctuating due to the fine structure errors in the coil and not responding to the gross structural errors that are described by these two distortions. For instance, an examination of Table 4.4.1 shows that an inner coil key angle fluctuation of 10 mils only changes b_8 by .29. This fluctuation from a 10 mil distortion is smaller than the rms error on this coefficient as can be seen by looking at Figure 4.1.6. It should be emphasized that 10 mils is considered an enormous fluctuation. Thus, we are forced into a situation where we have basically two measurements, namely b_2 and b_4 , and we would like to determine four unknowns which, of course, we can not do. Thus we will separately consider distortions A2 and D2 and see what we can learn by considering the errors in the multipoles due to either one or the other of these two errors.

To show the strategy of this technique, we will first consider a situation where D2 is supposed to be responsible for all of the errors in the multipole series that we are considering here, and that there is no A2. Figure 4.5.1 shows the calculated amplitude of the error in the outside and inside coil. The circles are the inner coil and the crosses represent the outer coil. The horizontal axis is the magnet number and the vertical scale has been converted to an amplitude in thousandths of an inch. What is shown is the distortion necessary to convert the measured magnet to a magnet whose b_2 is equal to -2 and whose b_4 is equal to 3.1. These values of b_2 and b_4 are typical of the magnets in the range between #110 and #120. It is seen that in order to fit the data, a large positive excursion in the inner coil compensates a large negative excursion in the outer coil, i.e., the inner and outer coils are fighting each other in order to get the proper combination of b_2 and b_4 to distort the real magnet into the assumed magnet. This correlated fluctuation of the inner and outer coil distortion is an unnatural state of affairs. There is no reason to expect that it would exist in the normal process of coil manufacturing. Hence, it is assumed that although D2 may exist, it does not by itself represent a very good description for the errors as actually found in the magnet.

We now proceed to the case of A2 and show a situation where the analysis is considerably more successful than it was in the last case. Here again we assume a standard magnet with $b_2 = -2$ and $b_4 = 3.1$ and calculate the errors at keys such that the standard magnet is converted into the physical magnet as measured. Results are shown in Figure 4.5.2; again

$b_4 = 3.1$

■ OUTER
○ INNER

MILS.

20
10
0
-10
-20

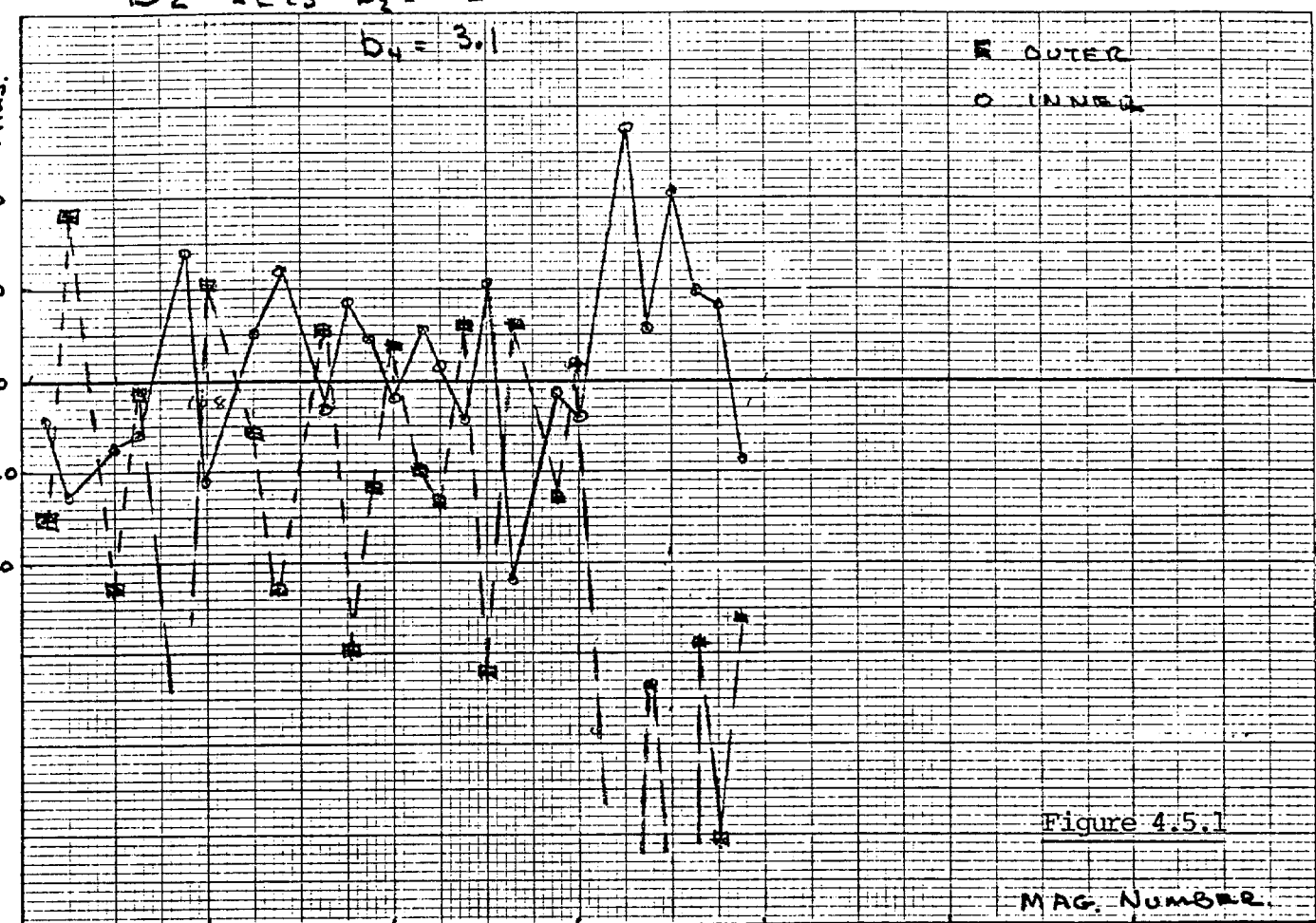


Figure 4.5.1

MAG. NUMBER

100 108 116 124 132 140 148

MILS OUTER

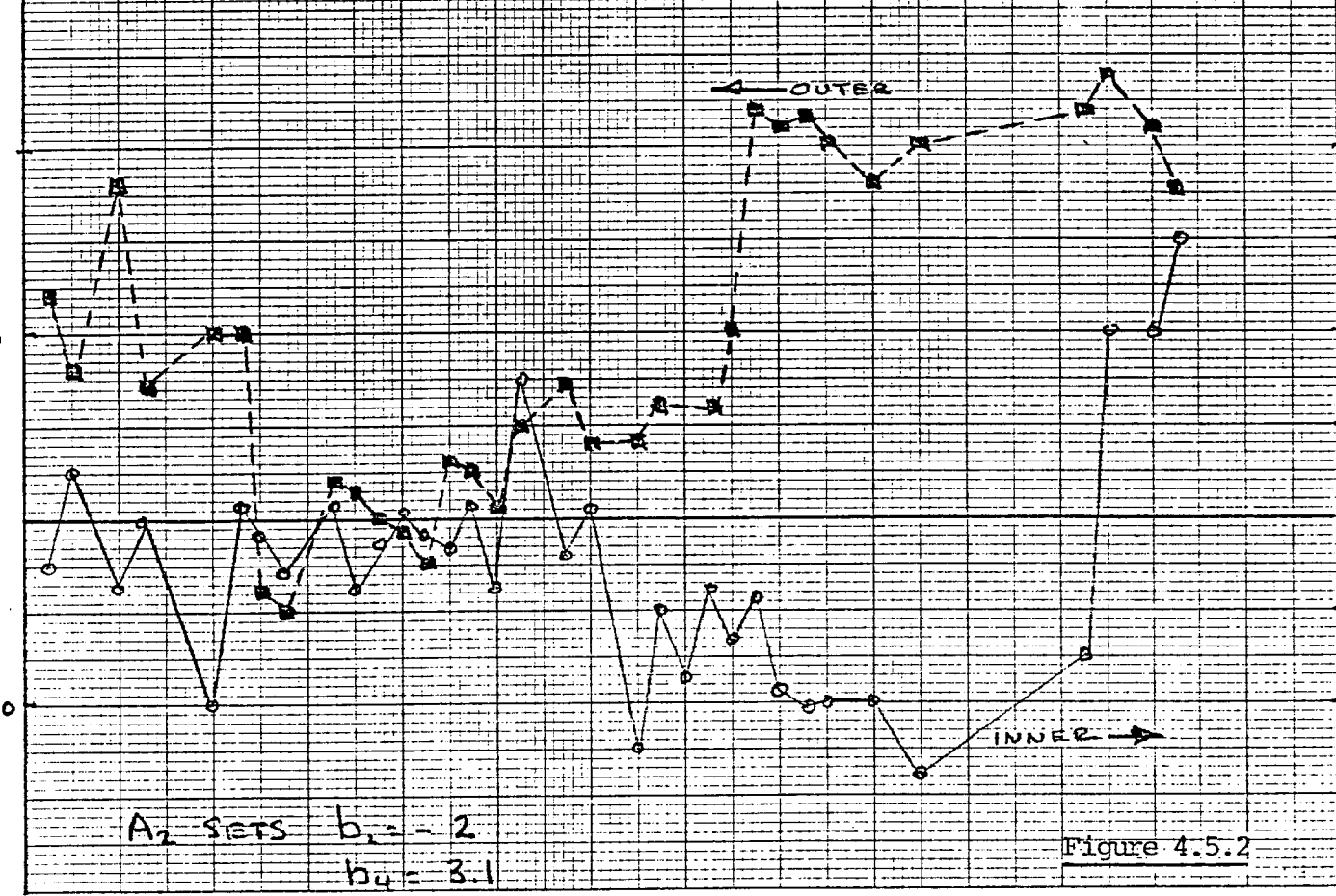
20
10
0
-10

MILS INNER

8
6
4
2
0
-2
-4

A₂ SETS $b_2 = -2$
 $b_4 = 3.1$

Figure 4.5.2



the horizontal scale represents magnets between #100 and #150. The boxes on the curve go with the left hand scale that goes from 0 - 20 mils and represent the shifts for the outer coil. The circles go with a scale on the right that represents the displacements associated with the inner key. First we notice that there is a rather coherent structure to these curves. At magnet #109 there is a big change in the size of the outer coil. This was caused by the collars closing. Since rather complicated things were happening between magnet #100 and #109 we will ignore this region in the analysis. It is seen that the errors between magnet #100 and magnet #120 are rather modest; the inner coil fluctuating by only ± 1 mil and the outer coil by only ± 2 mils. It appears that someplace between magnet #120 and #130 a change occurred such that the inner coil became bigger and the outer coil started to become smaller. At magnet #130 there was an intentional change in the size of both the inner and outer coils. The outer coils was made smaller by 15 mils and the inner coil was made smaller by 5 mils. The jump in the outer coil is clearly shown and it has the correct magnitude. After the jump this coil again maintains its size to ± 2 mils. However, the inner coil did not respond to this change but instead even grows slightly in size. Measurements of magnets in cryostats are not complete at this point, however, we do have measurements for magnets #145, 146, 148 and 149. Between magnet #145 and #146, we see that finally the inner coil responded to the size change and jumped in size by 5 mils. It is evident from the room temperature measurement that the magnets between #140 and #150 except #142 and #144, are of the type that are

shown as having an inner coil that is too big. This presents graphic documentation of the crushed irrigation channel episode. It would appear from these curves that magnets between #126 and #145 are all suffering from this syndrome. However, it is also apparent that someplace around magnet #120 something happened to decrease the size of the outer coil by about 5 mils. This effect was not known before this analysis and at present we are trying to ascertain what caused this defect.

This analysis is gratifying in that it shows that the fluctuations on the coils when they are properly constructed is actually rather small, and that the rather large fluctuations in sextapole and decapole observed in the magnets between #120 and #130 is probably not a normal error in our manufacturing process but rather came from a defect in the materials.

We can now carry the analysis a bit further. Since we have determined this amplitude S_1 and S_2 of the inner and outer coil fluctuations, we can calculate the corrected harmonics from harmonic number 6 on up and we can also calculate corrections to k , the transfer constant. If the distortion as calculated from b_2 and b_4 caused enormous fluctuations in the rest of the harmonics, we would assume that the distortion is not really present in the coil but is only mirroring some other error. Table 4.5.1 shows the rms errors in the harmonics before and after the correction is applied.

Table 4.5.1

Work in Progress

Figure 4.5.3 shows the transfer constant as measured for the same series of magnets. The circles show the values as measured at MTF and averaged over the central 8 feet of magnet. The cross show what the transfer constant would be if we corrected for the b_2 and b_4 errors by using the distortion A2. It is seen that the changes caused by correcting the multipole structure are very small compared to the other fluctuations that are taking place in the transfer constant. One can see the changes in radius of 1 or 2 mils is necessary in order to explain the rather large changes that are seen. Again it is interesting to note there is an indication of a change in the radius, and hence the transfer constant at a little bit after #120. This would seem to suggest that something in the collaring operation was happening between magnet #120 and #120 that we do not yet understand.

Conclusion: $\frac{\Delta r}{r} = 1\%$, $S1 = \pm 1$ mil, $S2 = \pm 2$ mils.
D2 undetermined.

In addition to these random errors, we assume that there has been a systematic failure at both the inner and outer keys during part of this series of magnets.

4.6 Error C1

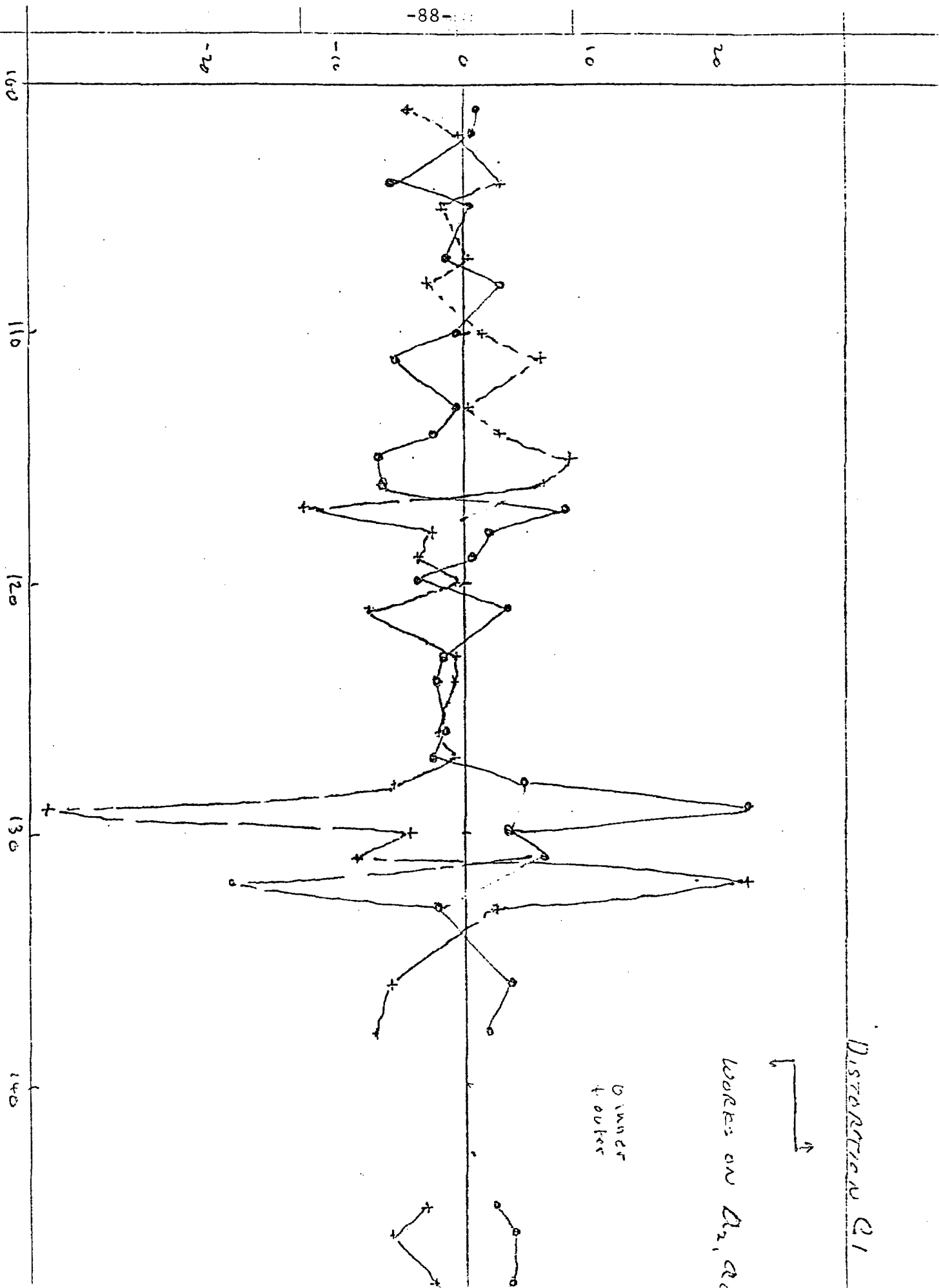
Error C1 influences a_0, a_2, a_4 , etc. As mentioned a_0 is eliminated by choice of the coordinate system at the time the measurements are made. Thus, C1 becomes the only source for the skew sextapole. There are two variables S1 and S2 the inner and outer coil displacement. We give two different approaches. The first involves using a_2 and a_4 to determine separately the displacements of the outer and inner coil. The second approach had to be invented because of failure of the first method.

Thus, we attempt first to set a_2 and a_4 equal to zero by means of distortions in the outer and inner coil. The necessary displacements are shown in Figure 4.6.1. The circle represents the inner coil and the crosses the outer. Again it is seen that we have a non-physical situation on our hands. When we choose to set these two harmonics equal to zero, the displacements are fighting each other in a non-physical way. However, it is clear that the coil package could be constructed in such a way that this distortion could be present. Furthermore, since this is the only distortion that drives a_2 , and a_2 is clearly present, we need to invent a new way to describe the situation. We do this by giving up the idea of separate motion of the inner and outer coils and assume that the error that is generating a_2 is coherently produced by these two coils

being the wrong size as described by distortion C1, but acting together instead of separately. This assumption may be near the truth in that the inner coil and outer coil are bonded together in the coil forming process, and hence, may both coherently be too small or too large. In any case, this average distortion says that the current is not dividing equally above and below the parting plane. Since a_2 exists, we know that this physical effect must exist in the magnet. Hence, the magnitude of C1 that we calculated will indicate how big an error in the parting plane would cause the a_2 that we observed. Figure 4.6.2 shows the amplitude of the distortion C1 as calculated by the new method. We assume that we have only one coordinate, S, to describe C1 for both the inner and outer coil. We ask that S be chosen by a least squares method so it minimizes a_2 and a_4 . Thus, we drive neither of these last coefficients equal to zero, but only determine the distortion so that they are minimized. Figure 4.6.2 shows the results of this calculation. Table 4.6.1 gives the resulting rms errors on the coefficients before and after this correction. It is seen that the major effect of this perturbation has been to reduce the A2 terms without much effecting anything else.

Table 4.6.1

k	a_k Before	a_k After
2	.52 ± .87	-.007 ± .07
4	.06 ± .78	.03 ± .73
6	-.17 ± .45	.18 ± .45



DISTORTION Q1



WORKS ON A₂, A₁

UNDER FOLK

Figure 4.6.1

(C1)

S cable by Least Squares (overcord)
MIN at 24.23106 C1

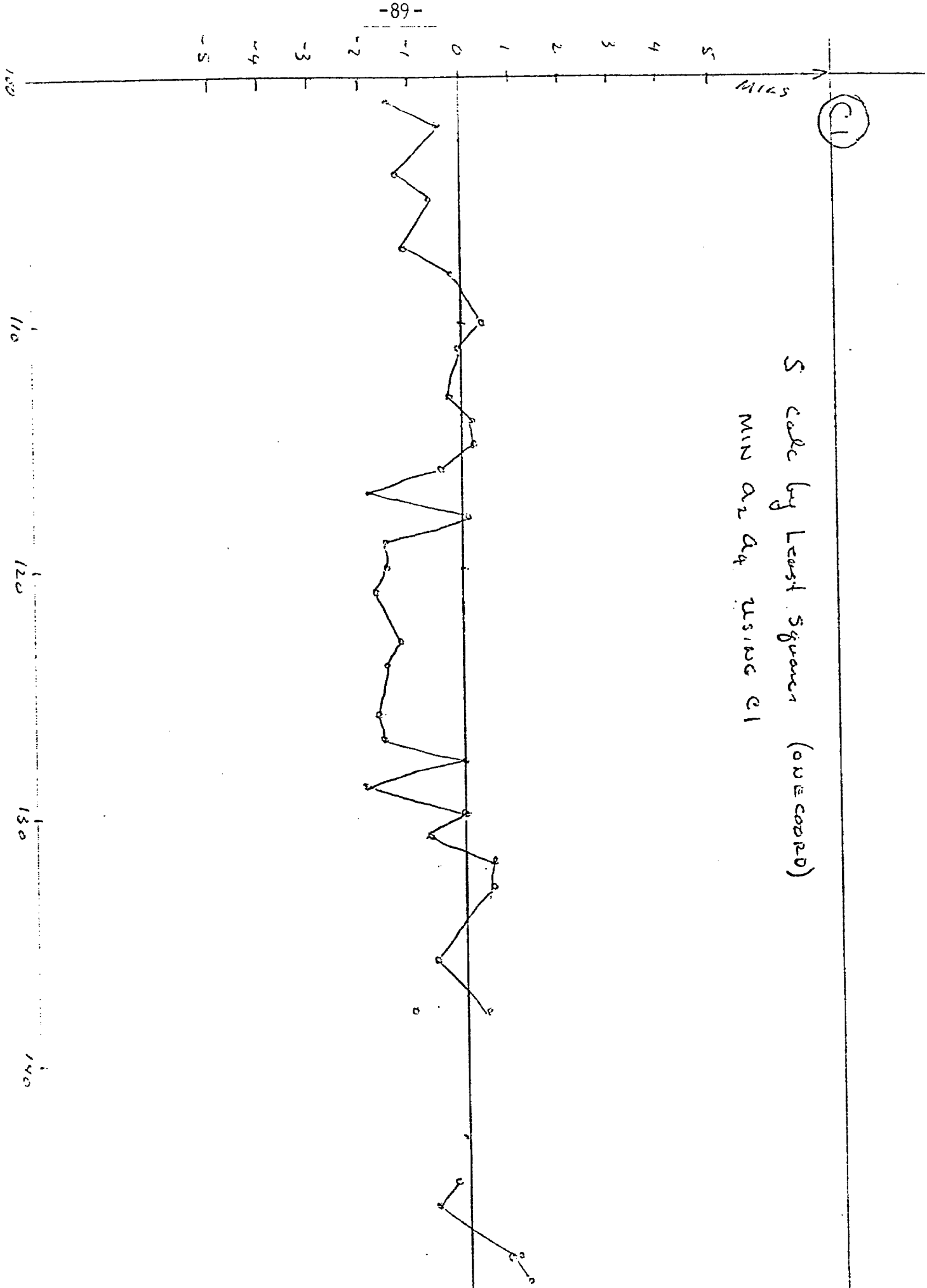


Figure 4.6.2

There is a suspicious region between magnet #118 and #130 where it looks like there is a systematic size error in the coils. This is the same region of magnet numbers where we had indications that something was happening to the outer key angle as described in Section 4.5. In any case, we see that a size difference of the order of 1.5 mils divided by 2 in the coils is sufficient to account for the random skew sextapole that seems to be present. Or, if one wanted to adopt an optimistic attitude, one could say that this calculation shows that the asymmetry in our coils is less than 1.5 mils divided by 2.

Conclusion: C1 amplitude is about ± 1 mil.

4.7 Distortions A1 and D1

These distortions give rise to the harmonics series b_1, b_3, b_5, b_7 . An examination of Figures 4.3.1 and 4.3.2 show that b_1 and b_3 are both fluctuating by rather large amounts. Again we get into a difficult situation analyzing both of these distortions together. We would need to use the first four harmonics to independently determine the amplitude of these two distortions for the inner and outer coil together. We again have the difficulty in that the errors for b_1 , the normal quadrupole, are also influenced by centering errors in the magnetic yoke. However, we have a method to estimate how big the centering errors are compared to how big the errors are due to asymmetries in the coil structure. We have investigated this point in Section 3.2.

Now that we have seen that the fluctuations due to centering the coil in the iron are small compared to the fluctuation of the quadrupole moment due to asymmetries in the coil, we will proceed to neglect this effect and treat b_1 as though

it were coming entirely from fluctuations in the coil structure. Figure 4.7.1 shows the results of the distortion A1 working on the coefficients b_1 and b_3 to set them to zero. The crosses show the amplitude for the outer coil and the circles show the amplitude for the inner coil. It is evident that the amplitude for the inner coil is rather small, less than ± 1 mil. However, it is again evident that for magnets in the range around #120 to #130 that the outer coil may be suffering some additional deformation. Again both the distortions C1 and A2 give indications that the outer coil is being disturbed during this period. This is not a very strong conclusion but at least it is suggestive in indicating that one should look at the outer coil as a source of uncontrolled errors.

We now investigate whether D1 can also fit this series of data. An attempt was made to use D1 to drive b_1 and b_3 to zero. The resulting curve is not plotted but it has all of the aspects of the previous cases where employing two distortions to drive two coefficients to zero results in rather large and coherent anti-fluctuation of the two displacements. Displacements of the gap in the outer coil of up to 20 or 30 mils were found. Hence, the attempt to determine A1 as a fit was not successful.

The least squares technique was used on D1 with rather interesting results. In this method as we indicated with C1 we use a single D1 working on b_1 and b_3 to minimize the sum of their squares. Thus, the amplitude considered here measures some kind of asymmetrical average parting plane gap for the right and left half of the total coil package. Curve 4.7.2 shows the result of this analysis. The scale on the right

17 x 6 - 41 quora

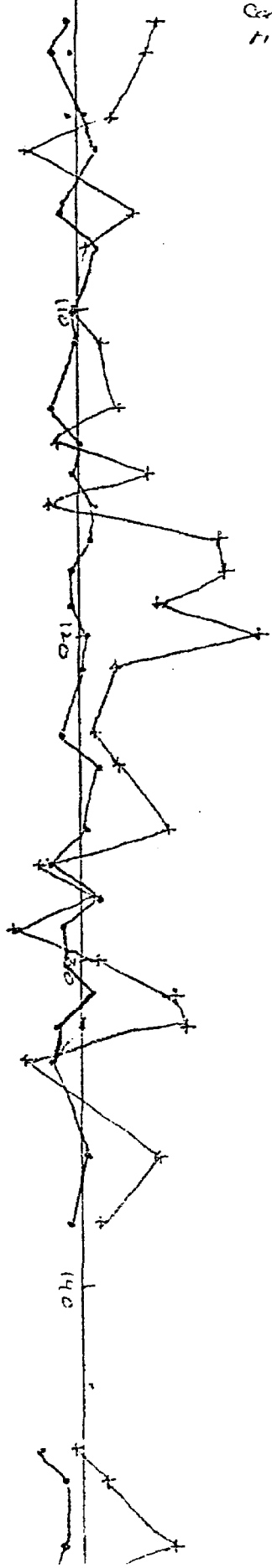
(A1) working on b1 b3

28145

-92-

10
5
0
-5
-10

Core. Smaller
right hand side



$$\overline{S(1)} = -0.0145 \pm 0.052$$

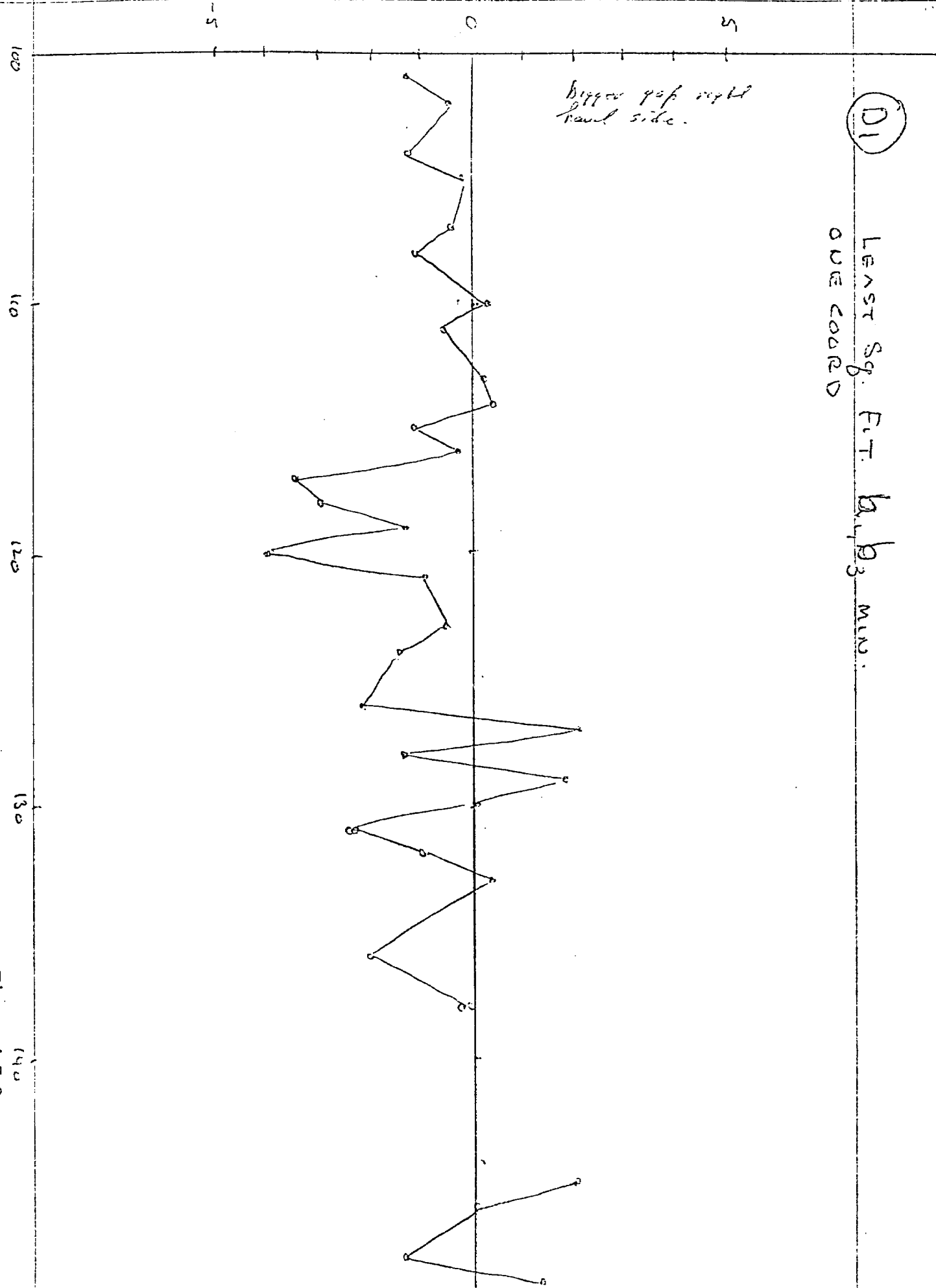
$$\overline{S(2)} = 0.13 \pm 0.18$$

\pm S(2) For
 PART A1
 on S(A)
 S(1)

110 120 130 140

Figure 4.7.1

b1, b3



D1

LEAST Sq. F.T. b₁, b₃ MIN.
ONE CORNER

bigger gap right hand side.

Figure 4.7.2

140

is the asymmetrical gap size. Both the inner and outer coils are assumed to have the same gap. It is seen that a gap variation of a few mils will minimize the coefficients b_1 and b_3 . To see how well this minimization works we display the coefficients b_1, b_3, b_5, b_7 in Figures It is seen that the minimization does a good job of driving b_1 to a rather small value. Table 4.7.3 lists the average value rms

Table 4.7.3

k	b_k Before	b_k After
1	0.75 ± 1.51	.09 ± .34
3	0.55 ± .72	.18 ± .60
5	0.31 ± .41	.099 ± .33
7	0.23 ± .43	0.19 ± .41

deviation of these four coefficients before and after the correction was applied. It is seen that the rms deviation and average value of both b_1 and b_3 are reduced, however, surprisingly enough, the average amplitude of b_5 and its fluctuation was also reduced as was b_7 . This result indicates that at least some of the errors of these higher multipoles are coherent with this D2 type of error in the lower multipoles. As a result, although we obtain a good fit with A1, there seems to be no way to rule out that the whole effect could also be coming

from D1. In either case, this analysis gives us an estimate for how big an error we could tolerate at the keys and at the parting plane. We use these errors as limits in the conclusion given below.

Conclusion: A1 inner is less than ± 1 mil.

A1 outer is less than + 5 and - 2, and displays perhaps systematic effects.

D1 for inner and outer summed has an amplitude of ± 2 mil with some systematic effects showing around magnet # 120 to #130.

It is useful to note that the distortion D1 as summed together for the inner and outer coils very closely duplicates the matrix for A1 for the outer coil. Since the main results of using A1 was mirrored in the coordinates of the outer coil it is not surprising that D1 summed is equally able to fit the data, however, A1 as a source of error is probably to be preferred. This is because A1 is the anti-symmetrical combination of distortions as compared to A2. We have already shown that there were large, uncontrolled errors in A2 and we would expect errors of the same order of magnitude in the opposite symmetry combination to show up. However, it is not inconceivable that an error in the parting plane of 2 or 3 mils could exist, and that the symmetrical combination of this error is the thing that is making itself felt in the analysis of A2 for the outer coil around magnet #120. This indicates the difficulty of uniquely unscrambling the structural errors in the magnet from a set of multipole measurements that have errors.

4.8 B2 and C2 Distortions

Finally we come to the errors B2 and C2 that drive the multipoles series a_1, a_3, a_5, a_7 , etc. The examination of Figures 4.3.15 through 4.3.18 that there are rather large fluctuations in this chain of coefficients. However, the analysis is very difficult. If we use B2 and C2 together we have four unknowns and if we take as our measurements a_1, a_3, a_5 , and a_7 , we can determine all four displacements. This yields a set of distortions for C2 that are unrealistic -- sometimes being as big as 20 or 30 mils, and furthermore, the inside and outside distortions are fighting each other. The reason for this is again evident if we examine the transfer matrices given in Tables 4.4.2 and 4.4.5 for B2 and C2. We see that for $K = 7$, the coefficients for B2 are rather small, and for C2 are very small. Thus, the relatively large fluctuations occurring in a_7 drive enormous fluctuations in the displacements.

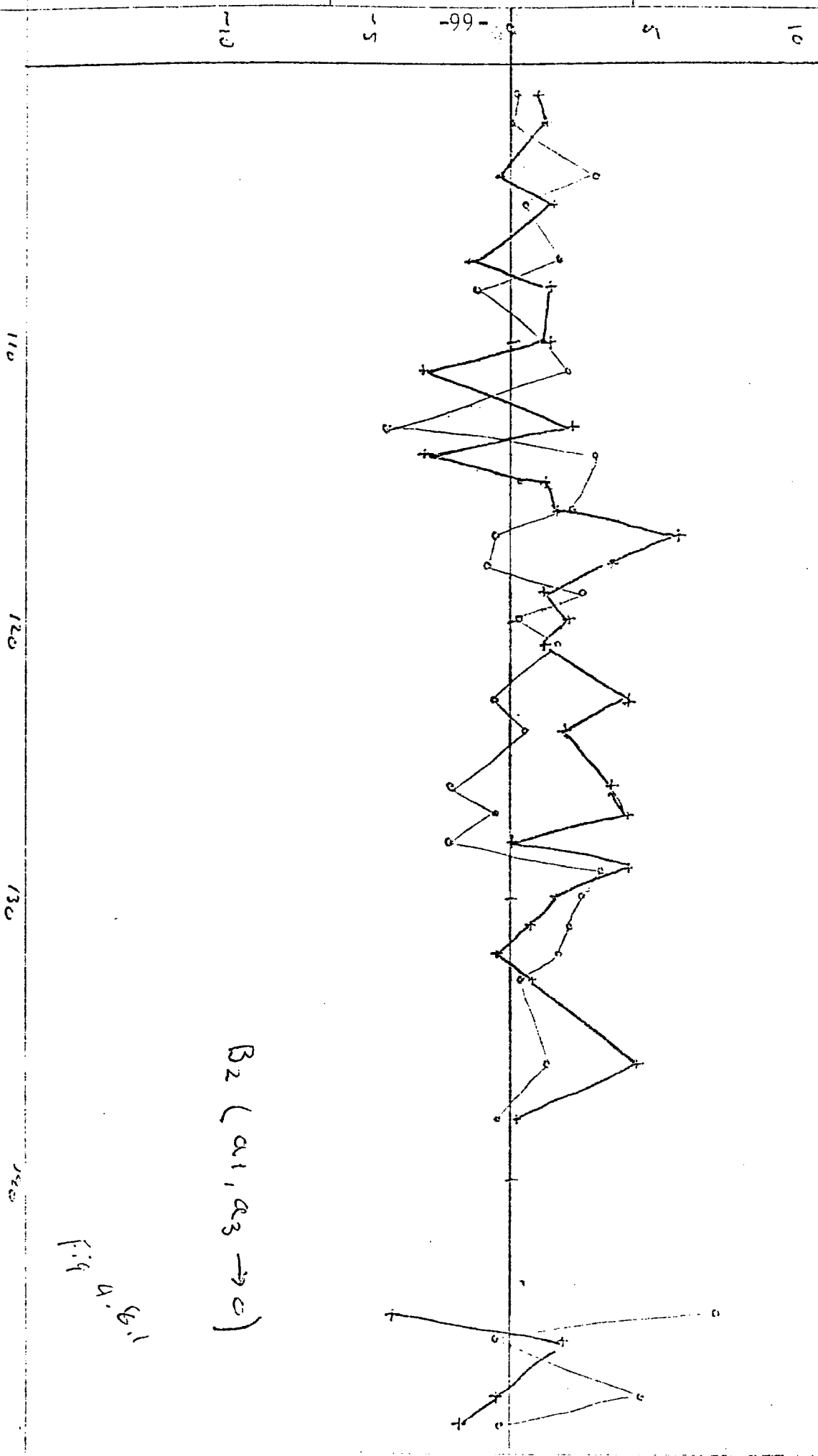
Using either B2 or C2 alone is the next thing to try. Figure 4.8.1 shows the results of letting B2 work on a_1 and a_3 , forcing them to zero. This is not an unreasonable fit. It is clear that the inner and outer displacements tend to fight each other a little bit, but there is certainly some truth in the amplitudes of the terms observed. On the other hand, an attempt to use C2 alone results in a terrible fit -- the inside and outside terms being very large and of opposite sign.

Conclusion: The amplitude of B2 inner is of the order of 2 mils; the amplitude of B2 outer is of the order of 2 mils. Again there may be some systematic structure between magnet #120 and #130 driving the outer coil.

It is worth noting that if one key is of the wrong size by an amount Δ that it will drive the four distortions, A1, A2, B1 and B2, to an amplitude $\frac{\Delta}{4}$. Therefore, if the coil is manufactured with an error at one of the keys, this error should show up in the distortions A1, A2, B1 and B2. In no case will a failure of the mechanical support structure at just one point result in a nice symmetrical or anti-symmetrical error. In other words, if we find a fluctuation in the symmetrical amplitude, we expect it to also appear in the anti-symmetrical amplitudes.

B₂

o S(1) —
+ S(2) —



B₂ (a₁, a₃ → 0)

Fig. 4.6.1